UNIVERSITÀ DEGLI STUDI DI SALERNO

UNIVERSITÀ DEGLI STUDI DI SALERNO
Dipartimento di Farmacia

PhD Program

in **Drug Discovery and Development**

XXXV Cycle – Academic year 2022/2023

PhD Thesis in

Role of H3K56 acetylation in Candida albicans virulence

Candidate

Marisa Conte

Supervisor

Prof. *Amalia Porta*

Co-tutor

Prof. *Alessandra Tosco*

PhD Program Coordinator: Prof. *Gianluca Sbardella*

Table of Contents

ABSTRACT

INTRODUCTION **1**

Chapter I: *Candida albicans* **1**

1.1. *Candida albicans*: a microorganism with unique features 1

1.2. *Candida albicans* cell wall 3

1.3. Morphogenetic states of *Candida albicans* 5

1.3.1. Yeast-like morphotypes 7

Chapter II: *Candida albicans* virulence **9**

2.1. Virulence factors of *Candida albicans* 9

2.2. Polymorphism 10

2.3. White-gray-opaque switching 13

2.4. Adhesion to host 14

2.4.1. Biofilm formation 18

2.5. Hydrolytic enzymes 21

2.5.1. Candidalysin 22

Chapter III: Candidiasis **25**

3.1. Epidemiology 25

3.2. Etiology and pathophysiology 26

3.3. Pharmacological treatment of candidiasis 27

3.3.1. Azoles 27

3.3.3. Echinocandins 30

3.3.4. Flucytosine 31

3.3.5. Allylamine 32

3.4. *C. albicans* antifungal resistance 33

3.4.1. Azole resistance 33
3.4.2. Resistance to other antifungal drugs 36
3.4.3. Tolerance pathways contributing to drug resistance 37

Chapter IV: *Candida albicans* – host interactions 39

4.1. *C. albicans* commensalism 39
4.2. Interaction with host immune cells 39
4.3. Host immune escaping 43
4.3.1. Reducing recognition by immune cells 44
4.3.2. Soluble factors promoting host-immune evasion 46

Chapter V: Epigenetic of *Candida albicans* 49

5.1. Chromatin: structure and functions 49
5.2. Histone acetylation 51
5.2.1. Histone deacetylases 51
5.2.2. Sirtuin family deacetylases 52
5.3. *Candida albicans* histone deacetylases 55
5.3.1. HATs/HDACs as potential antifungal targets 56

MATERIALS AND METHODS 61

6.5. Cell cultures 62
6.6. MTT assay 62
6.7. Treatment of J774A.1 with *Candida albicans* conditioned media 62
6.8. Infection of J774A.1 and Hotchkiss-McManus Stain 63
6.9. Immunofluorescence Assay and Confocal Microscopy 63
6.10. Histones extraction 64
6.11. Total RNA extraction and RNA sequencing 64
6.12. Chromatin Immunoprecipitation 65
6.13. Bioinformatic analysis 65

6.14. Metabolomic analysis 66

6.15. Recombinant Hst3 purification from *Saccharomyces cerevisiae* host 67

6.15.1. *S. cerevisiae* growth conditions 67

6.15.2. Transformation of INVSc1 competent cells 67

6.15.3. rHst3 purification by affinity chromatography and ion exchange 68

6.16. rHst3p purification from *Escherichia coli* host 69

6.16.1. Bacterial growth conditions 69

6.16.2. Cloning of *HST3* into pETM11-SUMO3 vector 70

6.16.3. Transformation of *E. coli* competent cells 70

6.16.4. Ni-NTA Agarose affinity purification 71

6.16.5. rHst3 purification from inclusion bodies 71

6.17. SDS-page, coomassie staining and Western Blotting 71

6.18. Statistical analysis 72

RESULTS 73

Chapter VII: H3K56 acetylation regulates the expression of virulence-related genes 73

7.1. Genome-wide analysis of H3K56ac across *C. albicans* genome in yeast and V-shaped forms 73

7.2. Sirtinol, SirReal2, and Inauzhin do not inhibit Hst3. 85

Chapter VIII: Acetylation of H3 Lys56 regulates the production of soluble metabolites influencing macrophages response 89

8.1. *C. albicans* soluble metabolites induce morphological changes in macrophages cytoskeleton 89

8.2. Hst3 inhibition induces the production of metabolites improving the phagocytic activity of J774A.1 cells 93

8.3. Genome-wide analysis of H3K56ac across *C. albicans* genome in hyphae-inducing conditions 96

8.3.1. Transcriptome analysis 99

DISCUSSION 109

BIBLIOGRAPHY 115

ABSTRACT

Candida spp., especially *Candida albicans*, represent the third most frequent cause of infection in Intensive Care Units worldwide, with a mortality rate approaching 40%. The increasing antifungal resistance drastically reduces therapeutical options for treating candidiasis. Moreover, finding new molecules that specifically recognize the microbial cell without damaging the host is further complicated by the similarity between fungi and human cells.

Epigenetic writers and erasers have emerged as promising targets in different contexts, including the treatment of fungal infections. In this context, histone acetylation-deacetylation plays a leading role since it regulates pathogenic processes and influences *C. albicans* virulence, especially the Lys 56 of the H3 histone acetylation, particularly abundant in yeasts. The fungal sirtuin Hst3, responsible for histone H3K56 deacetylation in *C. albicans*, is essential for the fungus viability and virulence, representing a unique and interesting target for the development of new antifungals since Hst family proteins diverge significantly from their human counterparts. In this study, using the non-specific Hst3 inhibitor nicotinamide (NAM), the effects of H3K56ac accumulation in *C. albicans* were evaluated. In particular, by Chromatin immunoprecipitation followed by sequencing (ChIP-seq) analysis the acetylation patterns of H3K56 were identified in yeast promoting conditions. In those conditions, Hst3 inhibition triggers the formation of a peculiar phenotype, namely V-shaped hyphae, associated with increased levels of H3K56ac. Moreover, by RNA-seq were identified some virulence-related genes regulated directly or indirectly by H3K56ac associated to the promoter. Furthermore, the roles of H3K56ac in *C. albicans* infection were evaluated. Specifically, since several studies pointed out the possible implication of *C. albicans* secretome in mitigating innate immune cells response, the supernatants from *Candida* cultures, treated with NAM (CaNAM-CM) or not

(Ca-CM), were used to treat J774A.1 macrophages. Interestingly, the exposure to the metabolites produced by NAM-treated *C. albicans* resulted in a rapid activation of macrophages and an improved phagocytic activity. By contrast, the macrophages pre-stimulated with Ca-CM displayed abnormal membrane ruffle and the phagocytosis resulted delayed. Of note, quantitative MS analysis showed that farnesol, a quorum sensing molecule that also affects innate immune system response, is significantly more abundant in CaNAM-CM. Finally, ChIP-seq experiments in infection conditions revealed a different genomic distribution of H3K56ac. Also, transcriptomic studies revealed a dysregulation of several genes associated to host immune evasion and PAMPs exposure. Overall, this study provides the first map of H3K56 acetylation across the *C. albicans* genome in two different growth conditions, representing a rich resource for future studies.

INTRODUCTION

Chapter I: *Candida albicans*

1.1. *Candida albicans*: a microorganism with unique features

Fungi represent one of the largest eukaryotic kingdoms, with estimated 1.5-5 million fungal species. However, the clinical diseases are attributed to a few hundred of them (1).

Species of the genus *Candida* are the main ones responsible for opportunistic infections and, in particular, *Candida albicans* represents the most common human pathogen associated with several sites of infection, including kidney, skin, nails, mucosal surfaces, and any other tissues or internal organs (1; 2). The ascomycetous *C. albicans* is a polymorphic fungus found, as a common member of the human microbiota, in the mucosal surfaces of gastrointestinal, respiratory, and genitourinary tracts (3). *C. albicans* genome consists of eight pairs of homologous chromosomes which are numbered from 1 (the largest) to 7 (the smallest), with the one carrying the ribosomal DNA called chromosome R. Being a eukaryotic organism, *C. albicans* has a cellular structure similar to that of animal cells, although some peculiar characteristics distinguish this opportunistic pathogen from other yeast species. *C. albicans* genome sequencing revealed the presence of mating type-like (MTL) regions, a discrete region on chromosome 5, related to mating type (MAT) loci in *S. cerevisiae*, encoding the transcriptional regulators that control the expression of mating specific genes (3). However, the *C. albicans* genome lacks key meiotic components essential for the proper execution of meiosis I in *S. cerevisiae* (3). Experimental evidence reveals that, in *C. albicans*, mating generates tetraploid strains that revert to diploidy by a parasexual process where a random chromosome loss generates phenotypic

variants of the fungus (4; 5). Furthermore, although the majority of progeny is reduced to the conventional diploid state during this process, aneuploid, triploid and tetraploid forms have been observed in *C. albicans* isolates (6). Indeed, changes in ploidy seem to be a strategy evolved by the fungus to adapt to changes in environmental conditions within the host or in response to antifungal drugs (7). All the essential elements of eukaryotic chromosomes have been identified in *C. albicans*. Nevertheless, the eight centromeres of *C. albicans* are 3–5 kb in size and do not show any common DNA sequence motif or repeat, suggesting an epigenetic regulation of the centromere without dependence on the primary DNA sequence. However, this fungus can form neocentromeres upon centromere deletion. Moreover, *C. albicans* telomeres contain tandem copies of unusually long 23-bp repeating units, a unique feature not shared with other eukaryotic species (3).

The major repeat sequence (MRS) is another unique feature of the *C. albicans* genome and consists of a long tract (10-100 kb) of repetitive DNA present in all the chromosomes (except chromosome 3) constituted by three subunits: the repetitive RPS subunit flanked by nonrepetitive elements RB2 and HOK (8). Interestingly, the MRS carries marks of both euchromatin and heterochromatin and is not assembled into classical heterochromatin as usually observed for other kinds of repetitive regions. The MRS is a preferred site for translocations between heterologous chromosomes and intrachromosomal recombination, but its functions remain unclear (8). Although the majority of the genomic diversity of *C. albicans* is attributed to asexual mitotic genome rearrangements, different repetitive loci have been shown to contribute to genotypic and phenotypic plasticity such as copy number variation (CNV), loss of heterozygosity (LOH) and chromosomal inversions (9).

C. albicans differs from other fungi also in codon usage, with higher frequency and longer repetitions of codons that were not found in other fungi (10).

All these unusual characteristics make *C. albicans* a peculiar microorganism that raises increasing interest in the scientific community.

1.2. *Candida albicans* cell wall

An important feature shared between all fungi is the presence of a cell wall outside the cytoplasmatic membrane. The cell wall might be considered like a skeleton with high plasticity that gives rigidity, defines the cellular structure**,** interacts with the environment, and protects the cell from different stresses (11). The main components of the fungal cell wall are glucans, chitin, chitosan, and glycosylated proteins structured in different layers that vary between different species of fungi. *C. albicans* cell wall consists of an outer layer of highly mannosylated proteins covalently attached to the inner layer through glycosylphosphatidylinositol (GPI) residues forming a fibrillar protein coat. These mannoproteins are frequently decorated with N- and/or O-linked mannans and represent up to 30–40% of the dry weight of the cell wall together with phospholipomannans (Fig. 1) (12; 13; 14). The inner layer contributes significantly to the overall integrity of the cell wall with structural polysaccharides such as β-1,6- and β-1,3-glucans and chitin (Fig.1) (14).

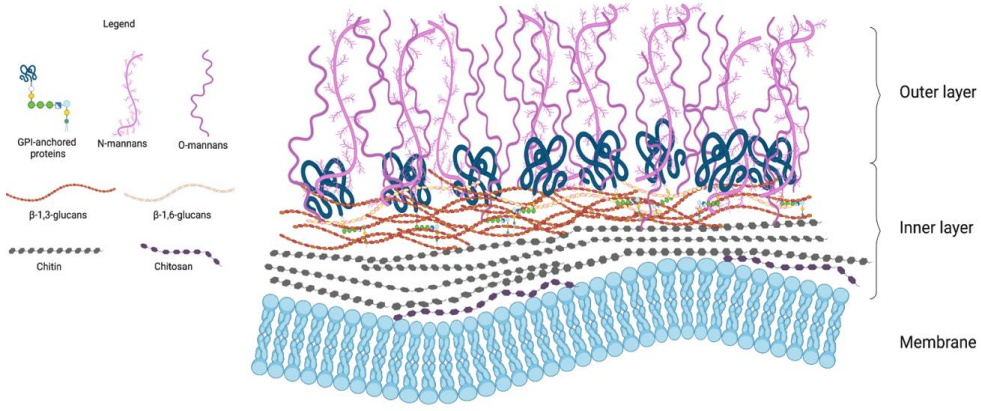

Fig.1 - *Candida albicans* cell wall structure (Created with BioRender.com).

Nevertheless, *C. albicans*, being a dimorphic fungus, can switch morphologies between yeast and hyphae with consequent changes in the cell wall composition. Usually, the chitin content is higher in the hyphal wall compared to the yeast form, whereas the structure of mannans remarkably changes between morphotypes (11). The 50–60% of the dry weight of the yeast cell wall is represented by β-Glucan, a structural polysaccharide composed of chains of glucose residues linked via β-1,3- or β-1,6 linkages. In particular, β-1,3-Glucan fibrils are the principal structural component of the *C. albicans* cell wall and are synthesized at the plasma membrane by the beta-1,3-glucan synthase complex and then extruded into extracellular space (11).

The chitin content of *C. albicans* cell wall varies according to the morphological phase from 1-2% of the dry weight of yeast cell wall up to 10-20% in hyphae (11). Chitin is a linear homopolymer of β-1,4-linked N-acetylglucosamine, which forms antiparallel chains linked by intrachain hydrogen bonds and in *C. albicans* is synthesized from n-acetylglucosamine by a family of four chitin synthases (11; 13). This strong fibrous structural component of the inner layer contributes significantly to the integrity of the cell wall. A small fraction of chitin is deacetylated to chitosan, which in this form makes the fibrillar layer more elastic and resistant to the action of chitinases (13). β-1,6-glucan structures are crosslinked to β-1,3-glucan in the inner layer and provide an additional platform for the covalent anchoring of some cell wall mannoproteins (Fig. 1). Several enzymes responsible for the β-1,6-glucan biosynthesis have been identified, but it is not clear where the β-1,6-glucan synthesis occurs (13).

Mannans do not influence the cell shape since they are less rigid than β-glucans and chitin, but they play a key role in the tolerance of the cell wall to antifungal drugs and host defense mechanisms (11).

Besides the well-known structural functions of the *C. albicans* cell wall, recent studies highlighted the role of this cellular compartment in host-immune evasion (see Chapters II and IV).

1.3. Morphogenetic states of *Candida albicans*

The modulation of morphogenesis is one of the most important abilities evolved by *C. albicans* to respond to environmental changes and represents one of the main virulence factors. These morphological changes include yeast-to-hypha transition, white-opaque switching, and chlamydospore formation (15). The yeast-to-hypha transition is promoted by several environmental stimuli such as nutrient starvation, N-acetyl glucosamine (GlcNAc), serum, CO_2 levels, neutral pH, and temperature (16). Yeast cells are the unicellular form of *C. albicans* at 25°C and acid pH. Cells appear round or oval, duplicate by budding and nuclear division occurs at the junction between the mother and the daughter cell (Fig 2a) (16). When unbudded yeast cells are induced to form hyphae (serum at 37°C), a single germ tube (a narrow, tube-like projection) evaginates from the mother cell and elongates exclusively from its tip, exhibiting a highly polarized growth. Noteworthy, the first cell cycle starts when the germ tube has already formed and may be up to 15–20 μm long. Growth at 37°C and neutral pH favors pseudohyphae, a multicellular form characterized by long, elliptic cells of different widths and lengths with features of both yeasts and hyphae (15; 16). There are no known *in vitro* conditions to induce pure, stable populations of pseudohyphae (16). Pseudohyphal cells remain attached following cytokinesis and generate mycelia after multiple rounds of cell division, but nuclear division in pseudohyphae occurs at mother-daughter junctions (Fig 2b) (16). Hyphae cells can be induced by a temperature of 37°C, N-acetyl glucosamine, embedding matrix, hypoxia, alkaline pH, and appear as multicellular long tube-like filaments (15). During hyphae formation, the cellular volume expands along a

polarized axis, and the ovoid yeast cells switch into elongated becoming more than 10 times larger in size (17).

In hyphae, nuclear division occurs within the hyphal daughter cell, and then one progeny nucleus migrates back to the mother cell. Following cytokinesis, hyphal cells remain firmly attached end-to-end, and subsequent rounds of cell division produce multicellular filamentous structures called mycelia (Fig 2c) (15).

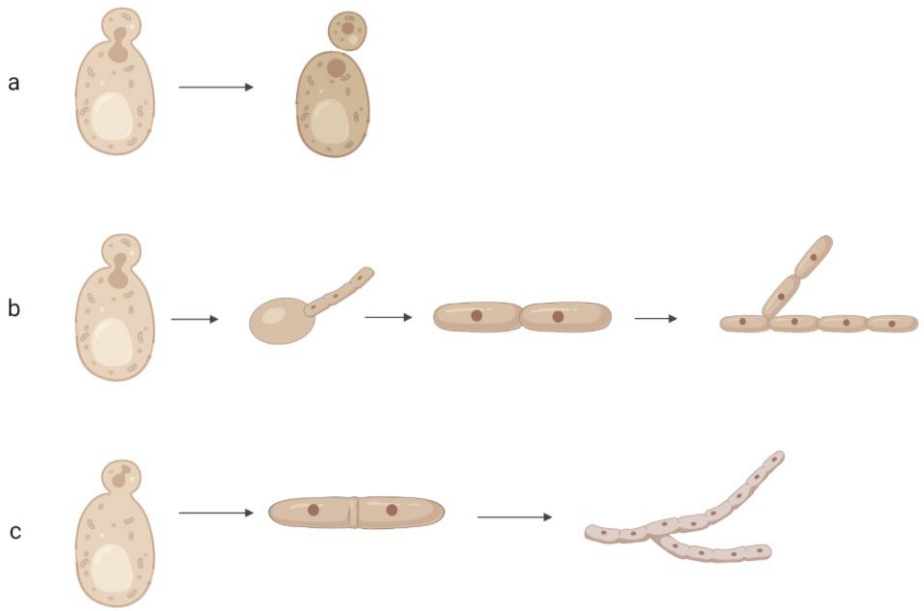

Fig. 2 - *C. albicans* morphotypes. (a) Budding yeast unicellular form; Pseudohyphae (b) and hyphae (c) formation. (Created with BioRender.com).

Although hyphae and pseudohyphae share some structural features, the latter displays a constriction in the neck of the bud and mother cell, a feature not observed in hyphae that are highly polarized and have parallel sides throughout their length (15).

This yeast-to-hypha transition is finely regulated by different mechanisms, including post-translational, transcriptional, and epigenetic mechanisms (18).

1.3.1. Yeast-like morphotypes

Besides the classical "white" round-to-oval yeast morphology, several more elongated yeast-like cell types (opaque, gray, and gastrointestinal cells) have been observed in *C. albicans* (17). As discussed in Section 1.1, a parasexual stage in the reproductive cycle has been observed in *C. albicans.* Indeed, *C. albicans* can exist as sterile "white cells" and mating-competent "opaque cells", characterized by the oblong shape, that form flatter and darker colonies (19). White-opaque transition is regulated by the configuration (a/α) of the (MTL) locus (19). The white state is considered the default cell type whereas the opaque state is the "excited state" since it requires the activation of specific genes which establish a series of positive feedback loops. Among them, *WOR1* is the "master regulator" of white-opaque switching (18).

Although the two cell types have the same genome, they express different genes (i.e., transcription factors encoded at MAT (the mating-type) loci), and they have some differences in morphology, metabolism, and susceptibility to antifungals (19).

Another cell type that has been reported in *C. albicans* is the gray phenotype (20). Gray cells are smaller than white and opaque cells, but similarly to the second ones show an elongated shape (20). The three cell types form a reversible switching system, and the balance between the three states is influenced by specific environmental stimuli (19; 20).

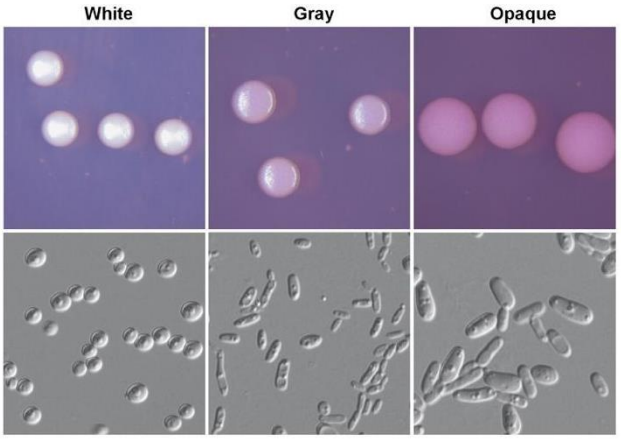

Fig. 3 - Colony and cellular morphologies of *Candida albicans* white, gray, and opaque cells
(Adapted from Ref. 21).

The other yeast-like morphotype identified in *C. albicans* is the Gastrointestinally indUced Transition (GUT) cells that, despite the cell shape and the dark colony similar to the opaque form, lack the classic features of white and opaque cells and are likely specialized for commensalism in the mammalian gastrointestinal tract (1).

Chapter II: *Candida albicans* virulence

2.1. Virulence factors of *Candida albicans*

Candida albicans is a commensal fungus that causes opportunistic infections in immunocompromised hosts with a mortality rate of about 40% (21).

The ability to establish opportunistic infections depends on many virulence factors (Fig. 4), which facilitate the adherence to the host, the tissue invasion, and the formation of resilient biofilm communities on medical devices and host surfaces (21).

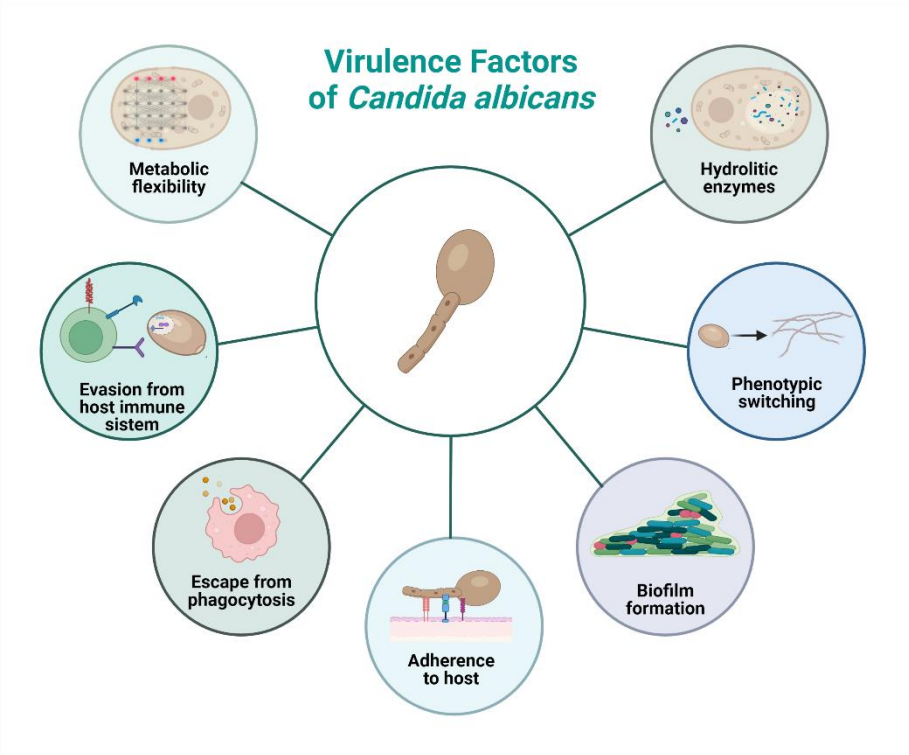

Fig. 4 - Main virulence factors of *C. albicans* (Created with BioRender.com).

Beyond the expression of a wide range of virulence factors, *C. albicans* also evolved several strategies to evade the host immune response, and escaping macrophages is the basis for establishing systemic infection (22). Furthermore,

several fitness attributes support the pathogenesis in *C. albicans*, including metabolic flexibility combined with potent nutrient acquisition systems, and robust stress response mechanisms (22).

2.2. Polymorphism

A strong association exists between *C. albicans* virulence and the ability to undergo a reversible morphological transition in response to host environmental cues.

The ability to switch between yeast, pseudohyphal and hyphal forms is one of the most investigated virulence attributes of this opportunistic pathogen (18; 23).

Both yeast and hyphal morphologies are necessary for the full virulence of *C. albicans;* hence the phenotypic switching is a finely regulated process accompanied by an extensive change in gene expression profile. In particular, the yeast form is mainly involved in dissemination, whereas the hyphal cells play a key role in tissue invasion (24).

The yeast-to-hyphal switch is mediated by different signal transduction regulators. Among them, the cAMP/PKA and MAPK are the most characterized pathways with a key role in integrating different environmental stimuli to drive hypha-specific gene (HSG) transcription (Fig. 5) (25).

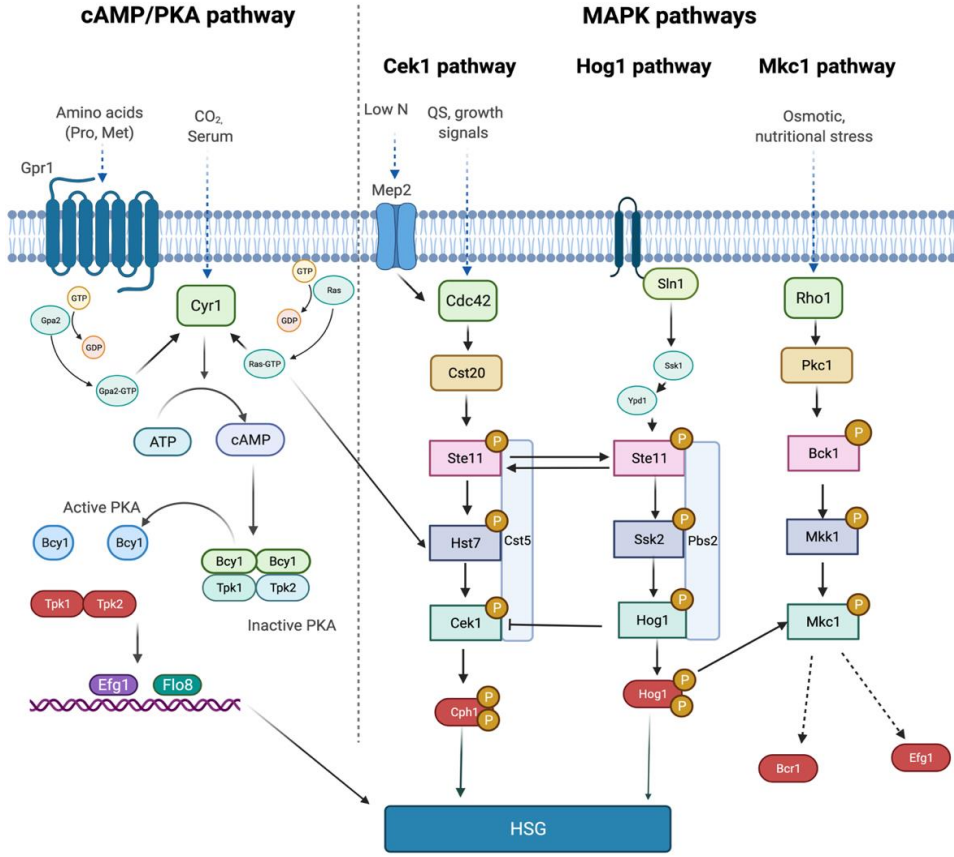

Fig. 5 - Major signaling pathway involved in *C. albicans* morphogenesis (Created with BioRender.com).

Whole-genome transcriptional profiling has demonstrated that several transcription factors regulate the *C. albicans* yeast-filament transition, including Tup1, Ngr1, Rim101, Cph2, Cph1, Czf1, Efg1, Tec1, Flo8, Ume6, Fkh2, and Mcm1 (18; 26).

Besides the well-known transcriptional control mediated by promoter-specific DNA-binding transcription factors, the transcription machinery components are equally important in the transcriptional regulation of *C. albicans* morphology and virulence (18).

Experimental evidence shows that *C. albicans* has a significant expansion in the TLO (TeLOmere-associated) gene family compared to less pathogenic *Candida* species, which do not produce filaments easily (18). The *C. albicans*

SC5314 genome contains 15 *TLO* genes close to each chromosome's telomeres, encoding the Med2 component of the Mediator complex, a large multi-subunit protein complex that functions as a general transcriptional co-activator in eukaryotes (18; 27).

C. albicans morphogenesis could also be regulated by a chromatin-mediated transcriptional mechanism involving the HIR histone chaperone complex, which facilitates chromatin assembly in a replication-independent manner (18). Indeed, Jenull S. and colleagues demonstrated that the deletion of *HIR1*, encoding a key component of this complex, dramatically reduces the HSG transcriptional amplitudes and the sensitivity to morphogenesis signals (28). In particular, they proposed a model in which the HIR complex acts downstream of cAMP/PKA signaling, promoting an open chromatin structure at promoters of HSG and, consequently, enhancing their expression (28).

The relevance of different components of complexes associated with chromatin-mediated regulation (i.e., Set3, Hos3, Hat1, Waf1, Yaf9) has already been elucidated, suggesting a central role of these mechanisms in regulating *C. albicans* morphogenesis and virulence (1).

Recently, a novel mechanism of morphogenesis regulation in *C. albicans* involving Hsf1 has been discovered. Hsf1 (heat shock transcription factor 1) is a conserved temperature sensor, highly expressed upon acute temperature increases to activate the cellular responses to thermal stresses inducing the expression of *HSP90* and other chaperone genes (29). Depletion of *HSF1* compromises the function of Hsp90, a critical molecular chaperone for *C. albicans* virulence, morphogenesis, drug resistance, and biofilm formation (29).

Specifically, Hsp90 has been shown to repress morphogenesis via the cAMP-PKA signaling pathway (30). Consequently, after HSF1 deletion, filamentation increased without external stimuli (29). Hsf1 also promotes the *C. albicans* morphogenesis through an Hsp90-independent mechanism

inducing the expression of positive regulators of filamentous growth, such as *UME6* and *BRG1,* and repressing negative regulators of filamentation, such as *NRG1* (29). Finally, a translational control exerted by the extensive 5′ untranslated regulatory sequences (5′ UTR) of filamentation and virulence genes has been shown for *UME6* and *EFG1*.

Specifically, the *UME6* 5′ UTR is likely to inhibit Ume6 protein expression under several filament-inducing conditions by reducing the association of *UME6* transcript with polysomes (31). In contrast, *EFG1* 5' UTR exerts a positive translational function by promoting the recruitment of regulatory factors during the emergence of the native transcript (32).

2.3. White-gray-opaque switching

The ability of *Candida albicans* to switch reversibly between the white to the opaque phenotype is also linked to virulence, as it allows yeast cells to survive and adapt to stress. Indeed, the replication of yeast cells in a host organism requires metabolic flexibility to ensure an active replication (17). Factors like temperature, CO_2, alkaline/neutral pH, carbon/nitrogen stress, quorum sensing molecules, hypoxia, serum, limited nutrition, adherence, and epigenetic mechanisms have been shown to regulate this phenotypic transition (33). In terms of pathogenicity, opaque phenotypes are overall less virulent than white phenotypes since they lack the ability to produce chemo-attractants for phagocytic cells, even if they are better at mediating cutaneous infections. On the other hand, white cells are more efficient in terms of fitness inside the host and are more efficient in causing systemic candidiasis (26; 34). Seven transcription factors (Wor1, Wor2, Wor3, Wor4, Ahr1, Czf1, Efg1) and one non-DNA-binding adapter protein (Ssn6) are involved in the regulation of white-opaque switching. *WOR1* is the master regulator involved in initiating the switching process to opaque cells and is repressed in white cells, whereas *EFG1* acts as a suppressor of this process (Fig 6) (35).

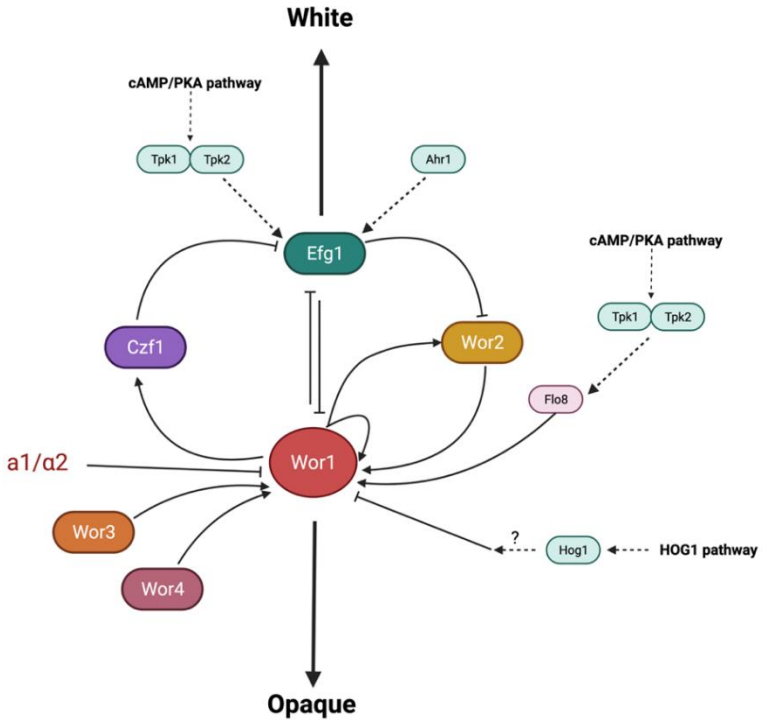

Fig. 6 - Regulatory network involved in the regulation of white opaque-switching (Created with BioRender.com).

However, recent studies suggest the possibility of alternative mechanisms regulating the white-opaque switching, considering that the switching from white to opaque can still be induced upon the simultaneous deletion of both *EFG1* and *WOR1* (36).

2.4. Adhesion to host

As a component of the human microbiota, *C. albicans* is adapted to live in the host, particularly in the gastrointestinal tract. Mucosal surfaces represent the main protective barriers during infection, given their role in the initiation and coordination of innate immune responses (37). The physical interaction between *C. albicans* and a mucosal surface is a requirement that precedes commensal colonization and pathogenic infiltration (37). The initial contact with the host usually involves the yeast form, which has evolved different

strategies to ensure successful adherence to the host epithelium (37). After the first interactions based on passive forces (Fig. 7a) (i.e., van der Waals forces and hydrophobic interactions), the adhesion of *C. albicans* is consolidated by numerous interactions with components of the host extracellular matrix (Fig. 7b; 7c) (37).

The adhesins are considered the main contributors to fungal adhesion. Among them, the agglutinin-like sequence (*ALS*) gene family, encoding a group of proteins GPI- linked to the β-1,6-glucans with adhesive properties, is the most studied in *C. albicans* (38).

The *ALS* gene family consists of eight members (*ALS1-ALS7* and *ALS9*), and distinct members of the ALS family are differentially expressed according to fungal morphology and body site (38). Als5 mediates the initial adhesion of yeast cells to epithelial cells (Fig. 8b). It presents a conserved tandem repeat region that facilitates the adhesion to numerous epithelial ligands and promotes yeast-to-yeast cell aggregation (37; 38).

ALS3 and the non-ALS adhesin Hyphal Wall Protein 1 (Hwp1) are mainly expressed by hyphae (Fig. 7c). *ALS1–5* and *ALS9* are up-regulated in human buccal epithelium model of mucocutaneous candidiasis, while *ALS1, ALS2, ALS3,* and *ALS9* result frequently expressed in clinical specimens of vaginal fluid (37; 38). Nevertheless, *C. albicans* adhesion is a finely regulated mechanism involving anti-adhesion factors, which may refine the process. The yeast-specific GPI-linked glycoprotein Ywp1 (Yeast wall protein 1) is highly expressed during yeast growth and is implicated in the dispersal of the yeasts to facilitate the dissemination (Fig. 8b). Indeed, deletion studies demonstrated that yeast cells lacking *YWP1* are more adhesive. The same phenomenon was observed for deletion mutants of *ALS5, ALS6,* and *ALS7*, suggesting that these proteins also possess antiadhesive properties (37).

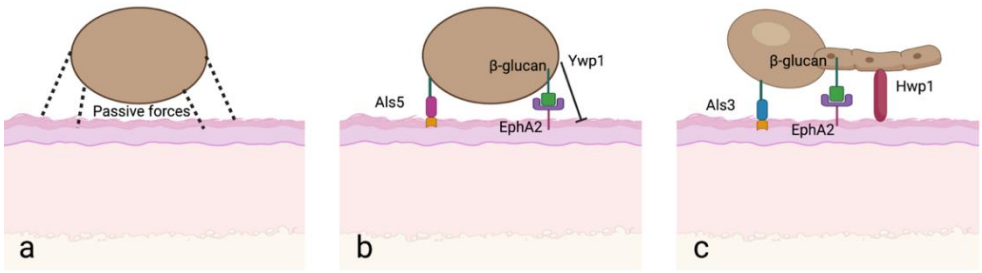

Fig. 7 - *C. albicans* adhesion to host cells (Created with BioRender.com).

Colonization may be followed by invasion, and subsequent infection, in immunocompromised hosts (Fig. 8). Host recognition is the first step in developing an innate immune response against *C. albicans*. In this phase, cells of the mucosal barriers, expressing pattern recognition receptors (PRRs), recognize pathogen-associated molecular patterns (PAMPs) on yeast and hyphal cells (37). *C. albicans* can invade epithelial cells by a passive host-mediated process called induced endocytosis, initiated by the recognition of invasins expressed on the fungal cell surface (Fig. 8) (39). Two invasins have been identified in *C. albicans*: Als3 and Ssa1. Interaction of E-cadherin or EGFR/Her2 complexes with Als3 or Ssa1 promotes the accumulation and co-localization of dynamin, clathrin, and cortactin at the site of contact, inducing the remodeling of the actin cytoskeleton required to endocytose the fungus (37; 39). Induced endocytosis can also occur through a mechanism involving the host GTPases (Cdc42, Rac1, RhoA) and the tight junction protein ZO-1, which are associated with actin remodeling during infection (37). Moreover, recent studies described the host epithelial aryl hydrocarbon receptor (AhR) as an essential upstream component involved in fungal endocytosis since the activation of AhR by *C. albicans* results in Src-mediated phosphorylation of EGFR and fungal internalization (39). Finally, siRNA knockdown of PDGF BB (platelet-derived growth factor BB) and NEDD9 (neural precursor cell-expressed developmentally downregulated protein 9) cause a reduction in

endocytosis, suggesting a role of these pathways in epithelial uptake of *C. albicans* (39). Recent findings described the ephrin type-A receptor 2 (EphA2) as a nonclassical epithelial PRR that recognizes the β-glucans present on *C. albicans* cell wall involved mainly in the initial interaction between *C. albicans* and epithelial cells (37).

Another mechanism of invasion, called active penetration, has been described in *C. albicans*, which requires a viable fungus and occurs by hyphal extension controlled by Ume6 and Eed1 through or between epithelial cells (Fig. 8) (26; 37; 39). Unlike induced endocytosis, this process depends on fungal attributes such as morphology, hyphal turgor pressure, continued extension of hyphal, and secretion of hydrolytic enzymes (see Section 2.6), which degrade host substrates facilitating the breaching of mucosal barriers (37; 39). Active penetration of *C. albicans* hyphae is the only driver of invasion across the epithelium in the gut, even though it may occur at all mucosal surfaces (39).

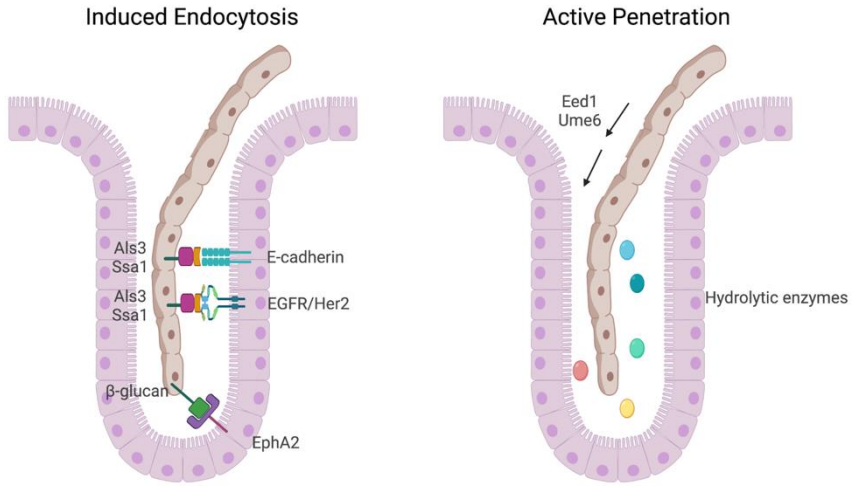

Fig. 8 - Well-known mechanisms of host invasion by *C. albicans*. The hydrolytic enzymes involved in active penetration will be discussed in Section 2.6 (Created with BioRender.com).

2.4.1. Biofilm formation

Biofilm formation represents a major virulence factor during candidiasis since it further complicates the treatment of these infections (40). Indeed, most of the manifestations of candidiasis, and around 15% of hospital-acquired cases of sepsis, are associated with biofilm formation on the surface of medical devices and host surfaces (40; 41). Biofilms are highly organized communities of microbial cells surrounded by a self-produced matrix of exopolymeric materials with distinct properties from their planktonic counterparts displaying an improved resistance to drugs and physical perturbation (40; 41). The biofilm extracellular matrix (ECM) is a major contributor to resistance as it sequesters antifungal molecules and prevents their penetration into the depths of the biofilm and, together with the overexpression of efflux pumps and the changes in the sterol composition of the cell membrane, significantly contribute to the drug tolerance (40). *C. albicans* biofilm developmental process can be divided into four phases: adherence, proliferation, maturation, and dispersion (Fig. 9) (40).

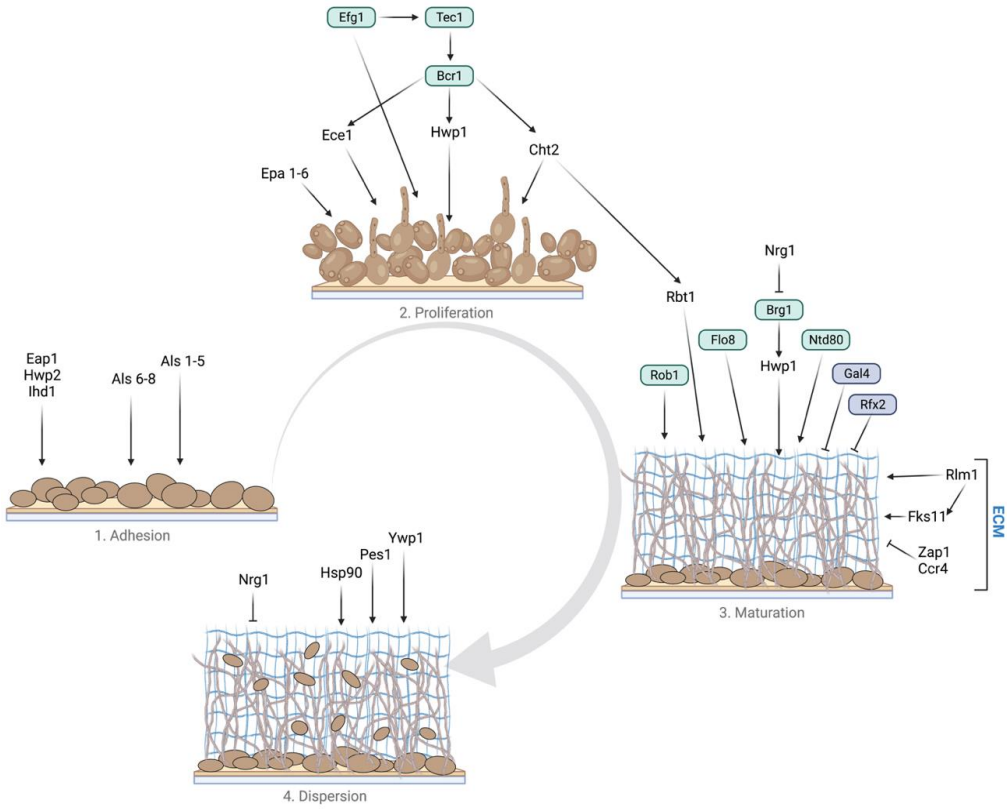

Fig. 9 - Biofilm development regulation in *Candida albicans* (Created with BioRender.com).

In *vitro* studies suggest that, during the early phase of the biofilm formation, yeast cells attach to a solid surface (biotic or abiotic) and form a basal layer that functions to anchor the biofilm (Fig. 9.1) (40; 41). These cells proliferate, remaining attached to the anchor layer, and during this proliferation phase, yeast cells begin to form pseudohyphae and hyphae (Fig. 9.2) (41). The filaments' elongation continues during the entire process, creating a complicated network that contributes to the overall robustness of the biofilm (40). Indeed, during the maturation phase, the hyphal scaffold becomes surrounded by a layer of self-produced exopolymeric substances (EPS) that holds the entire biofilm structure together and acts as a protective physical barrier from the environment (Fig. 9.3; 9.4) (40; 41).

Once fully matured, the biofilm slowly disperses yeast cells of a unique elongated morphology that contribute to the dissemination of the infection (40; 41).

More than 50 transcriptional regulators have been shown to regulate the formation of *C. albicans* biofilms (Fig. 9) (41). Als family proteins have a central role in *C. albicans* attachment to abiotic surfaces, but recent studies highlight the involvement of other factors since the deletions of *HWP2, IHD1,* or *EAP1* result in a complete loss of the initial attachment with the consequent collapse of biofilm, while the deletions of *ALS1, ALS2,* and *HYR1* lead to a reduction of biofilm biomass (42). Moreover, microarray studies showed an up-regulation of two groups of adhesion molecules, one at an early phase (*ALS1, ALS2, ALS3 ALS4, EAP1, MSB2, PGA6, SIM1, ORF19. 2449* and *ORF19.5126*) and another one at a late time point (*HYR1, FAV2, IFF4, IFF6, PGA32, PGA55, ORF19.3988, ORF19.4906, ORF19.5813,* and *ORF19.7539.1*) (43). Nine primary regulatory genes (*EFG1*, *BCR1*, *BRG1*, *NDT80*, *TEC1*, *ROB1*, *FLO8, RFX2, GAL4*) establish the transcriptional regulatory network involved in controlling the biofilm formation process (40; 44). These master transcription regulators control each other's expression and bind to the control regions of more than a thousand target genes (45). More than 500 proteins have been identified in the matrix, including glycoprotein and hydrolytic enzymes, in addition to carbohydrates (α-mannan, β-1,6-glucan, β-1,3-glucan), lipids, and nucleic acids (43). Several genes have been shown to be involved in regulating biofilm ECM production, including the positive regulator *RLM1* and the negative regulators *ZAP1* and *CCR4*. In particular, *RLM1* deletion promotes a reduction in matrix levels and regulates the expression of *FKS1*, responsible for β- glucan synthesis, while *ZAP1* and *CCR4* inhibit β- glucan production in ECM (43). Finally, several components, such as transcriptional regulators, cell wall proteins, and chaperones, have been shown to regulate biofilm dispersion. Beyond Ume6, Pes1, and Nrg1, known

regulators of cell dispersion from the biofilm, the GPI-anchor Ywp1 exerts anti-adhesive effects promoting the dispersion (43).

2.5. Hydrolytic enzymes

C. albicans produces different secretory products implicated in the pathogenesis since they play an essential role in adhesion, tissue penetration, invasion, and tissue damage by digestion of cell membranes and degradation of host surface molecules (46).

Almost all extracellular endopeptidases identified in *Candida* spp. belong to the aspartic proteinases class. The well characterized aspartic proteinases in *Candida albicans* are the candidapepsins, traditionally known as "secreted aspartic proteases" (Saps) (47).

In *C. albicans*, there are 10 different isoforms of Sap (Sap1-10), producing different clinical effects (48). Sap1–8 are secreted into the extracellular space, while Sap9 and Sap10 are membrane-anchored GPI proteins, and most of them have optimal activity in the acidic pH range, even if several studies suggested that each one has an optimum specific pH (49; 50).

Sap1−6 display the highest proteolytic activity at pH 3.0–5.0 but Sap7 and Sap8 show peculiar properties. In particular, Sap7 has optimal activity at neutral pH, whereas Sap8 optimum pH is 2.5, the lowest among all Sap isozymes. This property allows *C. albicans* to survive and cause infections in various host niches (50). SAPs expression is also related to the morphological state of the fungus. Sap 1-3 are mainly secreted by the yeast-like form; in contrast, Sap 4-6 are secreted by the filamentous form (47). Sap proteins also have great relevance in host-pathogen interaction since they destroy molecules of the immune system (antibodies, complement factors, cytokines) and thus limit microbicidal attacks (51).

2.5.1. Candidalysin

In *C. albicans ECE1* gene encodes the candidalysin, a cytolytic peptide known to be the first peptide toxin identified in any human fungal pathogen (52; 53). This peptide is critical for mucosal and systemic infections and, besides the direct damage to epithelial membranes, triggers a danger response signaling pathway activating epithelial immunity (53). *ECE1* is a hypha-associated gene strictly correlated with mucosal damage since the *ECE1*-deficient strain displays significantly reduced injury and immune activation in zebrafish (52). Ece1 sequence contains seven lysine-arginine (KR) motifs dispersed throughout the full-length protein. These motifs are known processing sites for the kexin, Kex2, suggesting that Ece1 is cleaved by Kex2 into at least eight smaller peptides and secreted, as confirmed by LC-MS/MS, but only one of them is involved in damage induction (52; 53). Specifically, Ece1 is processed by Kex2 at positions 61 and 93 to generate immature candidalysin (Clys), which Kex1 further processes to remove the terminal Arg93 generating the 31aa peptide (SIIGIIMGILGNIPQVIQIIMSIVKAFKGNK) named candidalysin (Fig. 10) (53).

Candidalysin is secreted from hyphae and interacts with the cell membrane to form pore-like structures resulting in membrane damage and calcium influx (Fig. 10a) (53).

It has been shown to induce p-MKP1, c-Fos, cytokines, and damage in oral epithelial cells (OECs). Moreover, it also directly lyses multiple human epithelial cell types and causes hemolysis of red blood cells (53).

Recent studies identified the epidermal growth factor receptor (EGFR) as a critical component of candidalysin-triggered immune responses showing that candidalysin induces the phosphorylation and activation of EGFR via indirect mechanisms, such as candidalysin-induced shedding of EGFR ligands

(predominantly epiregulin and epigen), activation of matrix metalloproteinase and calcium fluxes (Fig 10b) (53; 54).

EGFR activation induces the downstream MAPK- signaling and the consequent activation of c-Fos (via p38, ERK1/2), resulting in cytokine induction and neutrophil recruitment, while MKP1 activation (via ERK1/2) contributes to the regulation of the epithelial immune response (Fig. 10c-d) (53; 54).

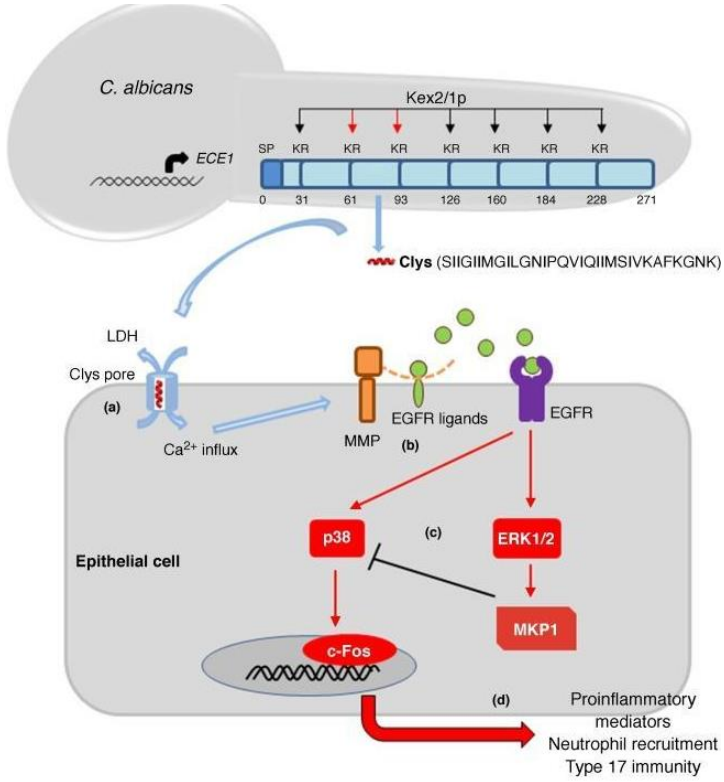

Fig. 10 - Candidalysin production and mechanism of candidalysin-triggered immune response
(Adapted from Ref. 53).

Chapter III: Candidiasis

3.1. Epidemiology

Candida species can cause superficial or invasive disease, mainly in patients with known acquired immunodeficiencies or iatrogenic conditions (55; 56).

The term candidiasis refers to infections caused by commensal fungi of the *Candida* genus, ranging from superficial infection to invasive candidiasis (56).

Invasive candidiasis (IC) is not limited to bloodstream infections (candidaemia) but includes a variety of deep-seated infections, such as intra-abdominal abscess, peritonitis, or osteomyelitis, with or without candidaemia (55; 56).

A substantial geographical variability in the prevalence of *Candida* spp. exists, even though *C. albicans* continues to be the most prevalent species causing disease in both adult and pediatric populations. Mortality due to candidaemia also depends from the specific patient population (56). An epidemiologic meta-analysis revealed that the European incidence of candidaemia is approximately 79 cases per day, of which an estimated 29 patients might have a fatal outcome on Day 30 (57). *Candida* spp. are the third most frequent cause of infection in Intensive Care Units (ICUs) worldwide and various risk factors are associated with the development of invasive candidiasis in ICU patients, including central venous catheters, treatment with broad-spectrum antibiotics, multifocal *Candida* colonization, surgery, pancreatitis, parenteral nutrition, hemodialysis, mechanical ventilation and prolonged ICU stay (55). During the last three years, IC has been a cause for great concern since several studies show an increment of candidemia incidence and mortality in hospitalized patients with COVID-19 (58; 59; 60).

3.2. Etiology and pathophysiology

Candidiasis, especially the invasive ones, are more often caused by *C. albicans* when perturbations of mucosal microbiota and/or weakening of host immunity occur (56; 61).

Due to the ability to adapt to a wide range of environmental conditions, this opportunistic pathogen could colonize different body districts. Besides superficial candidiasis, invasive candidiasis is an infection characterized by highly severe conditions (Fig. 11) (26).

Three major conditions predispose *Candida* spp. to invasive infection: long-term and/or repeated use of broad-spectrum antibiotics since antibiotics confer a selective advantage over commensal gut microbiota; breach of the gastrointestinal and cutaneous barriers which enable commensal *Candida* spp. to translocate from mucocutaneous sites into the bloodstream; iatrogenic immunosuppression as, impairing innate immune defenses in the tissues, facilitates *Candida* spp. invasion from the bloodstream into organs such as the liver, spleen, kidneys, heart, and brain (56).

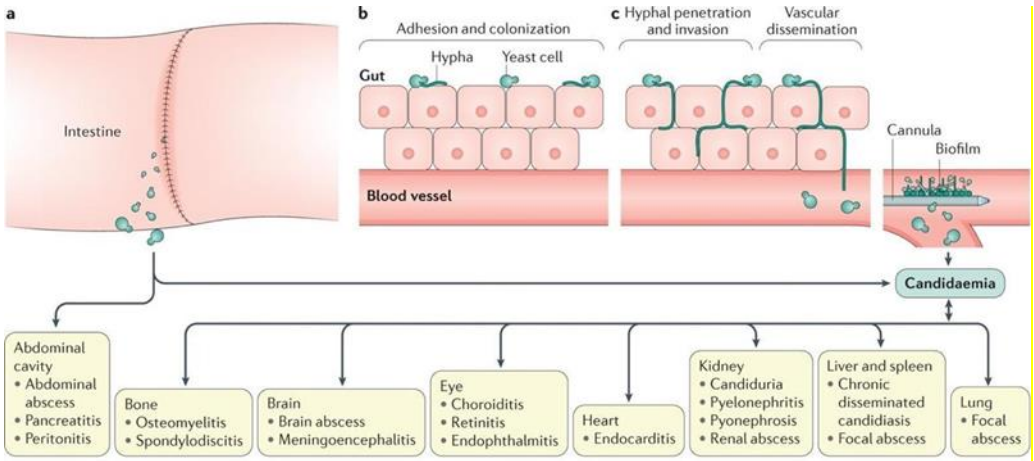

Fig. 11 - Pathogenesis of invasive candidiasis (Adapted from Ref. 57).

3.3. Pharmacological treatment of candidiasis

The similarity between fungal and human cells makes it difficult to identify molecules that specifically target the microbial cell without damaging the host, drastically reducing the therapeutic option for the treatment of fungal infections (62).

The classes of antifungals currently available include azoles, polyenes, echinocandins, pyrimidine derivatives, and allylamines. Even though azoles are the most used, different antifungal agents may be used for the treatment of IC depending on the patient's condition, including azoles (fluconazole, itraconazole, isavuconazole, posaconazole, and voriconazole), polyenes (amphotericin B and its lipid formulations) and echinocandins (caspofungin, anidulafungin, and micafungin) (63).

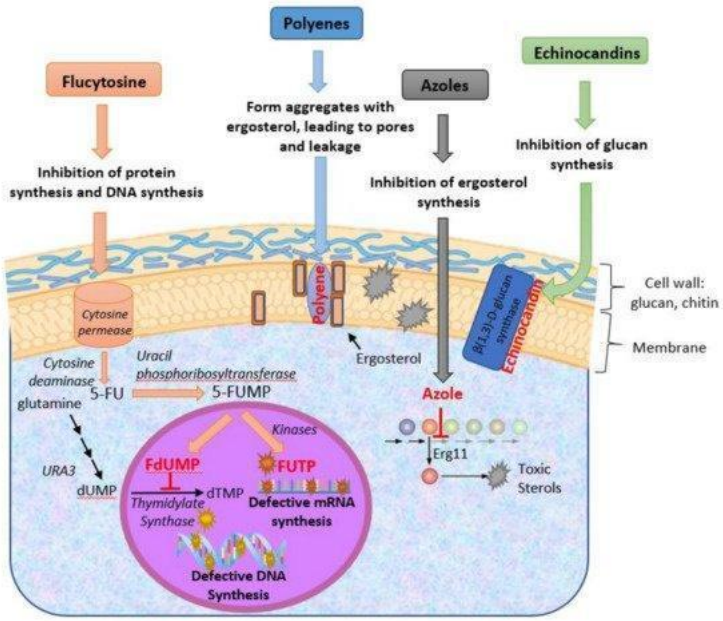

Fig. 12 - Mechanisms of action of the different classes of antifungals available for the treatment of candidiasis (Adapted from Ref 63).

3.3.1. Azoles

Azoles interfere with ergosterol synthesis by interacting with the enzymes of the cytochrome demethylase system of the fungal cells and disrupting the

oxidative membrane enzymes. Specifically, all azoles act by inhibiting the activity of the lanosterol-14α-demethylase enzyme Erg11 resulting in abnormal sterol retention, incomplete cell wall formation, retention of intracellular phospholipids, and ultimately fungal cell death (Fig. 12) (63). The first azoles used in clinical practice were three imidazoles: clotrimazole and miconazole (1969), followed by ketoconazole (1981) (Fig. 13). However, the use of imidazoles was limited by their inhibitory effect on the human hepatic CYP enzymes. Thus, in the early 90s they have been replaced by triazoles, among others fluconazole, itraconazole, the fluconazole-derived voriconazole (used for the treatment of IC caused by fluconazole-resistant species), posaconazole, isavuconazole (Fig. 13) (62; 63). Triazoles display many advantages over the imidazole ring, including increased polarity and improved solubility, reduced binding to plasma proteins, and increased specificity (62; 63). However, although reduced, triazoles also have an inhibitory effect on the cytochrome P450 of the mammalian enzymes system. Consequently, their oral and/or parenteral intake often leads to multiple side effects (62; 63). To date, imidazoles are mainly used for treating superficial candidiasis, while triazoles are preferred for treating invasive candidiasis (62).

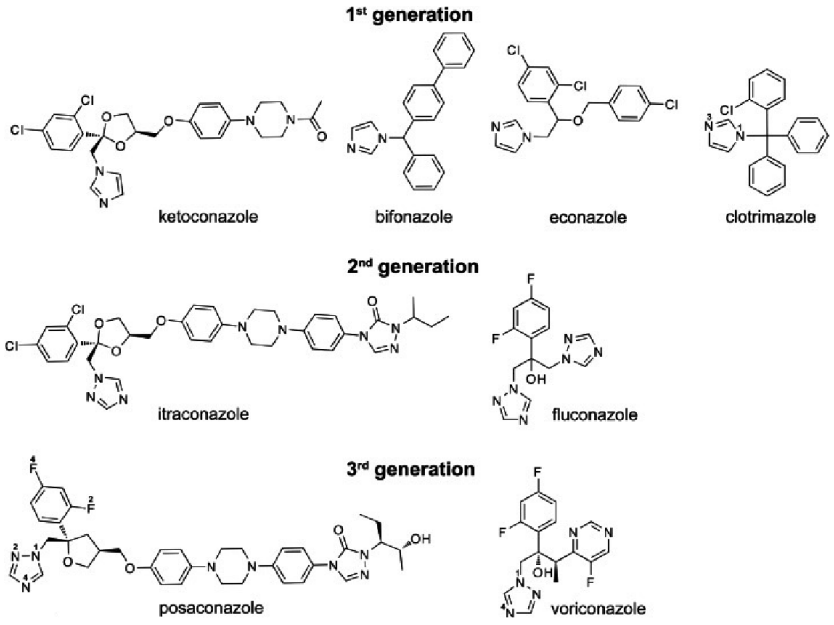

Fig. 13 - Chemical structures of the three generations of antifungal azoles (Adapted from Ref. 64).

3.3.2. Polyenes

Several polyene antifungal agents have been discovered, but only a few are practically used due to problems of solubility, stability, absorption, and toxicity (63). The most largely used polyenes are amphotericin B, the first antifungal developed for the treatment of disseminated candidiasis, and nystatin, used to treat oral infections (Fig 14) (62). Because of the high lipophilicity, all polyenes can penetrate the plasma membrane's phospholipid bilayer and quickly attach to sterols, especially ergosterol promoting the formation of pores (Fig. 12) (62; 63). Despite the potent effect of amphotericin B, its use is limited by its nephrotoxicity (62). Several formulations to vehicle this drug have been developed, mainly based on the use of liposomes, but their use is limited to second-line therapy due to the high cost (62).

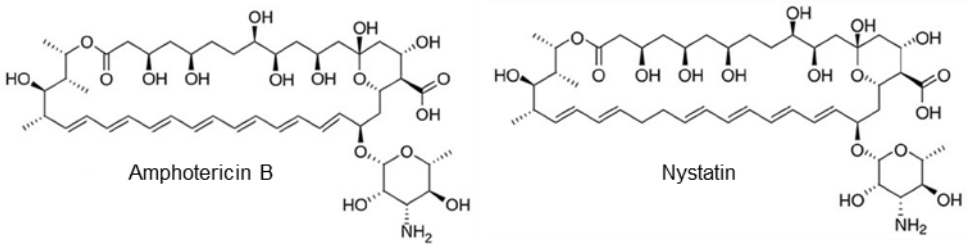

Fig. 14 - Chemical structures of amphotericin B and nystatin.

3.3.3. Echinocandins

The youngest antifungals are the echinocandins, which display fungicidal activity against many fungi, including *Candida* species, with few side effects compared to polyenes and azoles (62; 65). Echinocandins are secondary metabolites of fungi composed of a cyclic hexapeptide and lipid residues responsible for their antifungal activity (65; 66). Echinocandins act by blocking the cell wall synthesis by inhibiting Fks1, the catalytic subunits of β-(1,3)-d-glucan synthase, responsible for the elongation of (1,3)-β-d-glucans. The loss of β-(1,3)-d-glucan in the cell wall makes the cells highly susceptible to lysis (Fig. 12) (62).

Currently, they are commercially available in three forms: caspofungin, anidulafungin, and micafungin (Fig. 15). Caspofungin is a semisynthetic water-soluble lipopeptide, a derivative of the naturally pneumocandin B_0 produced by *Glarea lozoyensis* and is used to treat esophageal candidiasis, peritonitis, intra-abdominal abscess, and cavity infections caused by *Candida* spp. (66). Micafungin is formed by enzymatic deacylation of a natural hexapeptide derived from *Coleophoma empetri* used to treat patients affected by esophageal candidiasis. Also, it is employed as a prophylactic treatment against *Candida* infections in patients affected by neutropenia during hematopoietic stem cell transplantation (63; 66).

Micafungin has even been approved for pediatric patients > 4 months and patients under 4 months in case of invasive candidiasis (66). Anidulafungin is

a semi-synthetic derivative of echinocandin B, a fermentation product of *Aspergillus nidulans* used to treat esophageal candidiasis, candidemia, and deep-tissue candidiasis (66).

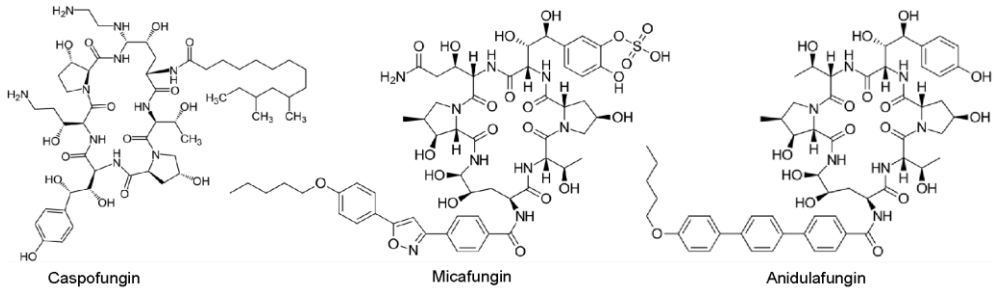

Fig. 15 - Chemical structures of commercially available echinocandins.

3.3.4. Flucytosine

The pyrimidine derivative 5-fluorocytosine (5-FC) exhibits a broad spectrum of activity against common pathogenic yeasts with a unique mode of action among all antifungal agents, as it targets DNA, RNA and protein synthesis (67). 5-FC is a prodrug that enters fungal cells through cytosine transporters and is then metabolized via the pyrimidine salvage pathway to 5-fluorouracil (5-FU). The latter is converted to 5-fluoro-uridylate (5-FUMP), phosphorylated by two specific kinases to 5-fluoro-UTP, and then incorporated into the RNA, causing premature chain termination. Furthermore, it is reduced to 5-fluoro-2′-deoxyuridylate, which inhibits the thymidylate synthetase, an enzyme essential for DNA synthesis. This antifungal also displays good selectivity since mammalian cells lack the enzyme cytosine deaminase responsible for the conversion of 5-FC to 5-FU (62; 67).

However, gastrointestinal side effects such as nausea, diarrhea, vomiting, and diffuse abdominal pain, but even more severe side effects such as hepatotoxicity and bone-marrow depression have been reported in patients under 5-FC therapy (67).

Due to its toxic effects, possibly explained by the ability of bacteria living in the human gut to convert 5-FC into 5-FU efficiently, 5-FC is used only in low concentration and in combination with other antifungals (62).

3.3.5. Allylamine

The allylamines are synthetic antifungals that target another critical biosynthetic enzyme involved in ergosterol synthesis, the squalene-2,3-epoxidase (Fig. 16) (68).

Unlike 14-α-sterol demethylase, the enzyme squalene epoxidase is not part of the CYP450 enzymes; hence allylamines have greater specificity than azoles (68).

Squalene epoxidase is the first enzyme in the biosynthesis pathway involved in the conversion of squalene to squalene epoxide resulting in an accumulation of the sterol precursor and inhibition of ergosterol synthesis (Fig. 16) (69).

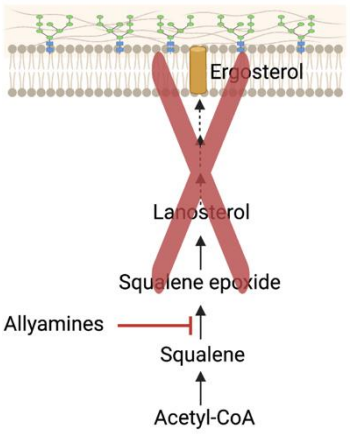

Fig. 16 - Allylamines mechanism of action (Created with BioRender.com).

Representative examples of allylamines include terbinafine, naftifine, and butenafine (Fig. 17), typically formulated as powders or creams for the treatment of cutaneous infections or in the form of oral preparations. Terbinafine has a fungicidal effect and is the only approved oral drug for the

treatment of onychomycosis, although its oral bioavailability is around 50% due to first-pass metabolism (68; 69).

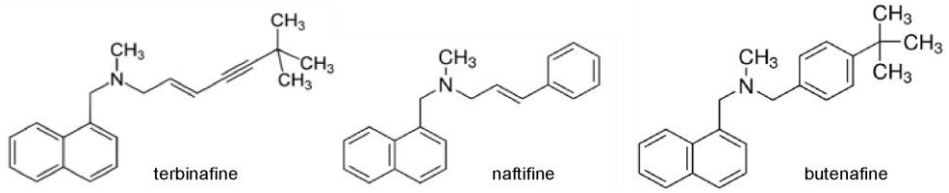

Fig. 17 - Chemical structures of representatives allylamine.

3.4. *C. albicans* antifungal resistance

The increasing antifungal resistance or tolerance further reduces the available therapeutical options for the treatment of candidiasis.

Three types of antifungal resistance have been described: primary or intrinsic, secondary or acquired, and clinical resistance. While the intrinsic resistance is exhibited independently from the exposure to antifungals, the acquired and clinical resistance require the exposure of the fungus to the drug and consequent development of mechanisms of adaptation and/or genetic alterations leading to drug tolerance (70). Specifically, microbiological resistance refers to nonsusceptibility of a fungus to an antifungal agent *in vitro*, whereas clinical resistance is the persistence or progression of an infection despite the appropriate therapy with antifungal with the effective activity *in vitro* (70). Clinical resistance can be attributed to a combination of factors, related both to the host and the pathogen and cannot be predicted (70).

3.4.1. Azole resistance

Azoles are the largest class of antifungal drugs in clinical use, and different mechanisms of azole resistance have been described in *Candida* spp. (70; 71).

These mechanisms include the up-regulation of drug transporters, overexpression or alteration of Erg11, and mutations in the *ERG11* gene (Fig. 18) (71; 72).

The ATP-binding cassette (ABC) transporters and the major facilitator (MF) transporters are the two classes of pumps mainly involved in regulating the accumulation of azoles inside the yeast cell (Fig. 18) (70). ABC pumps consist of two membrane-spanning domains (MSD) and two nucleotide-binding domains (NBD) and are active transporters requiring ATP as an energy source (71). The ABC transporters Cdr1 and Cdr2, whose expression is regulated by transcription factor Tac1, have been well documented as drivers of azole resistance (70; 72).

Azole resistance is often associated with Gain of Function (GOF) mutation in *TAC1* resulting in a constitutive increased expression of Cdr1 and Cdr2 (70; 72).

In contrast, MFS-transporters do not have the NBDs characteristic of ABC-transporters and require a proton gradient of the plasma membrane as an energy source to transport xenobiotics. Among MFS transporters, Mdr1 is a major player in fluconazole and voriconazole resistance (72). The GOF in the multidrug-resistant regulator (*MRR1*) transcription factor, regulating *MDR1* expression, followed by loss of heterozygosity, represents the main cause of *MDR1* overexpression associated with azoles resistance in *C. albicans* (71; 72). Azole resistance could also be related to altered ergosterol biosynthesis resulting from mutation and/or overexpression of ergosterol pathway genes. Overexpression of *ERG11,* encoding the target enzyme Erg11, is linked with azoles resistance in many fungi and is the consequence of point mutations affecting the azole binding in the active site of the enzyme (Fig. 18). Otherwise, *ERG11* up-regulation can result from GOF mutation in *UPC2,* encoding the transcription factor Upc2 that regulates the majority of ergosterol biosynthetic genes, or can be due to amplification of the copy number of the gene (71; 72).

Point mutations in *ERG3*, encoding the C5- sterol desaturase enzyme Erg3 are also associated with azole resistance, as well as the down-regulation of *ERG6* (71). Another mechanism of azole resistance has been described more recently: sterol import. Since azoles lower the ergosterol levels of the cell, *Candida* spp. and other fungi developed strategies to improve exogenous sterol import. Notably, while most fungi import sterols under anaerobic or microaerophilic conditions, *C. albicans* imports sterols aerobically, thus developing resistance by importing cholesterol and serum from the blood (Fig. 18) (71). Finally, genomic variations, including loss of heterozygosity (LOH) and aneuploidy, are linked with azole resistance in fungi. LOH correlated with increased resistance has been observed in *TAC1*, *ERG11*, and *MRR1*, in clinical isolates of *C. albicans* (71). Likewise, chromosomal alterations, such as aneuploidies and trisomies, are often observed in azole-resistant clinical isolates (Fig. 18) (71).

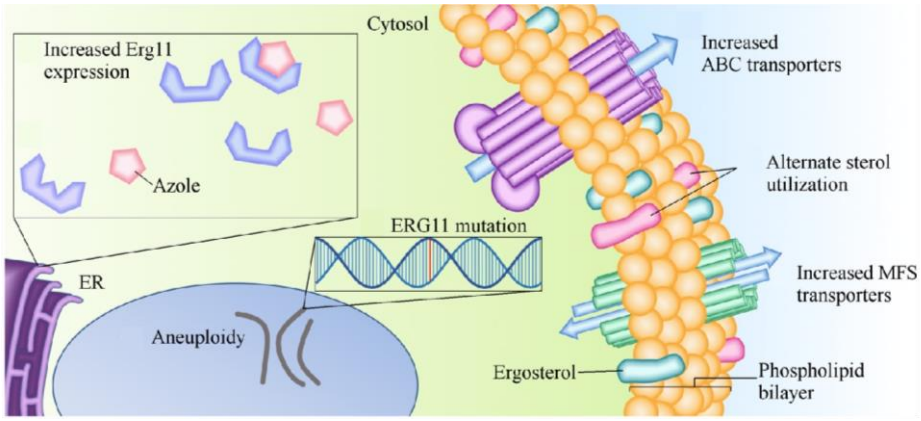

Fig. 18 - Known azole resistance mechanisms in *C. albicans* (Adapted from Ref. 72).

3.4.2. Resistance to other antifungal drugs

Resistance to polyenes, particularly to Amphotericin B, is relative unusual and results from mutations in *ERG3* and *ERG6* genes, even though polyene resistance in clinical isolates has not been fully characterized yet (Fig. 19a) (70; 71). In contrast, several studies highlight the mechanism of echinocandin resistance, which is often linked to mutations in *FKS1* and/or *FKS2*, the two homolog genes encoding for the target enzyme β-1-3 glucan synthase (Fig. 19b) (70; 71). In particular, mutations in *FKS1*, clustered in two regions, have been observed in echinocandin-resistant clinical isolates of *C. albicans*, whereas mutations in *FKS2* cause echinocandin resistance in *C. albicans* in *vitro* only (71).

Other phenomena trigger echinocandin resistance in *C. albicans*, such as chromosome anomalies and, in particular, chromosome 2 trisomy, although the specific mechanism behind that is still unclear (Fig. 19b) (71). Finally, point mutations in the *FCY2* gene, resulting in decreased activity of the cytosine permease Fcy2, as well as mutations in the enzyme uracil phosphoribosyltransferase (Fur1), lead to resistance to 5-Fluocitosine in *C. albicans* (Fig. 19c) (70; 71).

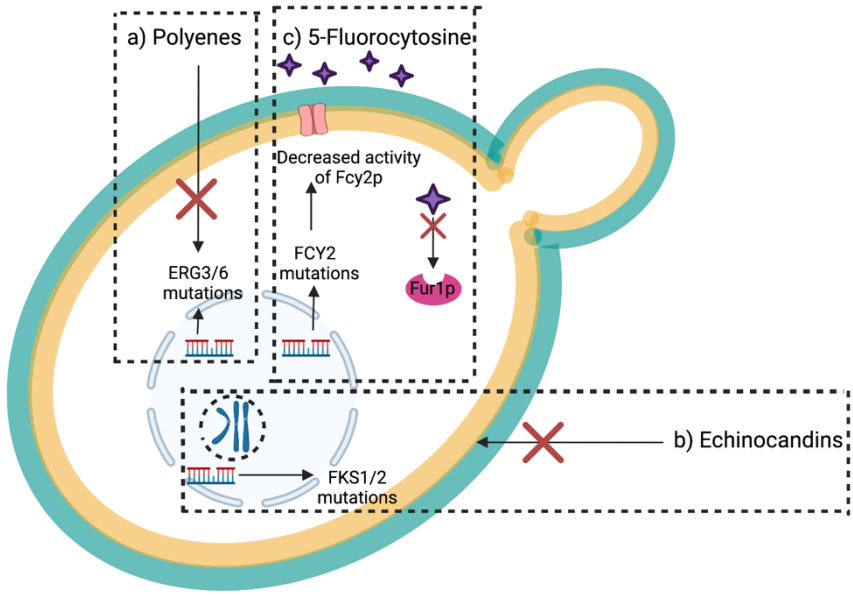

Fig. 19 - Schematic representation of known antifungal resistance mechanisms in *C. albicans*
(Created with BioRender.com).

3.4.3. Tolerance pathways contributing to drug resistance

Antifungal exposure, a stress factor for *Candida* cells, induces several cellular responses involving different signaling pathways (70).

cAMP- PKA signaling pathway mainly mediates the stress responses associated with azoles exposure since it is required to facilitate the adaptation to various stress conditions, like fluconazole exposure. Specifically, *CDC35* (encoding the adenyl cyclase enzyme) and the cyclase-associated protein Cap are the leading players in azole tolerance, as disruption of both genes results in hypersusceptibility to azoles in *Candida* spp. (70).

In *C. albicans*, the heterodimeric phosphatase calcineurin is also required for survival in the presence of antifungal drugs, especially fluconazole. Indeed, calcium-activated-calcineurin reduces the efficacy of fluconazole both in *vitro* and in *vivo* through the activation of the transcriptional factors Crz1 via Rta2 (70). In echinocandin drug tolerance, cell wall integrity signaling mediated via PKC, as well as calcineurin and Hsp90, have a central role (70).

Several studies showed that the compensatory increase in chitin synthesis following the inhibition of the β-(1,3)-glucan synthesis is mediated by the PKC, Ca2+-calcineurin, and HOG signaling pathways, resulting in high-chitin *C. albicans* cells that are less susceptible to echinocandins (70). Moreover, rearrangements of chromosome 5 may be involved in earlier tolerance development, resulting in changes in the expression of three genes on the right arm of Ch5: *CHT2*, implicated in cell remodeling, *CNB1*, and *MID1*, which belong to the calcineurin stress response-signaling pathway (70).

Chapter IV: *Candida albicans* – host interactions

4.1. *C. albicans* commensalism

Candida spp. are acquired during or near birth, becoming a significant part of the host microbiome (38). There are no detailed studies on *C. albicans* – host interaction focused on commensalism, although it is known that *C. albicans* establishes different kinds of relationships with the human host continuously interacting with epithelial cells, and it must be able to compete or cooperate with other members of the host microbiota too (38; 39; 73).

It is widely accepted that commensalism requires a homeostatic relationship among fungus, resident microbiota, and host immunity, and the balance perturbations lead to pathogenicity (74). Moreover, a recent study highlighted the role of the phosphate transporter Pho84 in promoting *C. albicans* commensalism, suggesting that other mechanisms might be involved in commensalism regulation. In particular, the study demonstrates that Pho84 triggers the induction of the transcription factor Try4, which regulates the expression of genes required for fungal commensalism via Pi uptake and Torc1 activation (75). Thus, colonization of *C. albicans* host niches likely depends on both intrinsic (i.e., gene regulation, cell morphology, adaptation) and extrinsic factors (i.e., competitive microbiome, diet, and host immune status) (74).

4.2. Interaction with host immune cells

The *C. albicans* cell wall components play a central role in host-pathogen interactions (73). The innate immune responses elicited during *Candida* infections are very different, although the majority are mediated by the interaction between Pattern Recognition Receptors (PRRs) expressed on the surface of innate immune cells and Pathogen Associated Molecular Patterns (PAMPs) on the fungal surface (76).

C-type lectin receptors (CLRs), RIG I-like receptors (RLRs), NOD-like receptors (NLRs), and Toll-like receptors (TLRs) are the main families of receptors involved in recognition of *C. albicans* PAMPs (76). *C. albicans*-host interaction depends on innate immune cells morphotypes and *C. albicans* morphology. Indeed, each innate immune cell has a distinct repertoire of receptors and interacts differently with the yeast or the hyphae since hyphae generally have less β-glucan exposed on their cell surface and, consequently, are less successfully recognized by Dectin-1 (76).

The hyphal orientation also influences phagocytosis, which occurs faster when macrophages encounter hyphal tips (76). Cell wall remodeling, and consequent masking/unmasking of PAMPs, is a key process in innate immune response controlled by *C. albicans*. Despite β-glucan - Dectin-1 recognition, also mannoproteins are targets of PPRs, and their exposure may be regulated in response to environmental stimuli (77). Neutrophils are the primary immune cells involved in controlling candidiasis, and the C-type lectin receptor Dectin-1 is the most critical neutrophil PRR in *C. albicans* recognition. (76). Also, tissue-resident macrophages (TRMs) are involved in *C. albicans* recognition in various niches since they function as the first line of defense against pathogens, while dendritic cells represent a bridge between the innate and acquired immune systems being specialized in presenting antigenic material from *Candida* to lymphocytes (76; 78). These innate immune cells recognize *C. albicans* by its cell wall PAMPs too: β-1,3-glucan is recognized by Dectin-1 and complement receptor 3 (CR3); N-mannan by Dectin-2, DC-SIGN, and MINCLE; and O-mannan by TLR4 (Fig. 20) (76).

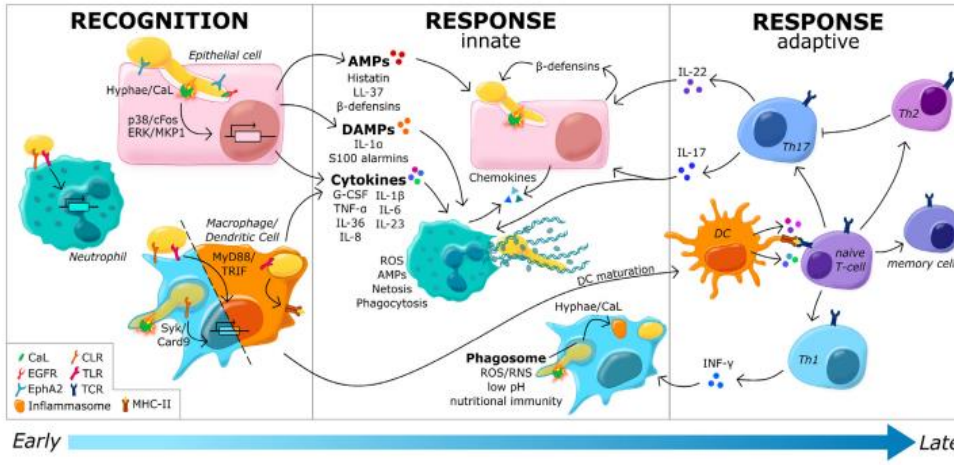

Fig. 20 - Schematic representation of immune recognition and responses against *C. albicans* (Adapted from Ref. 79)

PAMPs recognition initiates phagocytosis, which involves two main stages: phagosome formation and maturation. Phagosomes are formed upon binding of phagocytic receptors (i.e., CR3, Fcγ receptors (FcγRs), and Dectin-1) to phagocytic targets resulting in receptor clustering. Thus, the phosphorylation of their immunoreceptor tyrosine-based activation motifs (ITAM) and the subsequent activation of Rho-family GTPases activate nucleation-promoting factors, causing actin-driven protrusions from the plasma membrane to advance around the target (76). Phagosome maturation is a gradual process that differs between neutrophils and macrophages; even though, in both cases, it establishes a hostile and degradative environment (76). In neutrophils, phagosome maturation occurs quickly and involves fusion with lysosomes and neutrophil granules containing antimicrobial peptides (AMPs) and proteolytic enzymes. On the other hand, in macrophages, endosomal fusion is driven by the recruitment of active Rab5 and then Rab7 and begins early during phagosome maturation. Thus, lysosomes fuse with late phagosomes to form a phagolysosome armed with lytic enzymes and highly acidic (76). Finally, dendritic cells regulate their phagosomal contents for partial degradation since they prioritize antigen presentation, so ROS production is maintained at low

levels by the recruitment of NADPH oxidase Nox2 (76). The recognition of *C. albicans* by macrophages or epithelial cells results in the release of proinflammatory cytokines such as TNF-α, IL-1β, and IL-6, enhancing clearance and neutrophils recruitment (Fig. 20) (76). The latter represent critical players in *Candida* clearance by releasing proinflammatory cytokines such as TNF-α and IL-12 and inducing ROS oxidative *C. albicans* killing and non-oxidative killing by producing AMPs such as lactoferrin and β-defensins (Fig. 20) (76; 79; 80). Furthermore, the formation of neutrophil extracellular traps (NETs) and dendritic cell recruitment and activation significantly contribute to the resolution of infection (Fig. 20) (76). Nevertheless, recent studies showed that extracellular trap formation (ETosis) could also be induced in macrophages in the presence of *C. albicans,* triggering the formation of macrophages extracellular traps (METs) similar in functions and composition to NETs (81). Following innate immunity, DCs drive T-cell response in antifungal immunity activating the differentiation of T-lymphocytes into $CD4^+$ and $CD8^+$ (Fig. 20). Antigen presentation to MHC II triggers the differentiation of $CD4^+$ into Th1, Th2, Th17, Treg, nTh17 and γδ T-cells, even though Th1 and Th17 responses are considered the most successful adaptative immunity defense against *C. albicans* infections and allow the maintenance of tissue homeostasis (80).

MHC could also present antigenic peptides I to $CD8^+$ cells but the direct killing by $CD8^+$ T-cells is not well characterized yet. However, several studies suggest that $CD8^+$ T-cell response has an essential role in controlling fungal infections (80, 82).

By contrast, antibody response plays a minor role in immunity against candidiasis since B-cell deficient mice did not show increased susceptibility to *C. albicans* infections (80).

4.3. Host immune escaping

Being a common member of the microbiome, *C. albicans* has developed mechanisms to anticipate and protect itself against immune attacks during co-evolution with its host.

To date, several mechanisms have been discovered through which *C. albicans* is able to reduce recognition by immune cells, decrease the efficacy of killing mechanisms and escape immune cells following engulfment (79). As mentioned above, after recognition, phagocytes engulf *C. albicans* cells, entrap them within the phagosome and expose the fungi to a low pH, a nutrient-limiting microenvironment, and a potent mix of proteases, ROS and RNS, cation fluxes and AMPs. Exposure to this hostile environment triggers significant metabolic changes, allowing the cells to survive inside phagocytes. Experimental evidence suggests that once phagocytized, following the initial up-regulation of high-affinity glucose transporters to import the remaining glucose, *C. albicans* shifts to a starvation mode, with consequent up-regulation of genes for alternative carbon source utilization (83).

Moreover, *C. albicans* has evolved strategies to escape from the phagocyte oxidative burst, so that oxidative stress detoxification and repair proteins are rapidly induced upon phagocytosis by the transcription factor Cap1 and via Hog1 MAPK-pathway (83).

The third important adaptation promoting the survival of the fungus is the ability to form hyphae inside the phagocytes, resulting from the up-regulation of filamentation-associated and core-filamentation genes following engulfment. However, the molecular mechanisms promoting the yeast-to-hyphae transition despite the low phagosomal pH are still unclear (83). Different mechanisms associated with the hyphae development within the phagolysosome help *C. albicans* to evade macrophage killing. *C. albicans* is able to induce direct or indirect membrane damage to the phagocytes by simple

membrane piercing via mechanical force or through the production of the hypha-associated toxin candidalysin (Fig. 21) (79).

More recently, another peculiar escaping mechanism has been proposed. Indeed, several studies suggested that *C. albicans* is able to kill the macrophages by inducing early inflammasome-dependent cell death. This process, named pyroptosis, followed by membrane piercing, results in immune cell disruption (Fig. 21) (83). Finally, a less common event can occur, triggering the escaping from the phagosome, known as non-lytic expulsion or vomocytosis (Fig. 21) (83).

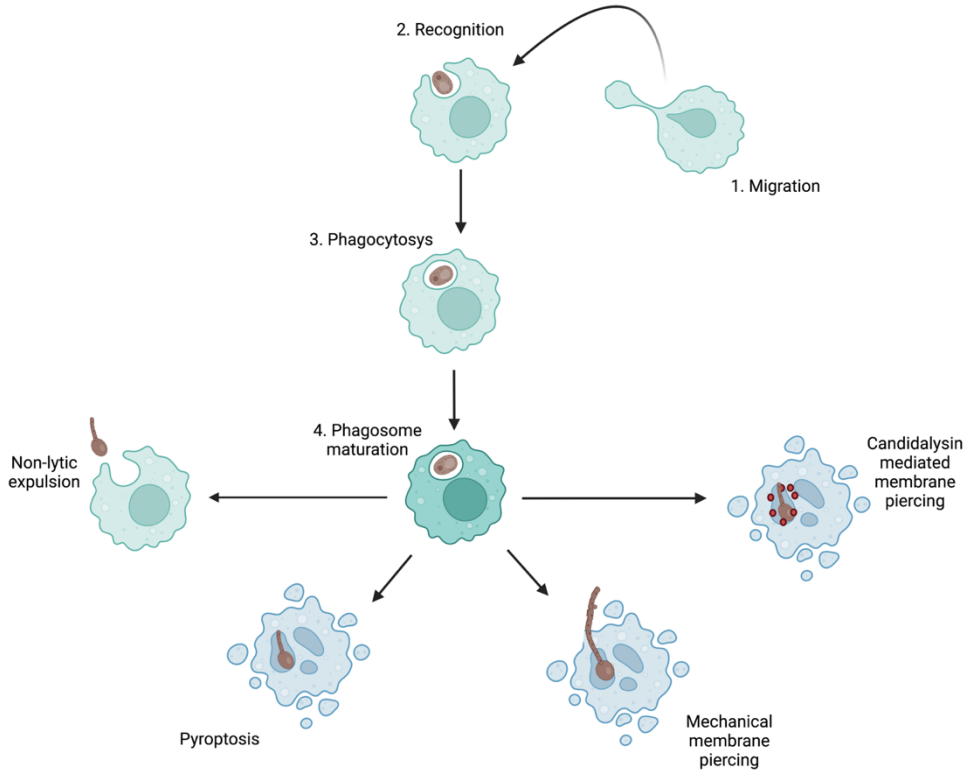

Fig. 21 - Four different mechanisms evolved by *Candida albicans* to escape from phagosome (Created with BioRender.com).

4.3.1. Reducing recognition by immune cells

Besides escaping from phagosomes, *C. albicans* also uses host signals to anticipate the immune attack. Indeed, recent studies showed that the fungus

actively regulates the exposure of PAMPs (i.e., β-1,3-glucan, mannans) by remodeling its cell wall in response to environmental stimuli preventing the recognition and phagocytosis (79).

Hypoxia is a common condition in several host niches. Upon hypoxic condition, *C. albica*ns induces robust changes in both metabolism and cell wall organization. In particular, a reduction in the levels of exposed β-1,3-glucan in response to hypoxia has been observed, resulting in reduced phagocytosis by murine macrophages and decreased cytokine production by human peripheral blood mononuclear cells (hPBMCs) (84). Hypoxia-induced masking depends on proper mitochondrial functioning, and in particular, the ROS processing to hydrogen peroxide within the mitochondria regulates the cAMP-PKA pathway leading to β-1,3-glucan masking (84). Nutrients availability also impacts β-1,3-glucan exposure. Glucose is the primary carbon source in different host niches, but in the lower gastrointestinal tract, short-chain fatty acids and lactic acid are particularly abundant. Recently, Pradhan and colleagues have shown that L-lactate and glycerol induce β-(1,3)-glucan masking while exposure to the short-chain fatty acids acetate or butyrate triggers β-(1,3)-glucan unmasking. Moreover, L-lactate induced masking results in decreased production of pro-inflammatory cytokines, including TNFα and MIP1, by murine macrophages and reduced phagocytosis (85). Two signal transduction pathways are essential in driving L-lactate induced masking. On the one hand, studies demonstrated that masking induced by L-lactate is mediated by the G-protein coupled receptor Gpr1 and the transcription factor Crz1. Gpcr1 and Crz1 both induce the expression of the exo-1,3-glucanase Xog1, which cleaves exposed (1,3)-glucan in the cell wall causing masking. On the other hand, it has been shown that deletions of both *CYR1* and *TPK1* blocked β-(1,3)-glucan masking, suggesting that the cAMP-PKA pathway is needed to induce masking in response to lactate as well (84).

Iron limitation is also correlated with a strong change in β-(1,3)-glucan exposure levels associated with decreased phagocytosis by bone marrow derived macrophages (BMDMs) and reduced secretion of the pro-inflammatory cytokines by hPBMCs. Iron-induced masking is again mediated by the cAMP-PKA pathway, even though a parallel signal transduction pathway involving the iron transporter Ftr1 and the iron-responsive transcription factor Sfr1 contribute to β-(1,3)-glucan masking (84). Finally, changes in pH significantly contribute to cell wall remodeling, and in particular acidic pH is likely to induce β-(1,3)-glucan unmasking, although the mechanism behind this phenomenon is not fully defined yet. Anyway, these changes correspond with enhanced immune recognition and increased phagocytosis by macrophages and neutrophils (84). In addition to cell wall remodeling induced by host stimuli, other factors contribute to β-(1,3)-glucan masking/unmasking, such as exposure to drugs and neutrophil extracellular trap (NET). Both canonical and non-canonical signaling pathways are responsible for inducing changes in *C. albicans* cell wall in response to a wide range of stimuli. In particular, Cek1 and Mkc1 MAPK pathways play a key role in the modulation of β-(1,3)-glucan exposure (84).

4.3.2. Soluble factors promoting host-immune evasion

Enzymes secretion (i.e., proteases and phospholipases) is another critical virulence factor of *Candida* spp. helping in dissemination or immune evasion through host physical barriers degradation (86). Besides candidalysin, SAP-family proteins, lipases, and hydrolytic enzymes responsible for immune host cell damage, recent studies pointed out that *C. albicans* also produces soluble factors interfering with immune homeostasis.

Recently, Luo and colleagues identified the protease Pra1 as a soluble factor involved in complement disruption through CR3 cleaving, thus acting as a fungal master regulator of innate immunity (87). Moreover, an increasing

number of studies speculate a potential immunomodulatory role of quorum sensing molecules (QSMs) typically produced by *C. albicans* cells to communicate with each other. QSMs function as transcriptional regulators binding to receptor molecules when the concentration reaches a cell density-dependent threshold. Quorum sensing (QS) is well-studied in prokaryotes, whereas the first evidence concerning the QS in unicellular eukaryotes come out with the discovery of farnesol as a QSM in *Candida albicans* (88). In addition to farnesol, tyrosol has been reported as a QSM in *C. albicans*. Both these molecules have a defined role in regulating filamentation. Specifically, farnesol inhibits the switch from yeast to hyphae (without effects on cells which already started hyphal development), whereas tyrosol promotes and accelerates hyphal development (89; 90). Nevertheless, some QSMs displayed an immunomodulatory effect on different immune cell morphotypes. In particular, farnesol is likely to modulate host immune recognition in multiple ways, including the regulation of β-glucan remasking in response to alkaline pH (91). Moreover, monocytes and neutrophils exposed to farnesol display increased expression of activation markers and promote the release of proinflammatory cytokines, whereas the exposure of macrophages to E,E-Farnesol secreted by white cells stimulates macrophage chemokinesis, improving macrophages migration through the infection site (92; 93). Finally, farnesol stimulates NETosis via Mac−1 and Tlr2, activating a ROS-dependent NETosis pathway (94).

Chapter V: Epigenetic of *Candida albicans*

5.1. Chromatin: structure and functions

In all eukaryotic organisms, including fungi, genomic DNA is packaged in the nucleus in a compact structure called chromatin. The core of this structure consists of positively charged histone octamers (nucleosomes), and 147 bp of DNA wraps around each nucleosome that, interacting with each other, form a compact 30 nm fiber which is, in turn, further organized into a higher-order structure, namely chromatin (Fig. 22) (95; 96).

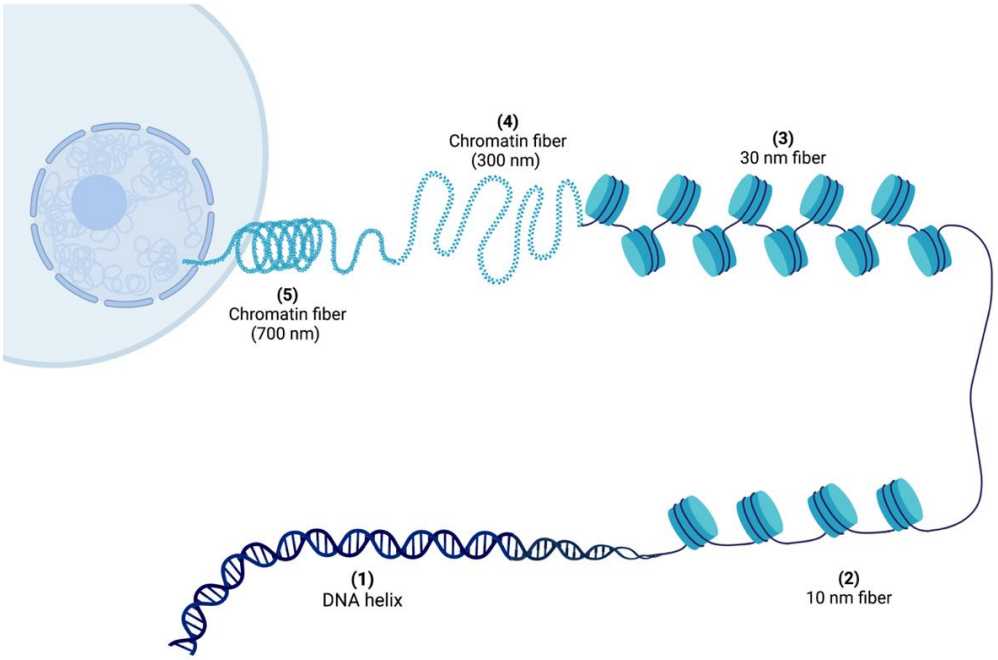

Fig. 22 – Levels of DNA condensation in eukaryotes (Created with BioRender.com).

While highly organized, chromatin is a very dynamic structure since the composition of nucleosomes and histones chemical modifications regulate the topological organization of nucleosomes across the genome (96; 97). Post-translational modifications (PTMs) in histones include acetylation, methylation, phosphorylation, ubiquitylation, acylation, hydroxylation,

glycation, serotonylation, glycosylation, sumoylation, crotonylation and ADP-ribosylation, each derived from metabolism intermediates (Fig.23) (96).

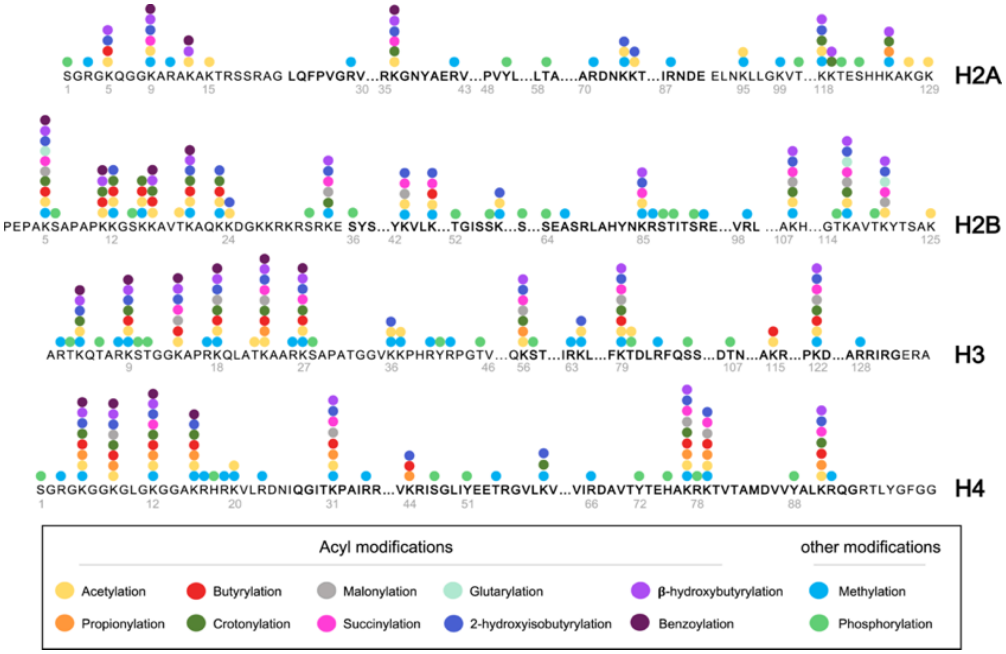

Fig. 23 - Schematic representation of PTMs distribution across the histones (Adapted from Ref. 98)

All histones (H2A, H2B, H3, H4) have a similar structure of the core globular domain, which is highly conserved from yeast to humans, and a disordered but evolutionarily conserved N-terminal tail (99). PTMs are mainly in the tails, although some modifications have also been observed in the histone-core domain and have a crucial role in regulating cell functions, including chromatin packaging, chromosome dynamics, gene expression, DNA replication, DNA repair, DNA damage response, cell cycle control (99).

The histone PTMs are often enriched in specific genomic regions, and their presence regulates positively or negatively the transcription of the gene. With a few exceptions, PTMs in the histone octamer's core directly affect nucleosome structure and trigger chromatin-dependent processes without any

specific reader. By contrast, histone tail PTMs have a limited direct effect on nucleosome stability and chromatin structure, and the downstream biological effect usually requires specific binding proteins (effectors) (100).

5.2. Histone acetylation

Histone lysine acetylation results from the balance between histone acetyltransferases (HATs) and histone deacetylases (HDACs) and is generally considered an active histone mark since neutralizing the positive charge of the lysine residues reduces the binding between histones and negatively charged DNA, resulting in more relaxed and accessible chromatin (101). However, acetylation on specific lysine residues, histone variants, and/or the crosstalk between different histone marks might result in different outcomes (101; 102).

More than 40 different Lys residues can be modified by acetylation within all four histones (Fig. 23), and the cell's metabolic state has a central role in regulating the targets and kinetics of acetylation. Indeed, HATs require acetyl-CoA as a substrate to trigger the addition of the acetyl to the ε-amino group of the Lys side chain, so the global levels of histone acetylation also depend on the abundance of such metabolite (103).

5.2.1. Histone deacetylases

Based on the presence of a conserved deacetylase domain and the dependence on specific cofactors, histone deacetylases are classified into two families: the histone deacetylase family and the sirtuin protein family (104).

The deacetylase family (HDACs) is, in turn, divided into three classes based on sequence similarity to yeast deacetylases: class I HDACs have high similarity with Rpd3 and exhibit an entirely conserved deacetylase domain, class II members are homologous to HDA1 and have a conserved deacetylase domain at their C-terminus, and class IV including only HDAC11 (homologous to yeast Hos3), that shares a catalytic domain with class I and

class II HDACs (104). All three classes HDACs are zinc-dependent and share similar tridimensional structures and catalytic mechanisms. The acetyl-lysine sits in a hydrophobic channel, and a zinc cation sits at the end of the substrate channel coordinated by aspartate and histidine residues. The water's nucleophilic attack on the carbonyl produces a tetrahedral oxyanion intermediate, which finally collapses into free lysine and acetate products (105).

5.2.2. Sirtuin family deacetylases

Class III HDACs belong to the sirtuin family and share homology with the yeast silent information regulator 2 (Sir2). These are NAD-dependent enzymes that exhibit a characteristic deoxyhypusine synthase-like NAD/FAD-binding domain and may localize in the nucleus (Sirt1, Sirt2, Sirt3, Sirt6, and Sirt7), cytoplasm (Sirt1 and Sirt2), or mitochondria (Sirt3, Sirt4, and Sirt5) (104). Sirtuins are evolutionarily conserved in all domains of life and are classified into five classes based on their sequence similarity. Crystallographic studies revealed the presence of a conserved catalytic core domain composed of 275 amino acid residues flanked by variable N- and C-terminal regions. The catalytic core displays an open α/β Rossmann-fold structure, characteristic of NAD^+/NADH-binding proteins, and a smaller globular domain composed of two insertions in the Rossmann fold, one binding a structural zinc ion coordinated by four conserved cysteine residues (Fig. 28) (106).

The active site is in a pocket between the two domains where both NAD^+ and acetyl-lysine substrates are bound (Fig. 24) (106).

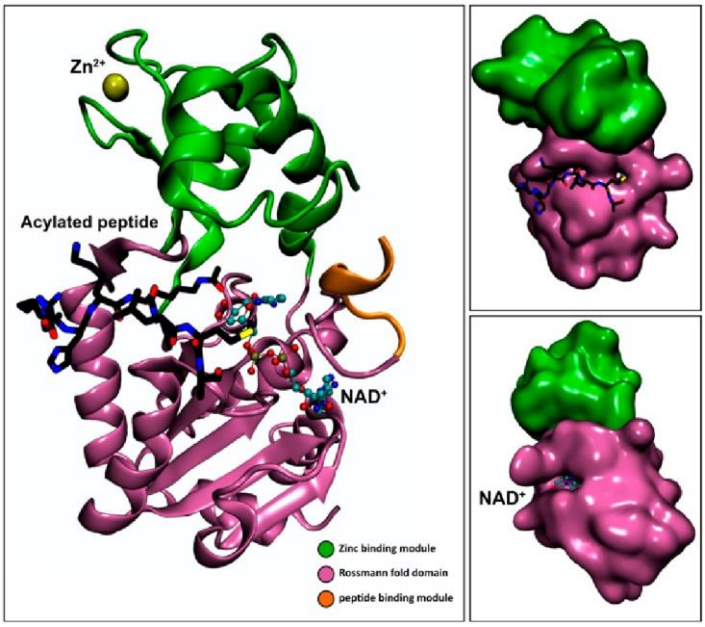

Fig. 24 - Crystallographic structure of *Thermatoga maritima* Sir2 (Adapted from Ref. 106).

The non-Zn^{2+}-binding module of the small Zn^{2+}-binding domain is the most variable region among the different Sir2 homologs and could be crucial for sirtuins substrate specificity, together with other regions distant from the active site and the distinct subcellular localizations (106). Sirtuins are catalytically active only when the lysine-acetylated peptide is correctly positioned inside the binding site, NAD^+ has its nicotinamide ring inside the hydrophobic C pocket with the α face of its N-ribose ring exposed to the acetyl-lysine carbonyl group, and the enzyme is in a closed conformation (106). The general sirtuin catalytic mechanism proceeds in two consecutive stages (Fig. 25).

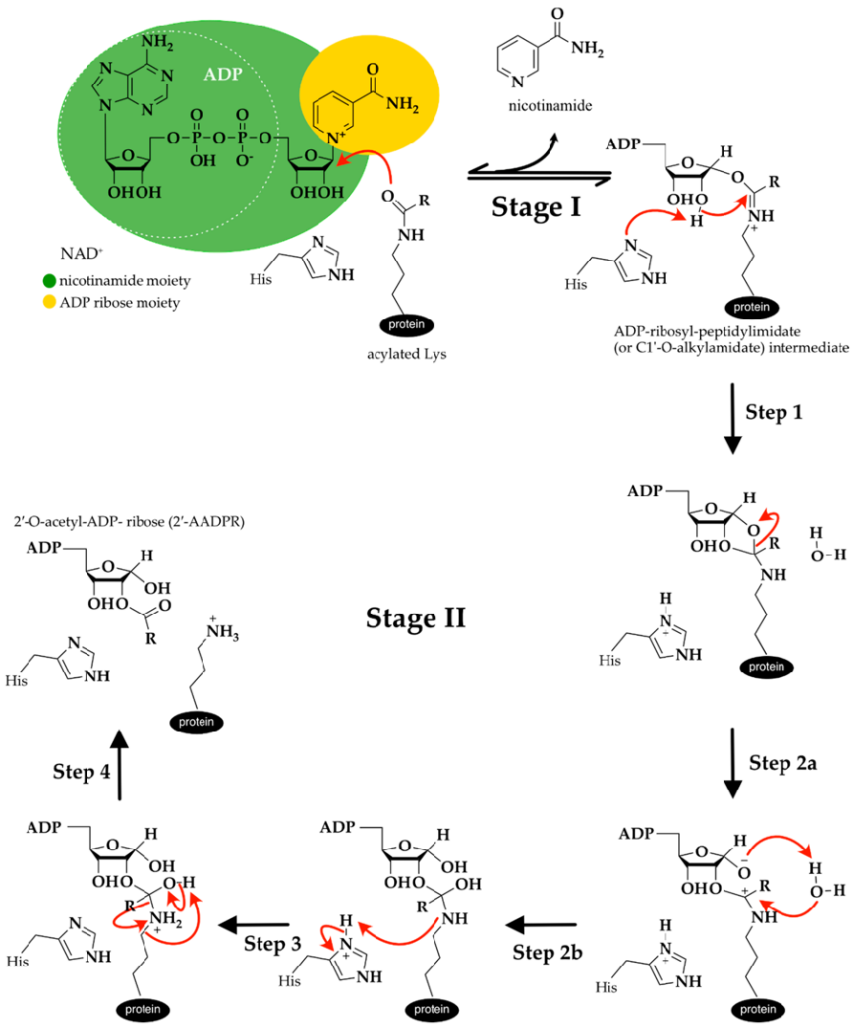

Fig. 25 - Sirtuins catalytic mechanism (Adapted from Ref. 106)

First, acetyl-lysine is ADP-ribosylated following the cleavage of the nicotinamide moiety of NAD^+ and the nucleophilic attack of the side chain of the acetylated lysine to form a positively charged ADP-ribosyl-peptidylimidate intermediate (or C1′-O-alkylamidate) and nicotinamide (Fig. 25). This is a reversible reaction which ensures that NAD^+ is resynthesized in the presence of elevated concentrations of nicotinamide (106).

The second stage starts with the deprotonation of the 2′-OH group by a conserved histidine residue that facilitates the intramolecular nucleophilic

attack of the 2′ hydroxyl and leads to the formation of a bicyclic intermediate that collapses in the presence of a water molecule and generates a tetrahedral intermediate (Fig. 25). Then a proton transfer from the positively charged histidine to the amino group of the tetrahedral intermediate triggers the breakdown of the tetrahedral intermediate into the reaction products, namely the deacylated lysine, the 2′-O-acetyl-ADP- ribose (2′-AADPR) and nicotinamide (Fig. 25).

5.3. *Candida albicans* histone deacetylases

Based on *S. cerevisiae* orthologs, *C. albicans* histone deacetylases have been divided into three groups. Class I and II HDACs are zinc-dependent, whereas Class III HDACs, namely the sirtuin family, are NAD^+ dependent (107). Rpd3, Rpd31, and Rpd32 belong to class I HDACs and are mainly located in the nucleus. Aside from their central role in cell survival and proliferation, these enzymes play an essential role in the development of azole resistance since it has been shown that *RPD3* expression increases during the acquisition of azole resistance and Rpd3 loss results in downregulation of efflux genes. Moreover, Rpd3 is likely to control the expression of *WOR1*, thus regulating the white-opaque switch (107).

Class II HDACs include Hda1, Hos2, and Hos, that commute between the nucleus and the cytoplasm depending on the cellular signals. Among them, Hda1 raised particular interest as the transcription factor Brg1 recruits it to the promoters of hypha-specific genes playing an essential role in establishing a specific chromatin state during hyphal elongation and maintenance (107, 108). Sirtuin family HDACs, composed of Sir2, Sir3, and Hst1–3, were characterized for the first time in *Candida* spp. with the identification of the *SIR2* gene in *C. albicans*, whose product, the Sir2 enzyme is responsible for the deacetylation of H3K9 and H4K16, also crucial for silencing at telomeres and ribosomal genomic regions (108). *HST* genes also belong to Class III

HDACs. Hst1 is a component of the Set3 complex (Set3C), which binds to the coding regions of four master biofilm regulators (*BRG1*, *TEC1*, *EFG1*, and *NRG1*), and has been shown to repress yeast-to-filament transition by attenuating the cAMP/PKA signaling pathway and to activate the white-to-opaque switch (107). Hst3, responsible for hydrolyzing H3K56ac in *C. albicans,* is an essential HDAC since conditional gene repression results in loss of cell viability associated with abnormal filamentous growth, histone degradation, and chromosomal aberrations (107, 109). Interestingly, *HST3* conditional mutants also displayed attenuated virulence in mice models (109).

5.3.1. HATs/HDACs as potential antifungal targets

Given the pivotal role of histone acetylation/deacetylation balance in *C. albicans* growth and/or virulence, HATs and HDACs represent promising targets for developing new antifungal drug. To date, various natural and synthetic antifungal compounds inhibiting HATs activity in *C. albicans* have been identified, and most of them also displayed an inhibitory effect on cell growth and biofilm formation (107).

Nevertheless, most studies focus on HDACs, inspired by mammalian studies where different HDACs inhibitors have been developed against cancers and immune diseases (107). Several known HDACs inhibitors have already been explored to identify the best compounds with antifungal activity (Fig. 26). However, possible side effects should be considered since HDAC inhibitors may also affect human enzymes, not only those from *C. albicans* (107).

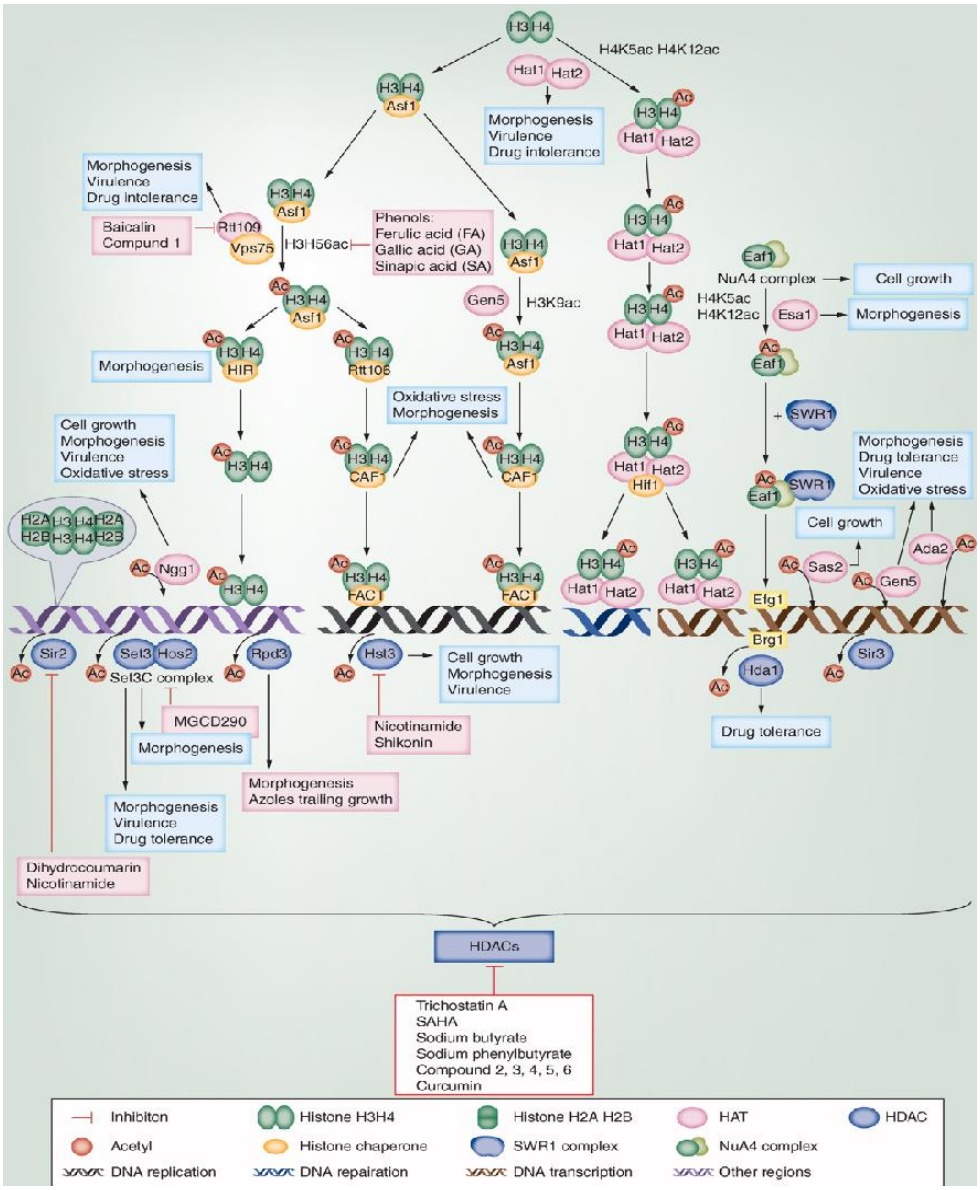

Fig. 26 - Histone acetylation/deacetylation in *Candida albicans* and antifungal compounds interfering with enzymes in these pathways (Adapted from Ref. 107).

Thus, targeting histone acetylation/deacetylation is an excellent perspective for developing new antifungal therapies, but the selectivity of such potential antifungals remains a challenge.

In this scenario, Hst3 represents a good therapeutic target since fungal enzymes that regulate H3K56ac levels diverge significantly from their human

counterparts (SIRT1 and SIRT2) (Fig. 27) and have higher substrate specificity (109).

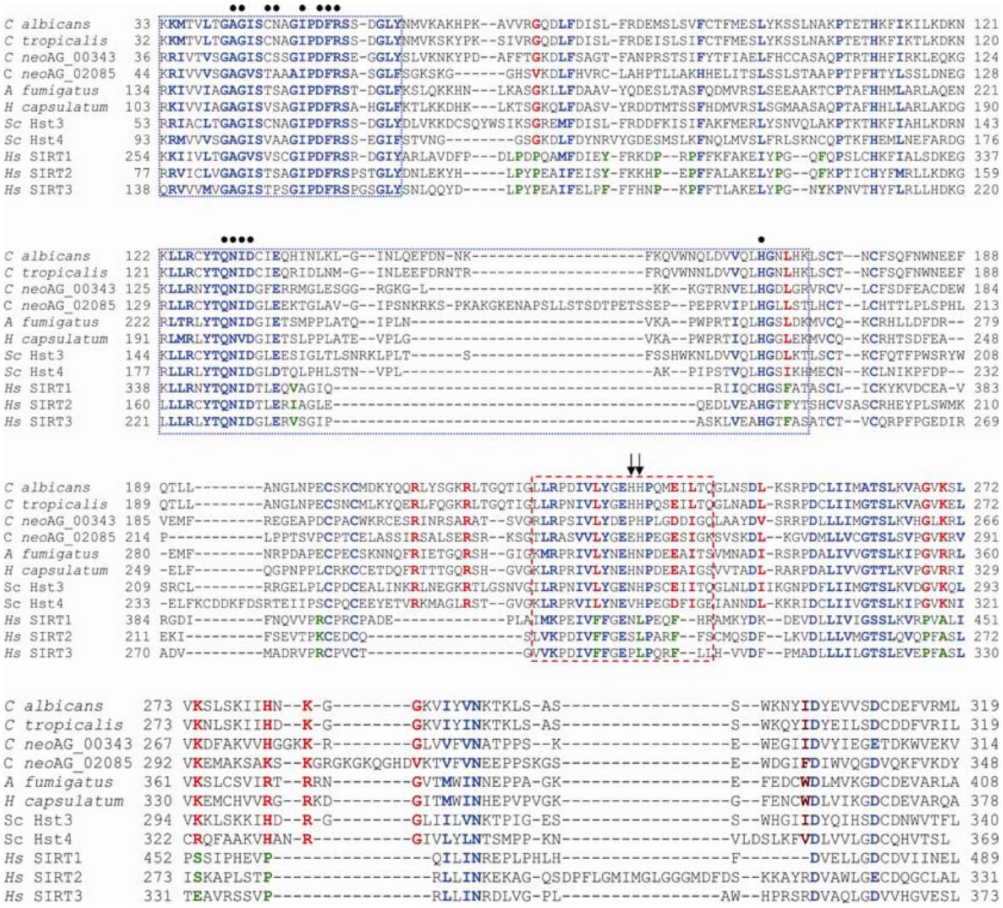

Fig. 27 - Hst3 orthologs and human sirtuins sequence alignment showing important sequence motif not shared between pathogenic fungi and human. The alignment is restricted to catalytic cores. Residues in red and brown are conserved among Hst3p family members; by contrast, residues in green are conserved among human class I sirtuins. The red box includes residues that bind acetylated peptides, and arrows show the residues implicated in peptide substrate selection. Black dots indicate the residues which directly interact with NAD^+
(Adapted from Ref. 109).

AIMS OF THE PhD PROJECT

The polymorphic fungus *Candida albicans* is the major human opportunistic fungal pathogen with a mortality rate of about 40%. The ability of *C. albicans* to adapt and proliferate in hostile environments, as well as the dynamic morphological transition from the yeast to the filamentous one, represent the most noticeable determinants of virulence.

An important clinical problem concerns the emergence of fungal strains resistant to the main antifungal drugs (including polyenes, azoles, echinocandins, and 5-Flucytosine), which drastically reduces therapeutic options. Epigenetic writers and erasers have emerged as promising targets in different contexts, including the treatment of fungal infections.

An increasing number of studies revealed that PTMs play a central role in regulating *C. albicans* virulence and morphological phenotype transition.

In *C. albicans*, H3K56 acetylation is the most abundant PTM whose homeostasis is dynamically regulated by the acetyltransferase Rtt109 and the sirtuin Hst3. The latter is an essential sirtuin for the viability and virulence of *C. albicans*. Since the Hst family proteins diverge significantly from their human counterparts, hst3 represents a unique and interesting target for developing new antifungals. However, little is known about the roles played by H3K56 acetylation dynamics.

Therefore, the present Ph.D. project aimed to highlight the molecular mechanisms behind Hst3-mediated epigenetic regulation. In particular, the non-specific sirtuin inhibitor nicotinamide (NAM) was used to evaluate the effect of Hst3 inhibition on *C. albicans* virulence and host immune escape.

Starting from preliminary results showing an alteration of normal morphological transitions following Hst3 inhibition, we investigated the effect of H3K56 acetylation levels on molecular pathways involved in the morphological switching of *C. albicans.*

Another peculiar characteristic of this opportunistic pathogen is the ability to escape or prevent the attack of innate immune cells. Indeed, during co-evolution with its host, *C. albicans* has developed mechanisms to protect itself against immune response. Specifically, the modulation of PAMPs exposure, the secretion of hydrolytic enzymes, and escaping from phagosomes are well characterized mechanisms of host immune evasion. Nevertheless, several studies highlighted the emerging role of QSMs in influencing innate immune cells. In this context, we evaluated the effects of Hst3 inhibition in host immune escaping and analyzed the molecular pathways regulated by H3K56ac during infection conditions.

In addition, since Hst3 represents a unique and interesting target for developing new antifungals, the present Ph.D. project aimed to set up an expression system to purify the recombinant protein to perform enzymatic assays to be used for the screening of new potential inhibitors.

MATERIALS AND METHODS

6.1. Chemicals

NAM was purchased by Sigma-Aldrich. For all the experiments, 2 M NAM in ultra-pure distilled water was used as stock and added to cultures to obtain the required concentrations. Sirtinol, SirReal2, and Inauhzin, purchased from Selleckchem, were dissolved in dimethylsulfoxide (DMSO) (Sigma-Aldrich, Milan, Italy).

6.2. Fungal strain and growth conditions

C. albicans wild-type strain SC5314 (ATCC-MYA-2876) was routinely cultured on YPD (1% Yeast extract, 2% Peptone, 2% Dextrose) agar plates and propagated in liquid YPD medium overnight at 25°C at 200 rpm. Depending on experimental conditions, *C. albicans* was grown in synthetic YNB medium (0.17% Difco Yeast Nitrogen Base, without amino acids and ammonium sulfate), supplemented with 2% glucose and 0.5% ammonium sulfate; M199 medium containing Earle's salts and glutamine (Sigma-Aldrich), buffered at pH 7.5 with 25 mM HEPES; 10% FBS (fetal bovine serum) (Euroclone); RPMI 1640 medium with L-Glutamine (Euroclone). Each medium was supplemented with 10 mM NAM, depending on the experimental needs. Solid media were prepared by adding 2% agar to the liquid broth before autoclaving. The optical density (OD) of each culture was measured at a wavelength of 600 nm (OD_{600}), considering that 1OD corresponds to 10^8 cells/ml. Three independent biological replicates were performed.

6.3. NAM, Inauhzin, Sirtinol, and SirReal2 treatments

A budding yeast culture was diluted in 6-well plates to a density of 10^5 cells/ml in 2 ml YPD with 10 mM NAM (CaNAM_YPD), 50 µM Inauhzin, 10 µM Sirtinol or 50 µM SirReal2. *Candida* cells treated with only vehicle

(DMSO) were used as control (CTRL). Plates were incubated at 25°C for 28 hours, and cell differentiation was followed by Time Lapse imaging (Leica DMI6000 T). A total of 5 x 10^8 cells were harvested by centrifugation (4,700*g*, 10 min at 4°C), washed with distilled water, and then stored at -80°C for subsequent histone extraction. Three independent biological replicates were performed.

6.5. Cell cultures

Murine macrophages J774A.1 cell line was supplied by LGC European partner of ATCC (LGC Standards) and cultured following the manufacturer's instructions.

Culture medium RPMI 1640 was supplemented with 10% fetal bovine serum (FBS; Euroclone), 100 U/ml penicillin, and 100 mg/ml streptomycin.

6.6. MTT assay

Macrophages viability was assessed by MTT assay. Briefly, 10^5 cells/ml were seeded onto a 96-well plate (100 µL/each well) in RPMI and incubated at 37°C and 5% CO_2 for 24 h with the following concentration of NAM: 10 mM, 25 mM, 50 mM, 100 mM.

After 24 h, the cells were washed with D-PBS (Euroclone) and incubated for 3 h at 37° C with MTT (1 mg/ml). After washing with PBS, 100 µL of DMSO was added until the formazan crystal was completely dissolved. The OD was determined spectrophotometrically at 540 nm wavelength.

6.7. Treatment of J774A.1 with *Candida albicans* conditioned media

C. albicans was grown at 37°C in RPMI and 5% CO_2 with or without 10 mM NAM. After 16 h, *C. albicans* conditioned media with or without 10 mM NAM were collected and sterilized using a 0.45 µm syringe filter to obtain CaNAM-CM and Ca-CM, respectively. RPMI with or without 10 mM NAM

was maintained at 37°C in RPMI and 5% CO_2, filter sterilized, and used as control media (NAM-M and CTRL-M). J774A.1 were seeded at a cell density of 10^5 cells/ml on polylysine-coated coverglasses, washed with D-PBS, exposed to CTRL-M, NAM-M, Ca-CM, and CaNAM-CM, and fixed at different time points (T0, T4h, T6h, T8h) for the following Immunofluorescence (IF) analysis.

6.8. Infection of J774A.1 and Hotchkiss-McManus Stain

Ca-CM and CaNAM-CM, collected as described in section 6.7 were used to pre-stimulate macrophages (10^5 cells/ml) for 8 h. Successively, *C. albicans* yeast cells grown in YNB at 25°C and resuspended in RPMI, were used to infect stimulated macrophages at a multiplicity of infection (MOI) of 1:1, at 37°C, 5% CO_2. The infection was followed by Timelapse microscopy (Leica DMI6000) for 24 h. The same conditions of infection were carried out also into Lab-Tek Chamber Slides (Nalge Nunc International). Macrophages pre-stimulated with CTRL-M and NAM-M were used as controls. After 2 h of infection, co-cultures were stained using the Hotchkiss–McManus method, by which *Candida* cells are highlighted in red while macrophages appear in dark green or blue (110). Brightfield microscopy (Axioplan Microscope, Zeiss) was used for observation.

6.9. Immunofluorescence Assay and Confocal Microscopy

For IF, cells were fixed with 4% paraformaldehyde for 20 min and washed with PBS-Tween (0.1%), permeabilized in 0.1% Triton-X-100 in PBS for 10 min and then incubated in blocking buffer (0.5% BSA in PBS-Tween) for 1 h. Slides were incubated for 1h with TRITC-Phalloidin 2 μg/ml and then washed with 0.5% BSA-PBS-Tween. For nuclei staining, 4,6-diamidino-2-phenylindole (DAPI) was used. Images were finally acquired by using a Zeiss LSM 710 confocal microscope.

6.10. Histones extraction

C. albicans pellets, obtained as described in section 6.3, were resuspended in 10 M EDTA, 10 mM Tris-HCl pH 7.4, 5 mM sodium butyrate, 5 mM NAM, 2.5% 2-Mercaptoethanol and 10% glycerol. The cellular suspension was grounded to a fine powder with a mortar and pestle in liquid nitrogen that was then resuspended in 10 mM EDTA, 10 mM Tris-HCl pH 7.4, 5 mM sodium butyrate, 5 mM NAM, 2.5% 2-Mercaptoethanol, 1% SDS, and 2% Triton-X 100 and acid-washed glass beads were added. Two or more cycles of freeze and vortex were performed. The suspensions were centrifuged at 12,000g for 15 min at 4°C, and the supernatants were collected. Acid-soluble proteins were extracted by adding 0.4 N H_2SO_4, followed by incubation at 4°C for 3h, under gentle inversion. Histones were acid-precipitated with 25% TCA (trichloroacetic acid, Sigma-Aldrich) overnight at 4°C. After two washing steps with ice-cold acetone, precipitated proteins were resuspended in Milli-Q H_2O.

6.11. Total RNA extraction and RNA sequencing

Cells, treated or not with NAM as described above, were harvested (8,000g for 10 min at 4°C) and washed with UltraPure™ DNase/RNase-Free Distilled Water (Thermo Fischer Scientific). The cell pellet was resuspended in 1 ml QIAzol Lysis Reagent (Qiagen) and disrupted mechanically with a BeadBug microtube homogenizer. Total RNA was purified following QIAzol manufacturer instructions. Three independent biological replicates were performed for either control or treated *C. albicans* cells. RNA quality was assessed with TapeStation (Agilent), and only RNA with RIN > 8 was used for RNA-seq library production.

For RNA sequencing, indexed libraries were prepared from 1 µg of purified RNA using TruSeq Stranded Total RNA Sample Prep Kit (Illumina Inc.),

according to the manufacturer's instructions. Libraries were pooled and sequenced (paired-end, 2 x 100 bp) on NextSeq 550 platform (Illumina Inc.).

6.12. Chromatin Immunoprecipitation

C. albicans cultures, treated or not with NAM as described above in YPD (ChIP-CTRL_YPD; ChIP-CaNAM_YPD) and RPMI (ChIP-CTRL_RPMI; ChIP-CaNAM_RPMI), were cross-linked with 1% formaldehyde for 15 minutes at room temperature with gentle shaking. The reaction was quenched by adding 125 mM glycine and incubating for 5 minutes at room temperature under gentle shaking. Chromatin immunoprecipitation was performed as previously described (111), except for cell lysis that was carried out using a cryogenic freezer mill (SPEX SamplePrep 6970EFM Freezer/Mill). ChIP-seq libraries were generated from two independent biological replicates of H3K56ac and input following a previously published protocol (112) and sequenced on Illumina NextSeq 500 using 2 × 75 bp reads.

6.13. Bioinformatic analysis

For RNA sequencing, analysis was performed using the Flaski RNAseq pipeline (113) and the reference *Candida albicans* SC5314 genome assembly GCA_000182965.3.

Data normalization and differentially expressed transcripts were identified using DESeq2 with standard parameters. A gene with FDR ≤ 0.05 (False Discovery Rate) and with a value of Fold Change ≤ -1.5 (for down-regulated genes) or Fold Change ≥ 1.5 (for up-regulated genes) was considered significantly differentially expressed.

For ChIP-sequencing, the analysis was performed using the Galaxy tool (114). Briefly, after FastQC quality check, the paired-end reads were aligned to the reference *Candida albicans* SC5314 genome (assembly GCA_000182965.3) using Bowtie 2 (Galaxy Version 2.4.4), and the generated

BAM file was filtered with Filter BAM (Galaxy Version SAMTOOLS: 1.8). Mapped reads were indexed and merged using samtools MergeSamFiles (Galaxy Version 2.18.2.1) and converted to bigwig files using deepTools bamCoverage (Galaxy Version 3.5.1.0.0) with a bin size of 10 and normalization to genomic content.

Peak calling was performed with MACS2 callpeak (Galaxy Version 2.2.7) using standard parameters for board regions. Peak annotation was carried out using ChIPseeker (Galaxy Version 1.28.3).

6.14. Metabolomic analysis

An orthogonal readout based on Multiple Reaction Monitoring Mass Spectrometry (MRM-MS) was performed. 30 µL of each secretome sample from *Candida albicans*, treated or not with NAM 10 mM, were submitted to UPLC-ESI-MRM-MS analysis to quantify farnesol. Appropriate blank samples of RPMI were also run. UPLC-ESI-MRM-MS analyses were performed on a 6500 Q-TRAP from Sciex equipped with Shimadzu LC-20A and Auto Sampler systems (Sciex). UPLC separation was performed on a Luna Omega Polar PS 1.6 µm C18 100 Å column (50 × 2.10 mm, Phenomenex) at a flow rate of 400 µL/min. 0.1% Formic Acid in H_2O (A) and 0.1% Formic Acid in Acetonitrile (B) were used as mobile phases, and the following gradient was performed: 0% B from 0 to 4 min, 0% to 95% B over 10 min, then held at 95% B for 5 min and re-equilibrated to 0% B over 5 min. Q-TRAP 6500 was operated in positive MRM scanning mode, with the declustering potential (DP) set at 30 V, entrance potential (EP) at 12 V, collision energy (CE) at 20 V, and cell exit potential (CXP) at 12 V. Farnesol was monitored through the 205.0/149.0, 205.0/121.0 and 205.0/109.0 transitions: the area of the peak related to the transition 205.0/121.0 was measured using the Analyst Software from Sciex and used for farnesol quantification in each sample. The other two transitions were used to confirm the occurrence of farnesol. An

external calibration curve has been prepared using pure farnesol (Sigma-Aldrich, Merck Group) at concentrations ranging from 10 nM to 50 µM.

6.15. Recombinant Hst3 purification from *Saccharomyces cerevisiae* host

The sequence of *HST3* of *C. albicans* SC5314 was optimized for the expression in *S. cerevisiae* and cloned into pYES/NT A vector (Invitrogen) by BioFab research company. The expression plasmid pYES/NT A/HST3 was transferred into INVSc1 competent cells (Invitrogen), where the recombinant protein was synthesized as a fusion protein with an N-terminal 6x Histidine tag.

6.15.1. *S. cerevisiae* growth conditions

S. cerevisiae INVSc1 cells were routinely cultured at 30°C on SC Minimal Medium Ura$^-$ plates [0.67% yeast nitrogen base (without amino acids); 2% glucose; 0.01% (adenine, arginine, cysteine, leucine, lysine, threonine, tryptophan, uracil); 0.005% (aspartic acid, histidine, isoleucine, methionine, phenylalanine, proline, serine, tyrosine, valine); 2% agar] and propagated in liquid SC Minimal Medium Ura$^-$. The recombinant protein (rHst3) expression was induced in SC Minimal Medium Ura$^-$ containing 2 % galactose (instead of glucose) for 8 h at 30°C, 200 rpm.

6.15.2. Transformation of INVSc1 competent cells

Following INVSc1 competent cells preparation using S.c. EasyComp™ Kit (ThermoFisherten 10 ng of plasmid DNA were added to 50 µL of competent cells. Yeast transformation was carried out with S.c. EasyComp™ Transformation Kit (ThermoFisher) following the manufacturer's instructions. Transformants were selected on SC Minimal Medium Ura$^-$ agar plates.

6.15.3. rHst3 purification by affinity chromatography and ion exchange

For affinity chromatography, the cell pellet was resuspended in 30 ml of lysis buffer [20 mM NaH_2PO_4/Na_2HPO_4, 500 mM NaCl, 0.5 mM DTT, pH 7.4] containing 1X protease inhibitors cocktail. The suspension was sonicated for 20 min, at 30% amplitude with 9.9 s on/9.9 s off pulses in a Vibra-Cell (Sonic) ultrasonicator, and cell debris were removed by centrifugation (10,000g for 30 min at 4°C) using a Beckman Coulter Avanti J-25 centrifuge.

One ml His-Trap HP column (GE Healthcare), connected to AKTA purifier FLPC system (Amersham Biosciences), was pre-equilibrated with binding buffer (20 mM NaH_2PO_4/Na_2HPO_4, 500 mM NaCl, 20 mM Imidazole, 0.5 mM DTT, 4 M urea, pH 7.4) before cell lysate loading. Then the column was washed with the same buffer. Proteins were eluted at a flow-rate of 1 ml/min in a 0%-100% linear gradient of elution buffer (20 mM Tris HCl, 10 mM NaCl, 0.25 M imidazole, 0.5 mM DTT, 4 M urea, pH 7.4) in 20 column volumes.

For affinity chromatography in denaturing conditions, 8 M urea was added to the elution buffer. For ion exchange chromatography, the cell pellet was resuspended in 30 ml of lysis buffer [20 mM NaH_2PO_4/Na_2HPO_4, 500 mM NaCl, 0.5 mM DTT, pH 7.4] containing 1X protease inhibitors cocktail. The suspension was sonicated for 20 min, at 30% amplitude with 9.9 s on/9.9 s off pulses in a Vibra-Cell (Sonic) ultrasonicator and cell debris were removed by centrifugation (10,000g for 30 min at 4°C) using a Beckman Coulter Avanti J-25 centrifuge.

One ml Mono Q 5/50 GL column (GE Healthcare) was equilibrated with binding buffer (20 mM Tris-HCl, 10 mM NaCl, 6 mM arginine, pH 8.5) ,and protein elution was performed with a step gradient in Mono Q elution buffer: 20 mM Tris-HCl, 1 M NaCl,six6 mM arginine, pH 8.5.

6.16. rHst3p purification from *Escherichia coli* host

The expression plasmid pET28/HST3 (purchased from GenScript company) was amplified into DH5α competent cells and then purified with PureYield™ Plasmid Maxiprep System (Promega). The plasmid was then used for *HST3* molecular cloning into the pETM11-SUMO3 vector (EMBL) (Fig. 28).

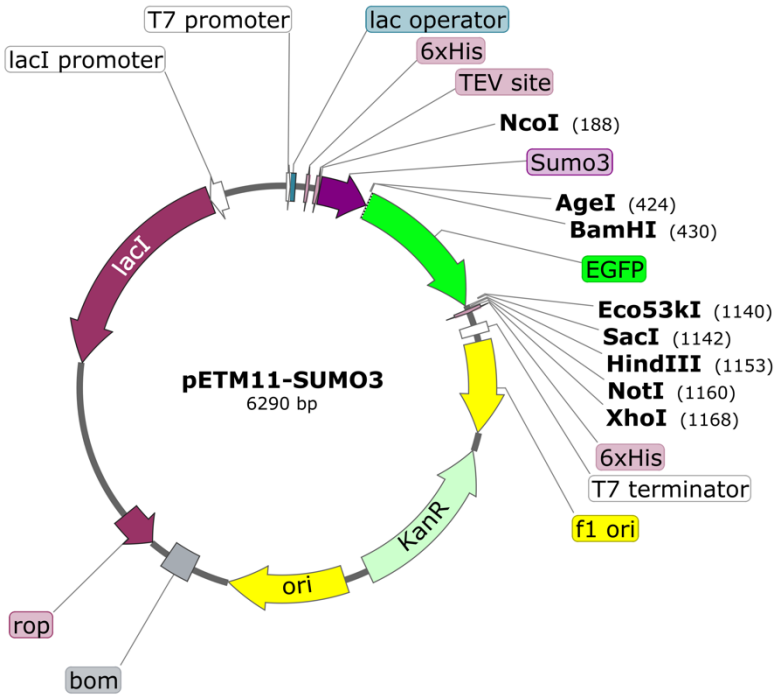

Fig. 28 - pETM11-SUMO3 vector map (Created with SnapGene)

6.16.1. Bacterial growth conditions

E. coli cells were grown at 37 °C in Luria–Bertani (LB) (1% tryptone, 0.5% yeast extract, 0.5% NaCl, pH 7.00) or LB agar plates, supplemented with 100 µg/ml kanamycin for DH5 α or BL21(DE3) cells carrying pET28/HST3 or pETM11/HST3 vectors respectively.

6.16.2. Cloning of *HST3* into pETM11-SUMO3 vector

PCR amplification of the *HST3* sequence cloned in the pET28a (+) vector was performed to insert the appropriate restriction sites for cloning into the pETM11-SUMO3 vector.

PCR was performed on 1 µg of pET28/HST3 using PCR Master Mix (2X) (Thermo Fischer Scientific); 0.5 µM forward (CTTGGATCCCATATGAAAAGCAAGAAAAT GACCGTTCTGAC); 0.5 µM reverse (AAGAAGCTTTTGTTAGCAGCCGGATCTCAGT) with the following conditions:

- 95 °C for 5 min;
- 95 °C for 45 sec;
- 60 °C for 45 sec; } x 40
- 72 °C for 1 min;
- 72 °C for 1 min
- Store 4 °C

The PCR product was purified on agarose gel, excising the band and using NucleoSpin Gel and PCR Clean-up (MACHEREY-NAGEL). pETM11-SUMO3 empty vector and PCR amplified *HST3* were then digested with BamHI-HF and HindIII-HF restriction enzymes (NEB) for 10 min at 37 °C in rCutSmart Buffer (NEB) and then again purified from agarose gel. For ligation with Rapid DNA Ligation Kit (Thermo Fischer Scientific) a molar ratio 1:3 of vector to insert was used.

6.16.3. Transformation of *E. coli* competent cells

10 ng of pETM11/HST3 were added to 50 µl of BL21(DE3) Codon Plus competent cells (Agilent) that were subsequently incubated on ice for 30 min, heat shocked for 45 sec at 42°C and then immediately placed on ice for 2 min. 500 µl of pre-warmed LB medium were added and cells were incubated at 37°C for 45 min.

Cells were plated on LB agar plates containing the appropriate antibiotic and incubated over-night at 37°C for transformants selection.

6.16.4. Ni-NTA Agarose affinity purification

rHst3 purification was performed using an Ni-NTA Agarose affinity chromatography matrix (Qiagen) as previously described (111).

6.16.5. rHst3 purification from inclusion bodies

The cell pellet was resuspended in 100 ml of washing buffer (20 mM Tris pH 7.5, 300 mM NaCl, 5 mM β-Mercaptoethanol, 10 mM Imidazole) containing 1X protease inhibitors cocktail. Suspensions were individually sonicated for 10 min, at 30% amplitude with 9.9 s on/9.9 s off pulses in a Vibra-Cell (Sonic) ultrasonicator and insoluble fraction was collected by centrifugation (10,000g for 30 min at 4°C). Cleared lysate (Supernatant 1) was recovered and pellet was resuspended in washing buffer for subsequent sonication (10 min, 30% amplitude, 9.9 s on/9.9 s off pulses). After centrifugation (10,000g for 30 min at 4°C) the soluble fraction (Supernatant 2) was recovered and inclusion bodies were resuspended in 10 ml of washing buffer supplemented with 8 M urea and incubated overnight under constant stirring at 4°C. Suspension was centrifuged (10,000g for 30 min at 4°C) and the pellet was solubilized in 5 ml of 6 M guanidine-HCl (Sigma-Aldrich) and 1 mM DTT. After centrifugation (10,000g for 30 min at 4°C) supernatant was recovered and analyzed by Western Blotting.

6.17. SDS-page, coomassie staining and Western Blotting

For Western blotting, 0.5 μg of each histone sample was resolved by SDS-PAGE on 15% polyacrylamide gel and transferred to a nitrocellulose membrane using the Trans-Blot Turbo Transfer System (Bio-Rad). The

following primary antibodies were used to detect histones: H3 (Abcam, ab1791), and H3K56ac (Active Motif).

To detect the recombinant protein, protein fractions were separated on 12% denaturing polyacrylamide gel, transferred to nitrocellulose membrane (Bio-Rad), and detected using an anti poly-Histidine (clone HIS-1, Sigma-Aldrich). Band intensities were assessed by densitometry using ImageJ analysis software.

For Coomassie staining of the chromatographic fractions, the proteins were resolved by SDS-PAGE (12% polyacrylamide gel), and the gel was stained with Coomassie G-250 Brilliant Blue (Sigma-Aldrich) and destained in destaining solution (20% methanol, 5% glacial acetic acid).

6.18. Statistical analysis

Data are from at least three independent experiments, and results are expressed as means ± SD. Data were analyzed with GraphPad Prism 7 (GraphPad Software). Two-tailed Student's t-test (2-group comparisons) or two-way ANOVA (>2-group comparisons) were performed as appropriate. P values <0.05 were considered significant.

RESULTS

Chapter VII: H3K56 acetylation regulates the expression of virulence-related genes

7.1. Genome-wide analysis of H3K56ac across *C. albicans* genome in yeast and V-shaped forms

Preliminary transcriptomic studies carried out in our laboratory showed a dysregulation of virulence associated genes following the inhibition of Hst3 with NAM (115). In particular, NAM was used at a concentration of 10 mM since it was able to induce the formation of V-shaped hyphae, which is the phenotype associated with H3K56ac accumulation (109) (Fig. 29a), also verified by Western blotting (Fig. 29b).

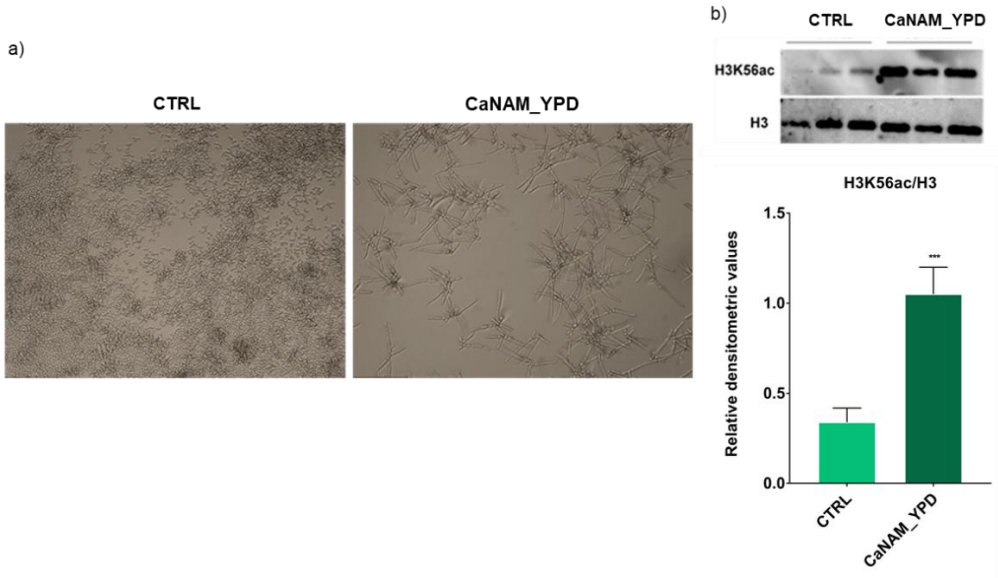

Fig. 29 - a) Representative pictures of *C. albicans* cells treated for 28 h with 10 mM NAM. Exposure to 10 mM NAM in yeast-promoting conditions induces an abnormal phenotype (V-shaped hyphae) associated with H3K56ac accumulation (109). b) Western Blot and densitometric analysis of H3K56ac normalized to H3 from three independent experiments. Values are the mean ±standard error of three independent experiments ***p<0.001 (t-test).

RNA sequencing experiments showed a significant difference between transcriptomes of *C. albicans* grown for 28 h in YPD medium (yeast cells, ChIP-CTRL_YPD) and *C. albicans* treated for 28 h with 10 mM NAM (V-shaped, ChIP-CaNAM_YPD) (Fig. 30).

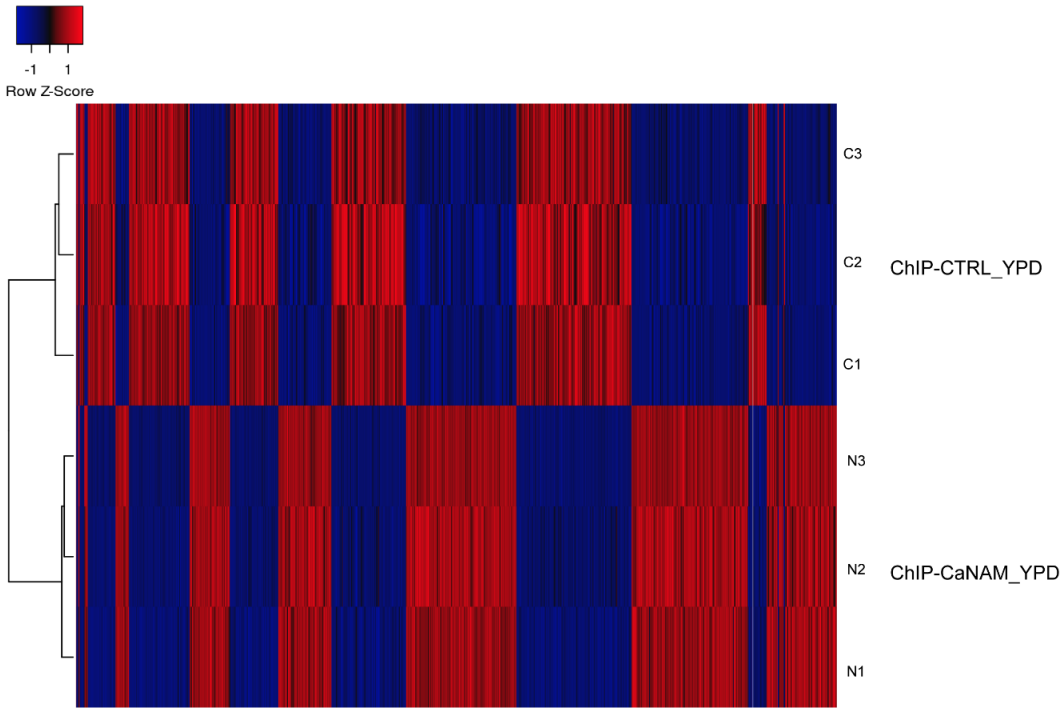

Fig. 30 - Heatmap showing the expression levels in $\log_2$ RPKM of differentially expressed genes upon NAM treatment (FDR ≤0.05).

Notably, most dysregulated transcripts are related to filamentation, white-opaque transition, cell wall organization, adhesion, biofilm, and virulence.

To deepen how H3K56 acetylation levels influence the transcriptome, *Candida* yeast (ChIP-CTRL_YPD) and V-shaped (ChIP-CaNAM_YPD) were used for Chromatin immunoprecipitation using an anti-H3K56ac antibody. Illumina high throughput sequencing revealed that acetylation patterns of H3K56 are mainly distributed in genomic regions across the TSS of genes (Figure 31).

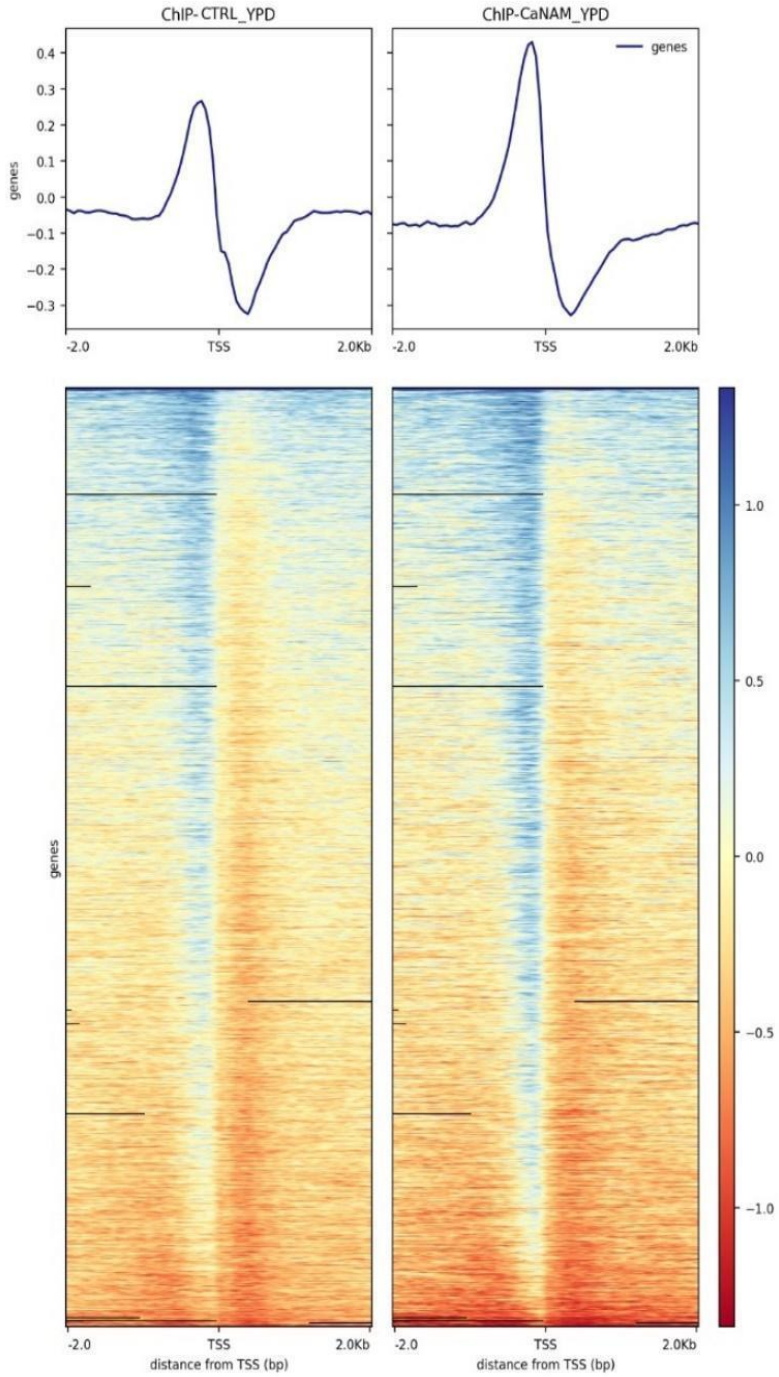

Fig. 31 - Representative profile heatmap around TSS of RefSeq genes showing the scores associated with genomic regions around the TSS of genes (± 2 kb). The gradient blue-to-red color indicates a high-to-low log2 ratio of the number of reads between the IP and the respective Input counts in the corresponding region.

Specifically, 671 and 843 ChIP-enriched regions were identified in ChIP-CTRL_YPD and ChIP-CaNAM_YPD, respectively. Among them, 283 enriched regions are common to both experimental conditions, and 477 regions resulted enriched exclusively upon NAM treatment.

To better understand the biological significance of differentially acetylated regions, a functional analysis was performed using ClueGo and CluePedia Cytoscape plugins, which integrates Gene Ontology (GO) terms to create a functionally organized GO term network. Biological processes GO-terms relative to filamentation, phenotypic switching and adhesion resulted significantly enriched (Figure 32a;b). In particular, the differentially acetylated regions include the promoters of several genes with a well-known role in cell differentiation and virulence (largely discussed in sections 1 and 2), including *OFI1*, *EFG1*, *ERG1*, *ACE2*, *WOR1*, *WOR2*, *WOR3,* and *WOR4*, *HWP1*, *HWP2*, *CRZ2, ALS3*.

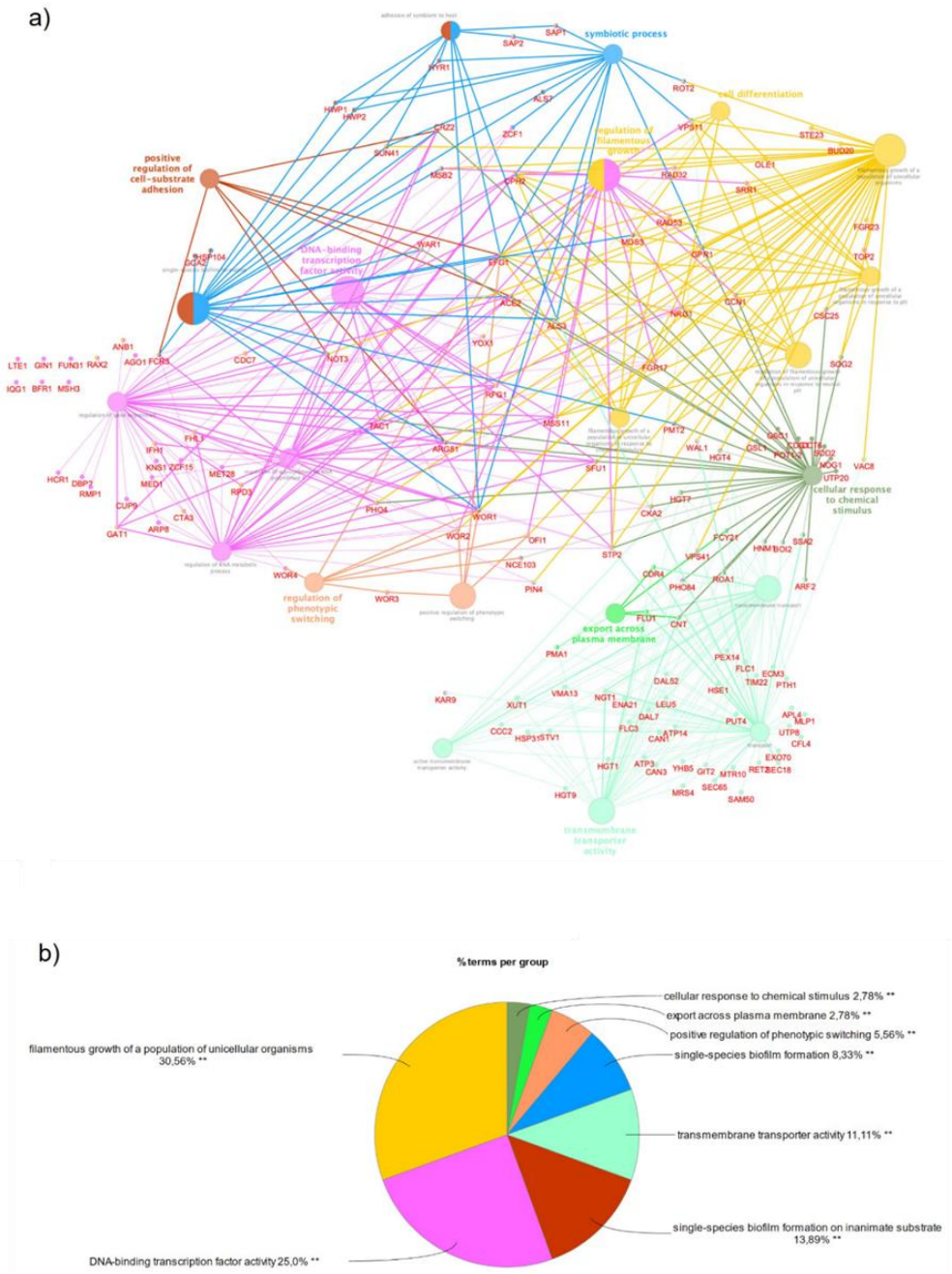

Fig. 32 - Biological process enrichment analysis using ClueGO and CluePedia Cytoscape plugins. a) Functionally grouped network of enriched categories. GO terms are represented as nodes, and the node size indicates the degree of significance; b) Pie chart showing significantly enriched GO-terms in 447 regions ChIP-enriched exclusively in ChIP_CaNAM_YPD. The most significant term defined the group name. Asterisks denote GO-term significance. (Bonferroni adjusted pValue ≤0.05).

Integrating RNA sequencing with ChIP-seq results, 87 genes showed a direct correlation between higher transcription and H3K56 acetylation associated with the promoters, including some virulence-related genes such as *OFI1*, *WOR1*, and *WOR2*, *HWP1*, *NRG1*, *ACE2*, *CRZ2*, and the secreted aspartyl proteinases *SAP1* and *SAP2* (Fig. 32; Table 1).

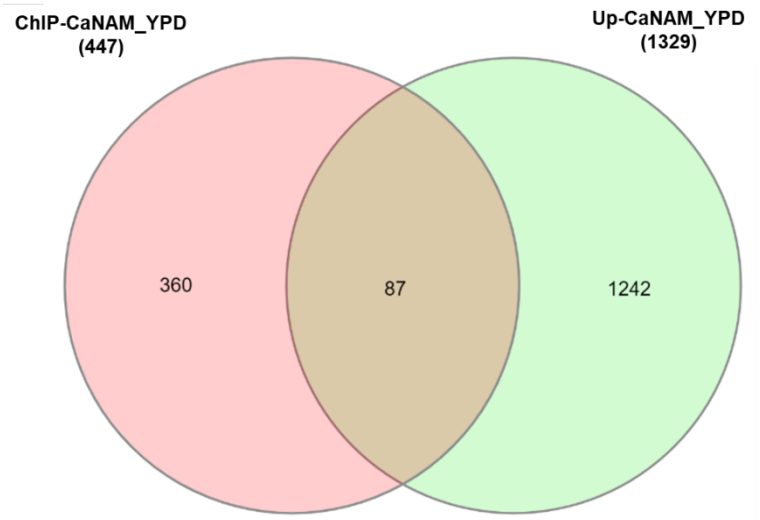

Fig. 33 - Venn diagram showing the overlapping genes between RNA-seq upregulated transcripts, and ChIP-seq enriched regions.

Table 1 – List of the 87 genes whose transcription directly correlates with H3K56 acetylation on their promoters.

Gene_ID	Gene_Name	Description
C1_01520C_A	SOD2	Mitochondrial Mn-containing superoxide dismutase; protection against oxidative stress; homotetramer active; N-terminal 34 amino acids removed on mitochondrial import; H2O2-induced via Cap1p; Hap43p-, alkaline-downregulated, farnesol-induced
C1_01920W_A	ROA1	Putative PDR-subfamily ABC transporter involved in sensitivity to azoles; Spider biofilm induced
C1_02390W_A		Putative nuclease required for DNA single- and double-strand break repair; rat catheter biofilm induced
C1_02470W_A		Ortholog of *C. dubliniensis* CD36: Cd36_02330, *C. parapsilosis* CDC317: CPAR2_106450, *Candida tropicalis* MYA-3404: CTRG_04653 and *Candida albicans* WO-1: CAWG_01134

C1_03240W_A		Ortholog of *C. dubliniensis* CD36: Cd36_03040, *C. parapsilosis* CDC317: CPAR2_108610, *C. auris* B8441: B9J08_000283, *Debaryomyces hansenii* CBS767: DEHA2G16500g and *Pichia stipitis Pignal*: PICST_32835
C1_03840W_A		Ortholog of *C. dubliniensis* CD36: Cd36_03580, *C. parapsilosis* CDC317: CPAR2_105090, *C. auris* B8441: B9J08_004984 and *Candida tenuis* NRRL Y-1498: CANTEDRAFT_106351
C1_04310C_A	GIG1	Protein induced by N-acetylglucosamine (GlcNAc); localized in cytoplasm; mutation causes increased resistance to nikkomycin Z
C1_06150W_A		Ortholog of Candida albicans WO-1 : CAWG_00792
C1_06340W_A		Ortholog of *C. dubliniensis* CD36: Cd36_05920, *C. parapsilosis* CDC317: CPAR2_803860, *C. auris* B8441: B9J08_000594, *Pichia stipitis Pignal*: PICST_30324 and *Candida guilliermondii* ATCC 6260 PGUG_04439
C1_07040C_A		Pry family pathogenesis-related protein; oral infection upregulated gene; mutant has reduced capacity to damage oral epithelial cells
C1_07330W_A	RME1	Zinc finger protein, controls asexual sporulation; white-specific transcript; upregulation correlates with clinical development of fluconazole resistance; Upc2-regulated in hypoxia; flow model biofilm induced; Spider biofilm
C1_07610C_A		Ortholog of *C. dubliniensis* CD36: Cd36_07090, *C. auris* B8441: B9J08_003145, *Candida tenuis* NRRL Y-1498: cten_CGOB_00237 and *Debaryomyces hansenii* CBS767: DEHA2F25542g
C1_07880C_A	GCS1	Gamma-glutamylcysteine synthetase; glutathione synthesis, required for virulence; induced in low iron, H_2O_2, Cd, or presence of human neutrophils; possibly adherence-induced; Spider and F-12/CO_2 biofilm induced
C1_07960W_A		Predicted nuclear exosome-associated nucleic acid binding protein; rat catheter and Spider biofilm induced
C1_08070W_A	CDR4	Putative ABC transporter superfamily; fluconazole, Sfu1, Hog1, core stress response induced; caspofungin repressed; fluconazole resistance not affected by mutation or correlated with expression; rat catheter and flow model biofilm induced
C1_09160W_A	AOX1	Alternative oxidase; low abundance; constitutively expressed; one of two isoforms (Aox1p and Aox2p); involved in a cyanide-resistant respiratory pathway present in plants, protists, and some fungi, absent in S. cerevisiae; Hap43p-repressed
C1_09540W_A		Protein of unknown function; Spider biofilm induced
C1_09550W_A		Protein of unknown function; transcript detected on high-resolution tiling arrays; rat catheter biofilm induced
C1_09710C_A		Ortholog(s) have role in endonucleolytic cleavage in 5'-ETS of tricistronic rRNA transcript (SSU-rRNA, 5.8S rRNA and LSU-rRNA), more
C1_10150W_A	WOR1	Transcription factor ("master switch") of white-opaque phenotypic switching; required to establish and maintain the opaque state; opaque-specific, nuclear; regulates its own expression; suggested role in regulation of adhesion factors
C1_10630C_A		Has domain(s) with predicted role in mitotic sister chromatid cohesion
C1_11340W_A	PRM1	Putative membrane protein with a predicted role in membrane fusion during mating; Hap43p-repressed gene; protein induced during the mating process
C1_11370C_A		Essential protein required for the DNA integrity checkpoint pathway; Spider biofilm induced
C1_11700C_A	MRF1	Putative mitochondrial respiratory protein; induced by farnesol, benomyl, nitric oxide, core stress response; oxidative stress-induced via Cap1; stationary-phase enriched protein; Spider biofilm induced

C1_13080W_A	OP4	Ala- Leu- and Ser-rich protein; secreted; N-terminal hydrophobic region; possible glycosylation; opaque-specific transcript; repressed by alpha pheromone in opaque MTLa homozygotes; fluconazole-induced; Spider biofilm induced
C1_13440C_A	OFI1	Putative transcription factor with zinc finger DNA-binding motif, involved in regulation of white-opaque switching and filamentous growth
C1_13450W_A	HYR1	GPI-anchored hyphal cell wall protein; macrophage-induced; repressed by neutrophils; resistance to killing by neutrophils, azoles; regulated by Rfg1, Efg1, Nrg1, Tup1, Cyr1, Bcr1, Hap43; Spider and flow model biofilm induced
C1_13740W_A	KAR9	Ortholog of S. cerevisiae Kar9; role in mitotic spindle positioning; nonessential; localizes to bud tip, bud neck, hyphal tip; wild-type localization requires actin and microtubule cytoskeleton; induced by alpha factor
C1_13750C_A		Ortholog of *C. dubliniensis* CD36: Cd36_12740, *C. parapsilosis* CDC317: CPAR2_201620, *C. auris* B8441: B9J08_002511 and *Candida tenuis* NRRL Y-1498: CANTEDRAFT_107586
C2_00880W_A		Predicted dihydrodiol dehydrogenase; ortholog of *S. pombe* SPAC513.06c; flow model and rat catheter biofilm repressed
C2_00890W_A		Ortholog of *C. dubliniensis* CD36: Cd36_15830, *C. parapsilosis* CDC317: CPAR2_212930, *Candida tropicalis* MYA-3404: CTRG_01155, *Candida albicans* WO-1: CAWG_03868 and *Candida metapsilosis*: CMET_2287
C2_02400W_A	ECM3	Has domain(s) with predicted role in transmembrane transport and integral component of membrane localization
C2_05320W_A	CDC7	Catalytic subunit of Dbf4p-regulated serine/threonine protein kinase; negative regulator of hyphal development; cell-cycle regulated periodic mRNA expression; *S. cerevisiae* ortholog is not cell-cycle regulated
C2_05640W_A		Putative helix-loop-helix (HLH) transcription factor with a role in filamentous growth
C2_07790C_A		Protein of unknown function; induced by alpha pheromone in SpiderM medium
C2_10000C_A		Ortholog of *C. parapsilosis* CDC317: CPAR2_407200.1, *C. dubliniensis* CD36: Cd36_24070, *Candida metapsilosis*: CMET_2070 and *Pichia stipitis Pignal*: PICST_31669
C3_00330W_A	UTP8	Essential nucleolar protein; involved in tRNA export from the nucleus and ribosomal small subunit biogenesis; physically interacts with TAP-tagged Nop1; Spider biofilm induced
C3_02300W_A	FGR23	Protein of unknown function; repressed by a1/alpha2 in white-phase cells, a-specific, alpha factor-induced; Hap43-repressed; flow model biofilm induced; Tn mutation affects filamentous growth;
C3_02330C_A		Protein of unknown function; Spider biofilm induced
C3_02390W_A		Protein of unknown function; Plc1-regulated
C3_02550C_A	DCG1	Protein of unknown function; ortholog of *S. cerevisiae* Dcg1; transcript regulated by Nrg1 and Mig1
C3_02660W_A		Protein of unknown function; Spider biofilm induced
C3_02750W_A		Protein with a ribonuclease III domain; flow model biofilm induced; Spider biofilm induced
C3_03720W_A	GTT11	Glutathione S-transferase, localized to ER; induced in exponentially growing cells, under oxidative stress; induced by nitric oxide; Spider biofilm induced
C3_05170W_A	WOR2	Zn(II)2Cys6 transcription factor; regulator of white-opaque switching; required for maintenance of opaque state; Hap43-induced

C3_05720C_A	KIP3	Putative kinesin, involved in mitotic spindle organization
C3_07160W_A	PGA32	Putative GPI-anchored adhesin-like protein; induced in high iron; Spider biofilm induced
C4_00920C_A		Possible similarity to mutator-like element (MULE) transposase; flow model biofilm induced; expression regulated during planktonic growth
C4_01650C_A		Putative cleavage and polyadenylation factor; heterozygous null mutant exhibits hypersensitivity to parnafungin and cordycepin in the *C. albicans* fitness test; possibly an essential gene, disruptants not obtained by UAU1 method
C4_03570W_A	HWP1	Hyphal cell wall protein; host transglutaminase substrate; opaque-, a-specific, alpha-factor induced; at MTLa side of conjugation tube; virulence complicated by URA3 effects; Bcr1-repressed in RPMI a/a biofilms; Spider biofilm induced
C4_04070C_A	PGA30	GPI-anchored protein of cell wall
C4_05970W_A		Protein of unknown function; Hap43-repressed gene
C4_06590W_A	CCJ1	Protein involved in cell cycle regulation; ortholog of S. pombe SPAC1071.09c DNAJ domain protein; Hap43-induced gene
C4_06600W_A	TOP2	DNA topoisomerase II; catalyzes ATP-dependent DNA relaxation and decatenation in vitro; Y842 predicted to be catalytic; functional homolog of S. cerevisiae Top2p; sensitive to amsacrine or doxorubicin; farnesol-upregulated in biofilm
C5_00710W_A	IFF8	Putative GPI-anchored adhesin-like protein; decreased transcription is observed in an azole-resistant strain that overexpresses MDR1
C5_01360W_A	CFL4	C-terminus similar to ferric reductases; induced in low iron; Sfu1-repressed; ciclopirox olamine induced; colony morphology-related gene regulation by Ssn6; Hap43-repressed; Sef1-regulated
C5_01570C_A	SPO1	Protein similar to phospholipase B; fungal-specific (no human or murine homolog)
C5_01670W_A	DAL52	Putative allantoate permease; mutant is viable; similar but not orthologous to S. cerevisiae Dal5
C5_02860C_A	GRP2	NAD(H)-linked methylglyoxal oxidoreductase involved in regulation of methylglyoxal and pyruvate levels; regulation associated with azole resistance; induced in core stress response or by oxidative stress via Cap1, fluphenazine, benomyl
C5_03080C_A		Predicted membrane transporter; monocarboxylate porter (MCP) family, major facilitator superfamily (MFS); Spider biofilm induced; rat catheter biofilm repressed
C5_03460C_A		Has domain(s) with predicted role in GPI anchor biosynthetic process
C5_03470C_A		Predicted membrane transporter, member of the L-amino acid transporter-3 (LAT3) family, major facilitator superfamily (MFS)
C5_04230W_A	MRV6	Ortholog of *Candida albicans* WO-1: CAWG_04796
C6_00290W_A		Protein of unknown function; regulated by yeast-hypha switch; induced by Mnl1 in weak acid stress; 5' UTR intron; repressed by chlamydospore formation in *C. albicans* and *C. dubliniensis*; rat catheter, Spider and flow model biofilm induced
C6_01680C_A	GBU1	Guanidinobutyrase (Gbase), enzyme involved in metabolism of guanidinobutyrate
C6_01810W_A		Protein of unknown function; transcription repressed by fluphenazine treatment

C6_02330W_A		Described as a Gag-related protein; hyphal induced; downregulation correlates with clinical development of fluconazole resistance; repressed by nitric oxide, 17-beta-estradiol, ethynyl estradiol
C6_02830W_A	MNN45	Mannosyltransferase; transcript upregulated in Ssk1 response regulator mutant or in nik1 null mutant, but not in chk1 or sln1 null mutants; pheromone induced; Spider biofilm induced
C6_03110C_A		Ortholog of *S. cerevisiae*: ASA1, *C. glabrata* CBS138: CAGL0K07920g, *C. dubliniensis* CD36: Cd36_63960, *C. parapsilosis* CDC317: CPAR2_600230 and *C. auris* B8441: B9J08_002518
C6_03490C_A	SAP1	Secreted aspartyl proteinase; acts in utilization of protein as nitrogen source; assessment of virulence role complicated by URA3 effects; regulated by growth phase, alpha-pheromone; produced by opaque cells
C7_01520W_A	FLU1	Multidrug efflux pump of the plasma membrane; MDR family member of the MFS (major facilitator superfamily) of transporters; involved in histatin 5 efflux; fungal-specific (no human/murine homolog)
C7_01840W_A	IQG1	Actomyosin ring component at bud neck; cell-cycle regulated ser phosphorylation at CDK sites regulate association with Bni1/Bnr1, Iqg1 degradation, and ring disassembly; mutation causes cytokinetic defects; rat catheter biofilm repressed
C7_03560W_A		Protein of unknown function; expression decreases by benomyl treatment or in an azole-resistant strain overexpressing MDR1; Spider biofilm induced
C7_03570W_A	ARG4	Argininosuccinate lyase, catalyzes the final step in the arginine biosynthesis pathway; alkaline downregulated; flow model biofilm induced; Spider biofilm induced
C7_04230W_A	NRG1	Transcription factor/repressor; regulates chlamydospore formation/hyphal gene induction/virulence and rescue/stress response genes; effects both Tup1 dependent and independent regulation; flow model biofilm induced; Spider biofilm repressed
CR_00010C_A		Protein similarity to mutator-like element (MULE) transposase
CR_00060C_A		DNA helicase involved in rDNA replication; Spider biofilm repressed
CR_01330W_A	CPA2	Putative arginine-specific carbamoylphosphate synthetase; protein enriched in stationary phase yeast cultures; rat catheter biofilm induced; Spider biofilm induced
CR_04710W_A		Ortholog(s) have U2-type spliceosomal complex localization
CR_06870C_A		Protein similar to ferric reductase Fre10p
CR_07060C_A	CRZ2	C2H2 transcription factor, involved in regulation of early adaptation to murine GI tract; Rim101-repressed at pH 8; required for yeast cell adherence to silicone substrate; Spider biofilm induced
CR_07440W_A	ACE2	Transcription factor; similar to S. cerevisiae Ace2 and Swi5; regulates morphogenesis, cell separation, adherence, virulence in a mice; mutant is hyperfilamentous; rat catheter and Spider biofilm induced
CR_07800W_A	SAP2	Major secreted aspartyl proteinase; utilization of protein as nitrogen source; role in virulence complicated by URA3 effects; immunoprotective; regulated by growth, albumin, drugs, white cell-type; flow model biofilm induced
CR_07810W_A	YHB5	Flavohemoglobin-related protein; not required for normal NO resistance; predicted globin/FAD-binding/NAD(P)-binding domains but lacks some conserved residues of flavohemoglobins; filament induced; rat catheter and Spider biofilm induced
CR_09700W_A		Predicted membrane transporter, member of the aromatic acid:proton symporter (AAHS) family, major facilitator superfamily (MFS)
CR_09890C_A	BET2	Putative Type II geranylgeranyltransferase beta subunit; transcript regulated by Mig1

CR_10180W_A		Protein of unknown function; Spider biofilm induced

Moreover, the transcriptome analysis also suggested that H3K56ac indirectly regulates the expression of virulence-related genes. Indeed, Hst3 inhibition results in acetylation associated with the promoter of *EFG1*, a key transcription factor involved in the regulation of several morphogenesis and virulence-related genes, whose transcription is not only negatively autoregulated by Efg1 (116; 117), but is also repressed by a series of positive feedback loops established by Wor1, Wor2, and Czf1 (132). Moreover, *ECE1*, which encodes for the cytolytic peptide candidalysin, and *UME6*, the filament-specific transcriptional regulator, are up-regulated in RNA-seq upon NAM treatment and directly regulated by *EFG1* (Moyes et al., 2016; Banerjee et al., 2008).

Unexpectedly, a subset of 85 genes whose promoters displayed H3K56 acetylation only in ChIP-CaNAM showed an opposite trend, with higher acetylation but lower transcript abundance in CaNAM_YPD compared to CTRL_YPD (Fig. 34) suggesting that a higher transcription rate does not always follow H3K56 acetylation.

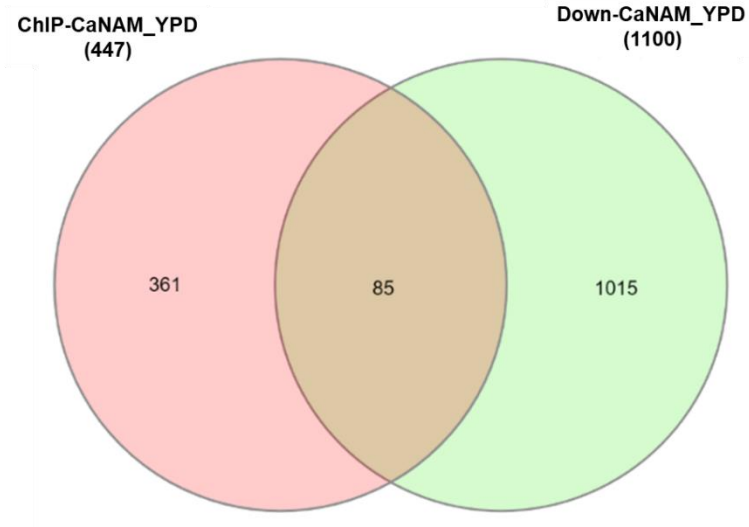

Fig. 34 - Venn diagram showing the overlapping genes between RNA-seq downregulated transcripts, and ChIP-seq enriched regions.

This could be explained by the fact that, in eukaryotes, a wide range of mechanisms contribute to transcriptional control (including mRNA stability control, Pol II termination, and Pol II attenuation) and this is consistent with NET-seq analysis carried out by Topal and colleagues in *S. cerevisiae* (118) who showed that, besides the central role in enhancing transcription initiation, H3K56ac might transiently functions as a transcriptional repressor by promoting nucleosome assembly. Furthermore, our ChIP-seq analysis revealed that Hst3 also regulates H3K56ac across the promoters of *MED1*, encoding the RNA polymerase II mediator complex subunits, the RNA polymerase II regulator *EED1*, besides other putative proteins with a predicted role in mRNA 3'-end processing, mRNA polyadenylation, and pre-mRNA cleavage. These results suggest a possible role of H3K56ac in the modulation of a fine-tuning mechanism of transcriptional control, highlighting the importance of such histone mark in controlling a wide range of biological processes in *C. albicans*.

7.2. Sirtinol, SirReal2, and Inauzhin do not inhibit Hst3.

As a member of a NAD^+-dependent histone deacetylases family, Hst3 is inhibited, in a non-specific and non-selective way, by NAM. To verify if currently available sirtuin inhibitors have an effect on Hst3, we tested Sirtinol, SirReal2, and Inauhzin, specific Sirt1 and Sirt2 inhibitors. In detail, yeast cells from an overnight culture were inoculated in YPD containing 10 µM Sirtinol, 50 µM SirReal2, or 50 µM Inauhzin (the highest concentrations at which the inhibitors are fully soluble), or with 10 mM NAM, here used as control. Yeast growth was followed up to 24 h by Time Lapse imaging. No morphological alterations were observed with any inhibitor used, whereas cells with NAM formed hyphae with V-shaped branches (Figure 35a). Moreover, Western blotting of histones extracted from overnight treatment confirmed that Sirtinol, SirReal2, and Inauhzin did not induce a significant accumulation of H3K56ac, whereas NAM inhibits Hst3 as demonstrated by the higher level of acetylated H3K56 (Figure 35b).

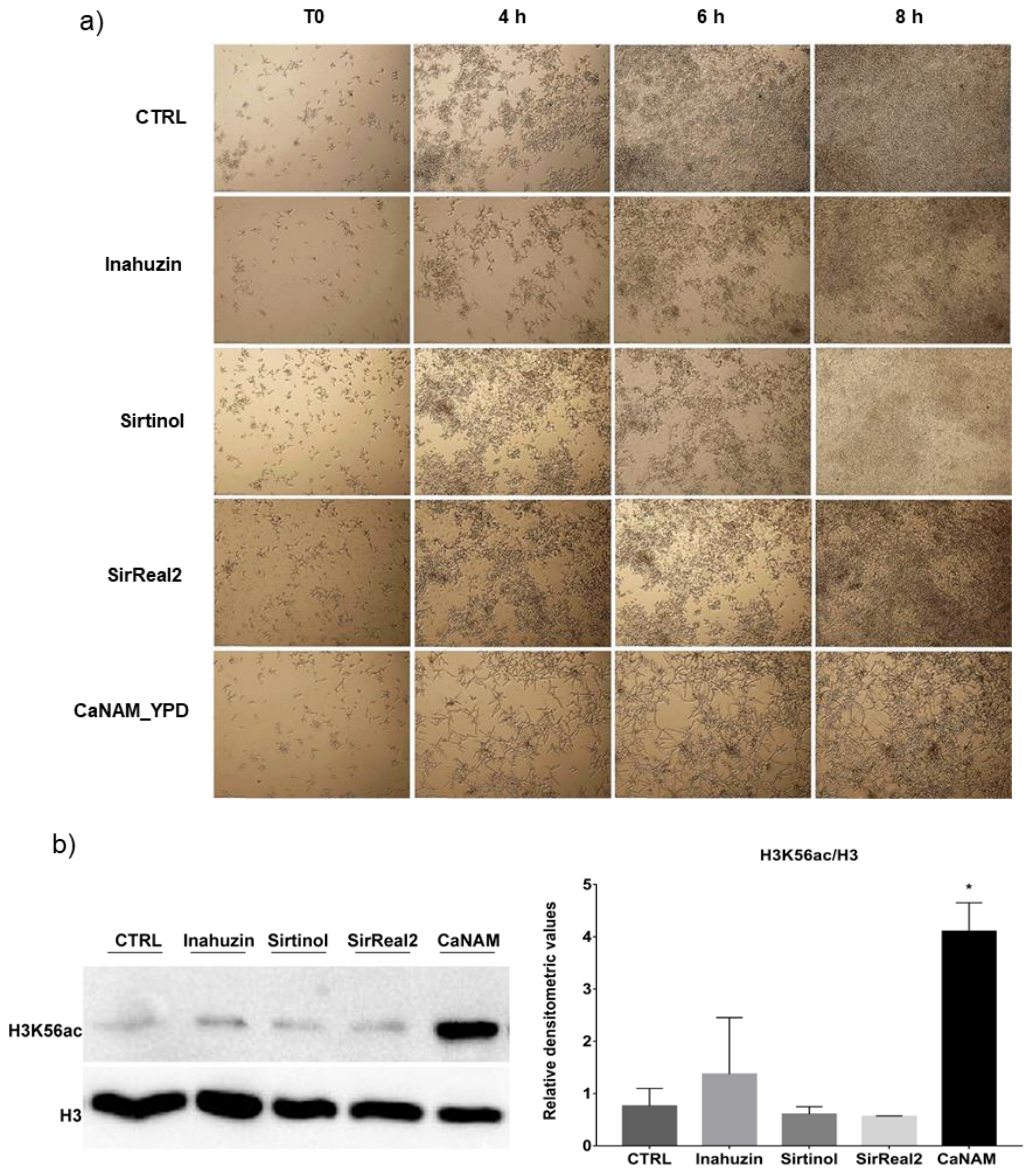

Fig. 35 - (a) *C. albicans* cells were treated with 50 µM Inauzhin, 10 µM Sirtinol, 50 µM SirReal2, or 10 mM NAM, and the morphology was imaged by Time-Lapse microscopy (10X magnification). (b). Western blotting and densitometric analysis of *Candida* cells treated with 50 µM Inauzhin, 10 µM Sirtinol, 50 µM SirReal2 and 10 mM NAM for 16 hours, and H3K56ac. Values are mean ± standard error of three independent experiments *p<0.05 (t-test).

The results reported in Chapter VII have been published in Frontiers in Cellular and Infection Microbiology: **Conte M**, Eletto D, Pannetta M, Petrone AM, Monti MC, Cassiano C, Giurato G, Rizzo F, Tessarz P, Petrella A, Tosco A and Porta A. Effects of Hst3p inhibition in Candida albicans: a genome-wide H3K56 acetylation analysis. Front. Cell. Infect. Microbiol. 2022 Oct 27. 12:1031814.

Chapter VIII: Acetylation of H3 Lys56 regulates the production of soluble metabolites influencing macrophages response

8.1. *C. albicans* soluble metabolites induce morphological changes in macrophages cytoskeleton

As widely discussed in Section 4.3, the opportunistic pathogen *C. albicans* has evolved different strategies to escape the host immune system and most of them have not been fully characterized yet. A growing number of studies pointed out the possibility that *C. albicans* secretome influences host immune response (91; 92; 93; 94). Of interest, previous studies demonstrated that *C. albicans* metabolites induce actin rearrangement in human epithelial cells and macrophages cytoskeleton (119; 120).

Since chromatin modifying enzymes have been shown to epigenetically modulate the pathogenicity of *C. albicans*, to characterize the role of H3K56 acetylation in the regulation of *C. albicans* secretome-related to immune escape, we analyzed the effects of *C. albicans* secretome on immune cells. In particular, conditioned culture media collected from *Candida* control cells (Ca-CM) or *Candida* grown with 10 mM NAM (CaNAM-CM) were used to treat the murine macrophages J774A.1. To identify the minimum concentration of NAM that, under these growing conditions (RPMI, 37°C and 5% CO_2 for 24 h), was able to inhibit Hst3 without having cytotoxic effects either on *Candida* or macrophages, 5 different concentrations of NAM were tested (10 mM; 25 mM; 50 mM; 75 mM; 100 mM). As already demonstrated for *Candida* grown as V-shaped (in YPD at 25°C; Fig. 29), also in these growing conditions, 10 mM NAM was sufficient to induce an accumulation of acetylation on H3K56 (data not shown) without affecting the viability of J774A.1 cells (Fig. 36a) Notably, in hyphae-inducing conditions the treatment with 10 mM NAM slows down hyphae elongation (Fig. 36b).

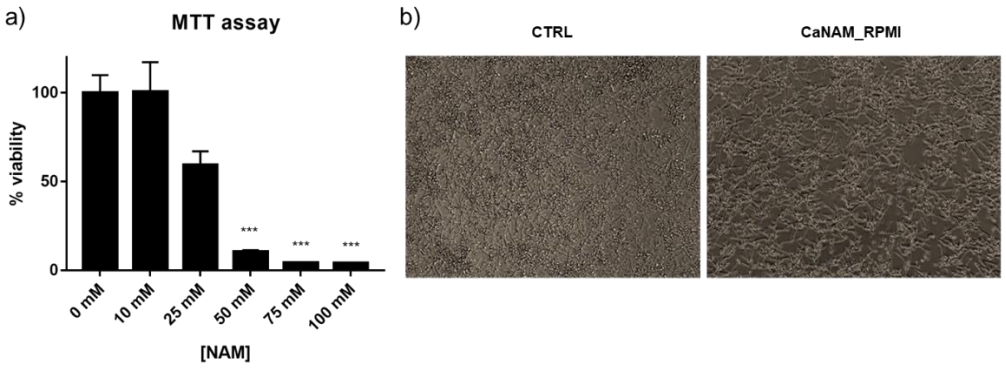

Fig. 36 - a) J774A.1 cell viability following the treatment with different concentrations of nicotinamide for 24 hours. Values are mean ± standard error of four replicates. *** P< 0.001 (t-test). b) Representative pictures of *C. albicans* cells treated for 6 h with 10 mM NAM. Exposure to 10 mM NAM impairs filamentation in hyphae-inducing conditions.

Furthermore, the stability of the nicotinamide in the designed experimental conditions was assessed by UV-Vis Spectroscopy (spectral range 200-350 nm). As expected, being a highly unstable molecule, NAM is rapidly degraded in a concentration-dependent manner and degradation subproducts occur after only 3 h when a 50 mM NAM solution in RPMI is incubated at 37ºC (data not shown).

All together these results suggest not only that the concentration used to obtain the *Candida* conditioned medium (Ca-CM), is not cytotoxic, but also that NAM degrades so fast that after *Candida* treatment and after filtration, the molecules present in the medium cannot have any cytotoxic effect on J774A.1 cells. Therefore, *C. albicans* was grown in RPMI medium at 37 ºC and 5% CO_2 with or without 10 mM NAM, the supernatants were collected from overnight cultures and filter-sterilized. J774A.1 macrophages were treated with Ca-CM and CaNAM-CM and successively stained with TRITC-Phalloidin at different time points to follow changes in actin cytoskeleton by confocal microscopy.

Interestingly, morphological changes in the actin cytoskeleton were observed already after 4 h of exposure to CaNAM-CM, with activated macrophages having linear filopodia (Fig. 37, CaNAM-CM). This effect was not observed in cells treated with Ca-CM, where the actin appears more localized around the nucleus with abnormal membrane ruffle (Fig. 37, Ca-CM). Moreover, none of these effects were observed in macrophages treated with only NAM (NAM-M), which appeared more similar to non-treated control cells (CTRL_M), further excluding the possibility of cytotoxic effects resulting from the exposure to NAM (Fig. 37 top panels).

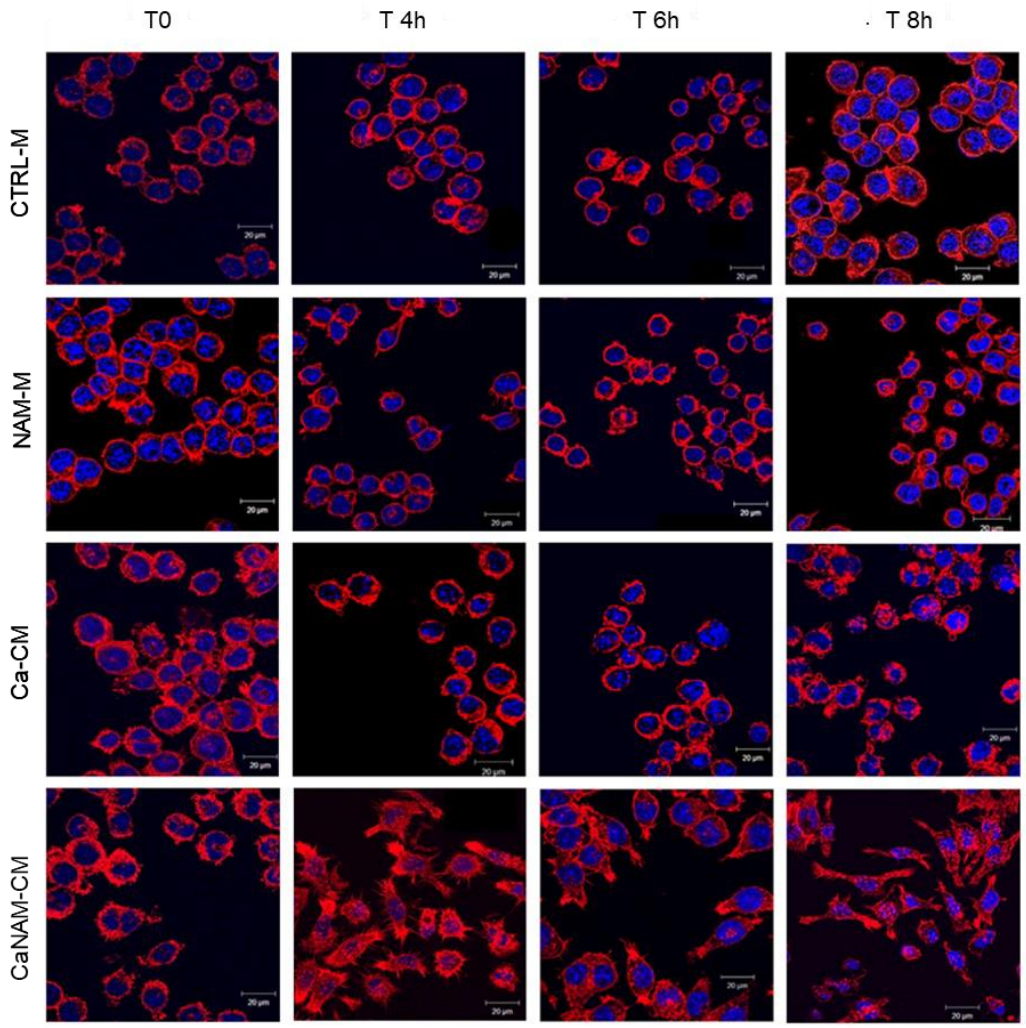

Fig. 37 - TRITC- phalloidin stained J774A.1 analyzed by confocal microscopy after 4, 6, and 8 hours of exposure to filter-sterilized supernatants collected from *C. albicans* (Ca-CM) or *C. albicans* + 10 mM NAM (CaNAM-CM) compared to cells treated with 10 mM only and non-treated (CTRL).

These observations suggest that *C. albicans* H3K56 acetylation levels influence the production of metabolites that compromise macrophages response by affecting the actin structure of the cytoskeleton.

8.2. Hst3 inhibition induces the production of metabolites improving the phagocytic activity of J774A.1 cells

Given the role of actin remodeling during phagocytosis, the observed cytoskeleton remodeling leads to hypothesize a direct effect on the phagocytic activity of macrophages. To verify this hypothesis, J774A.1 cells were pre-stimulated for 8 h with Ca-CM or CaNAM-CM and then infected with *Candida* yeasts. Again, the infection was also monitored in RPMI only and upon treatment with 10 mM NAM as a control. The infection was followed by Time-Lapse imaging up to 2 hours, revealing that the stimulation with CaNAM-CM results in an improved phagocytic activity, with an almost complete *Candida* phagocytosis after only 30 min (Fig. 38a, orange arrows). On the contrary, phagocytosis was delayed upon exposure to Ca-CM, and *Candida* cells were still outside macrophages even after 2 hours of infection (Fig. 38a, red arrows). Furthermore, no significant differences in phagocytic activity were observed between the macrophages pre-treated with CTRL-M and NAM-M. These findings are consistent with the different cytoskeleton organizations observed by confocal microscopy and were confirmed by Hotchkiss–McManus stain, which emphasized the clear difference both in morphology and phagocytic activity of macrophages (Fig. 38b).

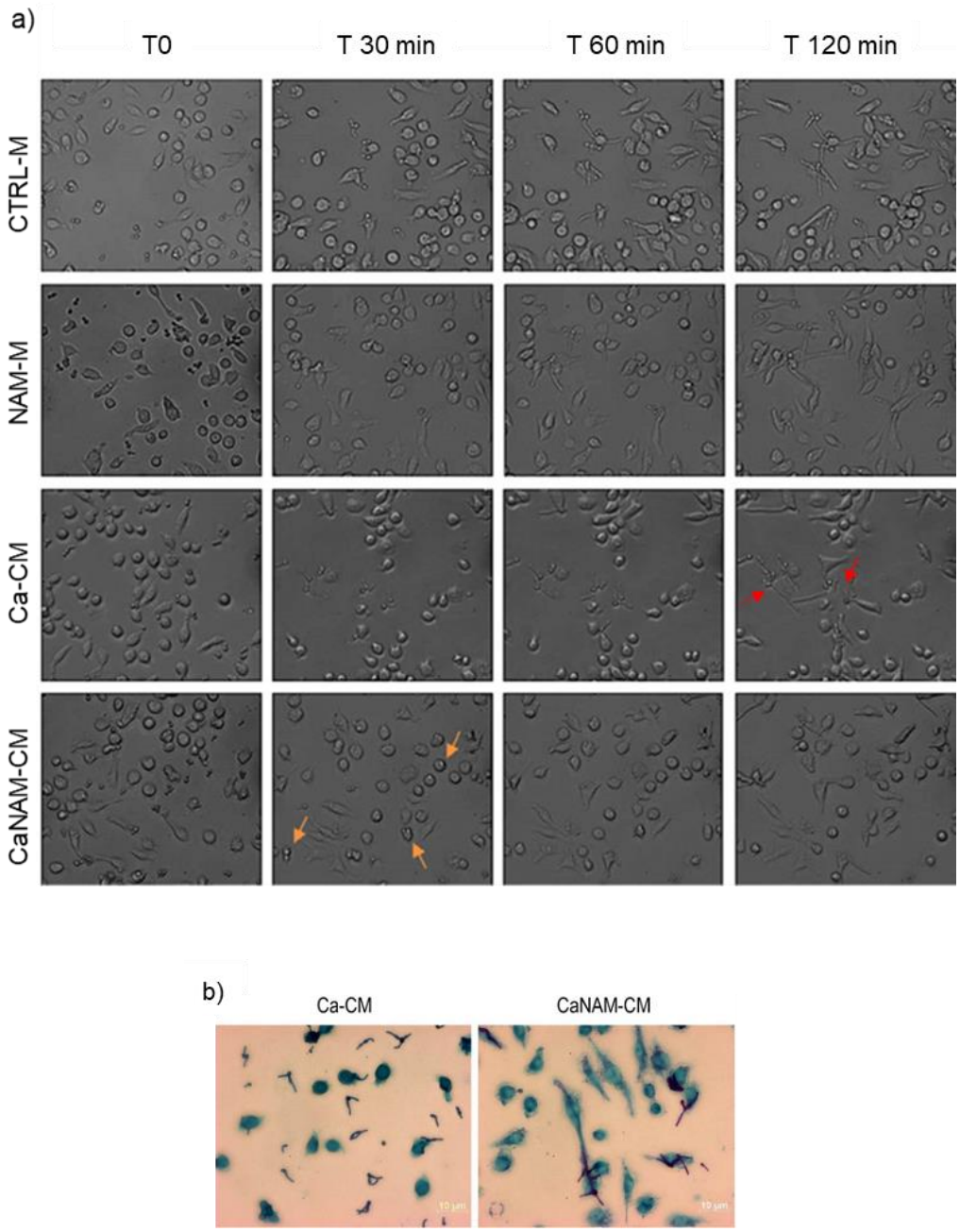

Fig. 38 - a) Automated Time-Lapse imaging of *C. albicans* infecting J774A.1 cells pre-stimulated with filter-sterilized supernatants collected from *C. albicans* (Ca-CM) or *C. albicans* + 10 mM NAM (CaNAM-CM) compared to cells treated with 10 mM only and non-treated (CTRL). b) Hotchkiss–McManus stained cells after 2 hours of infection. Macrophages are blue-stained, while the purple-stained are *Candida* germ tubes.

Overall, these results show that the inhibition of the histone deacetylase Hst3 induces an alteration in the production of metabolites that modulate the phagocytic activity of J774A.1 macrophages by inducing changes in the actin structures of the cytoskeleton, pointing out the possible role of H3K56 acetylation in regulating the metabolic pathways involved in the biosynthesis of such molecules.

8.3. Farnesol production is induced upon Hst3 inhibition.

Several studies have already demonstrated that *C. albicans* is able to modulate the activity of immune cells in multiple ways. In particular, host-immune recognition depends on cell wall rearrangements with consequent exposure of PAMPs. Nevertheless, the finding that *C. albicans* supernatants have some activity on J774A.1 cells suggests that the fungus could also produce soluble and stable molecules influencing the macrophage response, regardless of the presence or absence of viable *Candida* cells.

Quorum sensing molecules (QSMs) are emerging players in modulating immune cell response, and several studies have shown that farnesol activates innate immune cells and stimulates macrophages migration (92; 96). Based on these considerations, a quantitative MS Analysis of Ca-CM and CANAM-CM was performed to assess if H3K56ac levels could regulate the production of such QSM. To this purpose, *C. albicans* supernatants were collected from overnight cultures and used for the metabolomic analysis in collaboration with Prof. Maria Chiara Monti of the University of Salerno. As shown in Figure 39, farnesol was significantly more abundant in the supernatants of *C. albicans* grown upon Hst3 inhibition (CaNAM-CM) compared to supernatants control (Ca-CM), suggesting that the production of such a molecule is likely to be regulated by an epigenetic mechanism involving H3K56 acetylation.

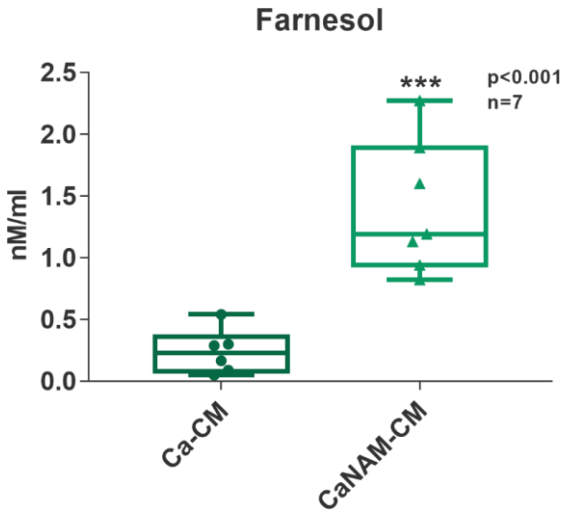

Fig. 39 – Farnesol quantification of Ca-CM and CaNAM-CM by MS Analysis.

8.3. Genome-wide analysis of H3K56ac across *C. albicans* genome in hyphae-inducing conditions

Epigenetic modifications are highly dynamic and changes in histone mark patterns may occur quickly in response to external stimuli. For instance, hypoxia impacts both histone acetylation and methylation inducing changes in chromatin accessibility (121). Indeed, while increasing global histone methylation, hypoxia decreases the acetyl-CoA level, resulting in a reduction in histone acetylation (121). To assess how H3K56ac patterns can influence *C. albicans* transcriptional expression in environmental conditions that mimic an *in vitro* infection, *C. albicans* cells were grown in hyphae-inducing conditions (RPMI, 37°C, 5% CO_2), with or without 10 mM NAM, and successively subjected to ChIP-seq analysis. Interestingly, as shown in the plot profiles in Figure 40, a different distribution in genomic regions across the TSS of genes was observed in CTRL_RPMI. By contrast, the profile distribution of CaNAM_RPMI was quite similar to that observed in both CTRL_YPD and CaNAM_YPD, yeast and V-shaped morphology respectively (Figure 31).

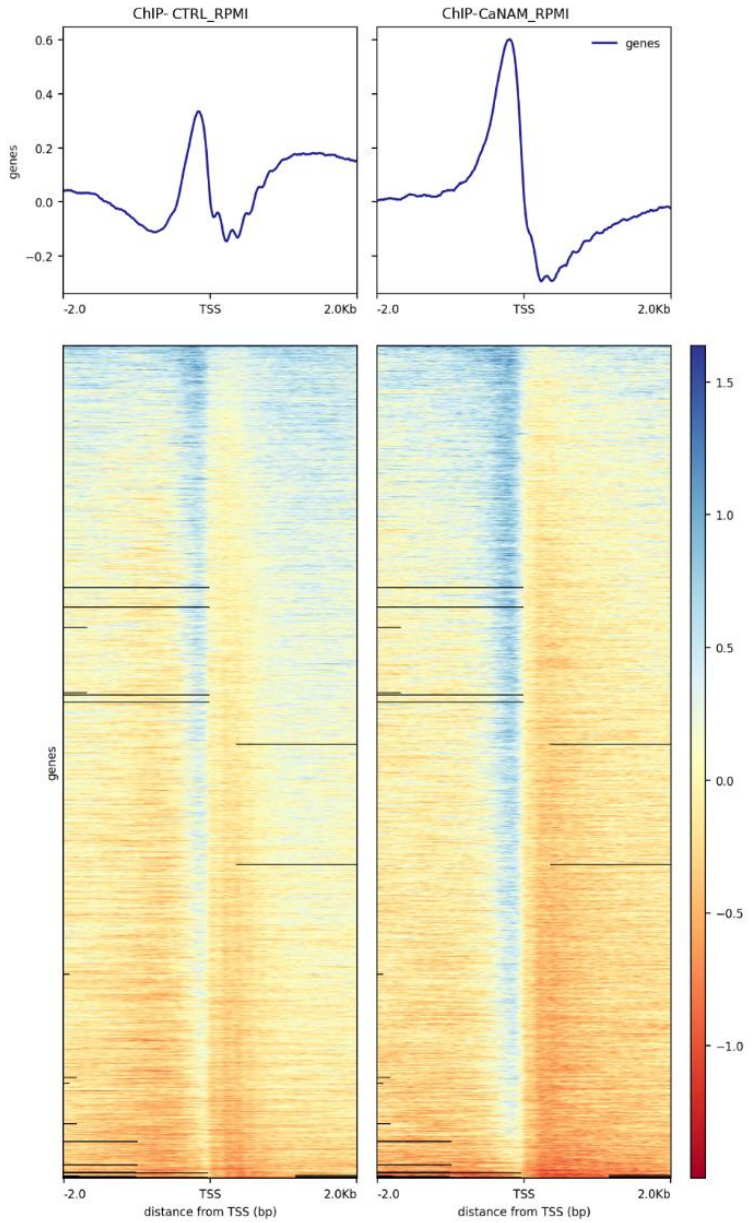

Fig. 40 - Representative profile heatmap around TSS of RefSeq genes showing the scores associated with genomic regions around the TSS of genes (± 2 kb). The gradient blue-to-red color indicates the high-to-low log2 ratio of the number of reads between the IP and the respective Input counts in the corresponding region.

ChIP-enriched promoters in hyphae-inducing condition were 509 and 717 for ChIP-CTRL_RPMI and ChIP-CaNAM_RPMI, respectively. Focusing on

the ChIP-enriched promoters, 181 regions were common to both experimental conditions, and 429 regions were enriched exclusively upon NAM treatment. ClueGO analysis revealed a weaker enrichment of GO terms relative to filamentation and biofilm formation compared to ChIP-CaNAM_YPD. This is consistent with the fact that the experimental conditions (basic pH, CO_2) promote the formation of hyphae, even though NAM treatment slows down their elongation. Also, no significant enrichment was observed for genes involved in white-opaque switching (Fig. 41).

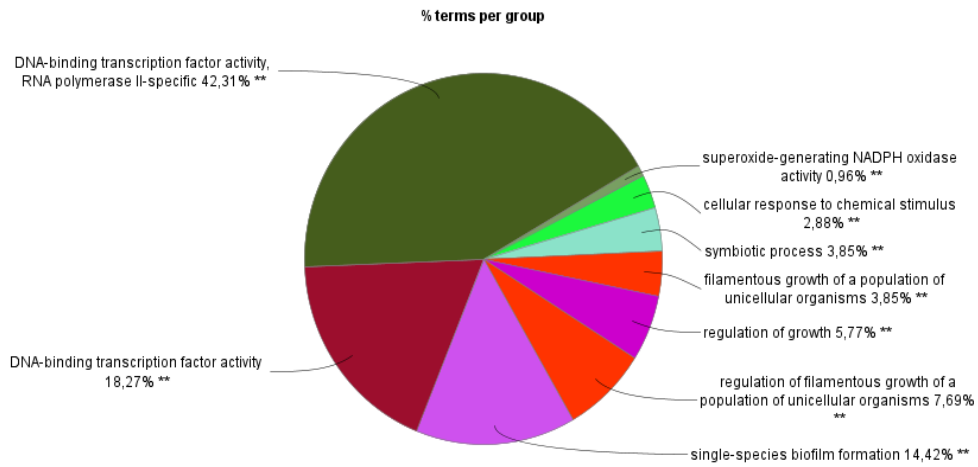

Fig. 41 - Biological process enrichment analysis using ClueGO Cytoscape plugin. Pie chart showing significantly enriched GO-terms in 429 regions ChIP-enriched exclusively in CaNAM_RPMI. The most significant term defined the group name. Asterisks denote GO-term significance. (Bonferroni adjusted pValue ≤0.05).

Noteworthy, GO analysis pointed out a strong enrichment for GO terms related to transcription factors activity (Fig. 41), confirming a possible role of such histone mark in transcriptional response. To clarify how acetylation patterns of H3K56 change in hyphae-inducing condition *vs* yeast-promoting condition (RPMI, 37°C, 5% CO_2 vs YPD, 25°C), ChIP promoter annotation enriched only upon NAM treatment of both experimental conditions were

compared. As a result, only 79 regions were shared between CaNAM_RPMI and CaNAM (Fig. 42), including key transcription regulators involved in morphological and phenotypic switching such as *OFI1*, *EFG1*, *NRG1*, *WOR2*, *WOR3*, *RFG1*.

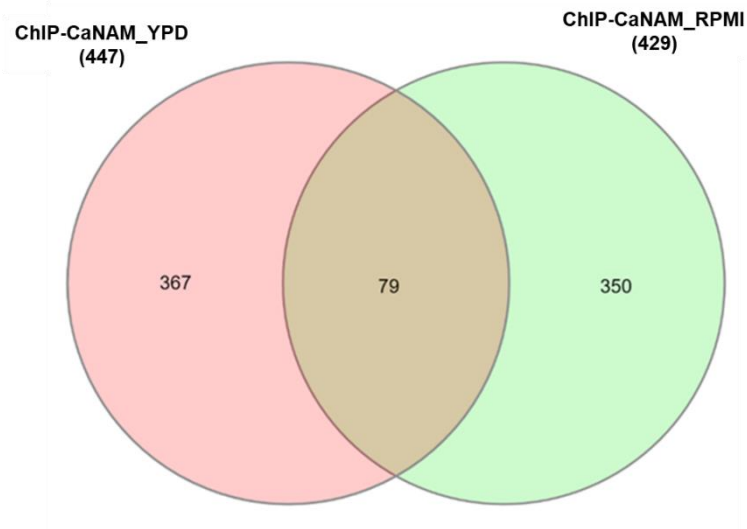

Fig. 42 - Venn diagram showing the overlapping ChIP-enriched region upon NAM treatment in the two experimental conditions assayed.

Altogether, these results highlight the consistent changes in chromatin organization in response to environmental stimuli that could contribute to the peculiar resilience of this opportunistic fungus.

8.3.1. Transcriptome analysis

To integrate the ChIP-seq results, RNA sequencing was performed, revealing a transcriptome dysregulation following the exposure to NAM, as already observed in V-shaped *versus* yeast. Specifically, 958 up-regulated and 985 down-regulated genes (FDR ≤ 0.05) were identified in CaNAM_RPMI *vs* CTRL_RPMI (Fig. 43).

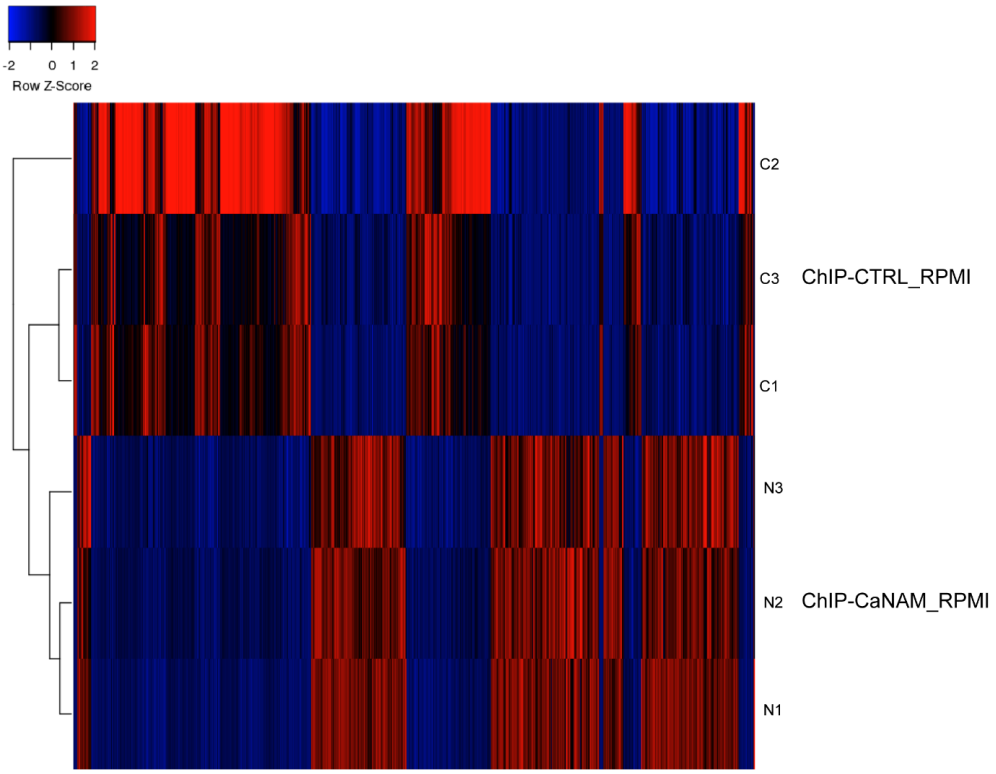

Fig. 43 - Heatmap showing the expression levels in log2 RPKM of differentially expressed genes upon NAM treatment in hyphae-inducing conditions (FDR ≤0.05).

Among them, an important dysregulation was observed in transcripts abundance of genes involved in β-glucan and mannan exposure, cell wall proteins biosynthesis and hydrolytic enzymes secretion (i.e. *PGA5*, *YWP1*, *KRE1*, *XOG1*, *ACF2*) (Fig. 44), pointing out a possible role of H3K56ac in interfering with the host-immune recognition and facilitating the host immune escaping.

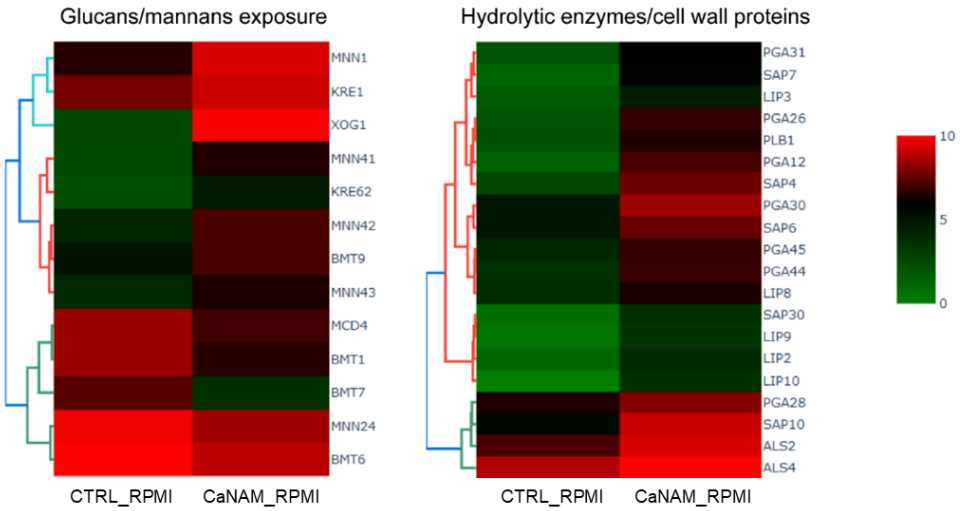

Fig. 44 - Heatmaps showing the expression levels in log2 RPKM of selected genes involved in glucans/mannans exposure, cell wall remodeling and hydrolytic enzymes biosynthesis (FDR ≤0.05; distance measure: Euclidean; clustering algorithm: Ward).

Moreover, RNA-seq showed a down-regulation of *EPT1* in NAM-treated cells (CaNAM_RPMI). This enzyme, responsible for the final step of phosphatidylethanolamine and phosphatidylcholine biosynthesis, has been shown to modulate the host immune recognition and its overexpression increases hyphal length (122). Therefore, its lower transcript abundance in CaNAM_RPMI cells is consistent with the reduction in hyphae length observed phenotype following NAM treatment. Among the up-regulated genes, 481 were common to both RNA-seq experiments (hyphae inducing and yeast promoting conditions) (Fig. 45) and, also in this case, most of them are genes involved in cell wall and β-glucan biosynthetic processes. In addition, 294 down-regulated transcripts were common to both experiments (Fig. 45). Of interest, most of the down-regulated genes are involved in biosynthesis, processing and transport of acetyl-CoA, suggesting a possible balance mechanism activated in response to the hyperacetylation due to NAM treatment. For instance, *CAT2*, the major carnitine acetyl transferase responsible for intracellular acetyl-CoA transport (123), *PXP2*, the acyl-CoA

oxidase responsible for the first step of acetyl-CoA biosynthesis from imported fatty acids (124), the citrate synthase *CIT1*, the pyruvate dehydrogenase kinase *PDK2*, along with several glucose transporters.

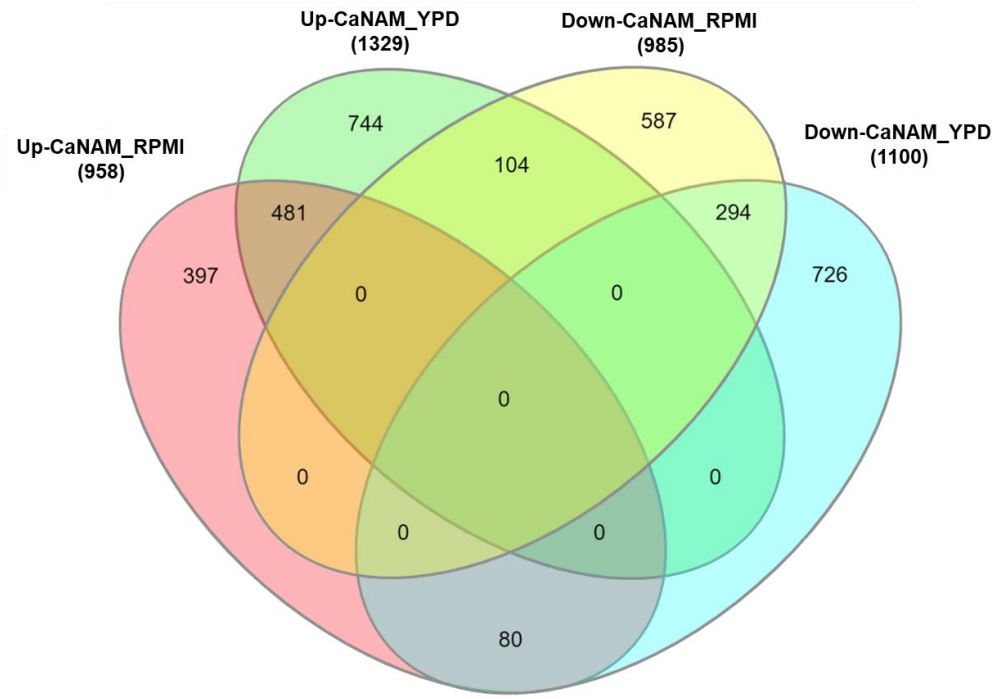

Fig. 45 - Venn diagram summarizing all the significant (FDR ≤ 0.05) dysregulated transcripts in both RNA sequencing experiments.

Integrating RNA-seq with ChIP-seq results, only 37 genes showed a direct correlation between promoter acetylation and transcript levels (Fig. 46), including *DPP1*, one of the three pyrophosphatases (*DPP1*, *DPP2*, *DPP3*) with a possible role in farnesol biosynthesis (125), further explaining the higher amount of this molecule in CaNAM-CM. Moreover, a correlation was observed between acetylation associated to the promoter and increased transcription of *YWP1*, encoding for the cell wall protein Ywp1, a yeast-specific protein that has been detected also in the pseudohyphae (126). Ywp1 is responsible for biofilm dispersion and in the β-glucan masking control,

consequently its overexpression might have a role in dissemination and host-immune evasion.

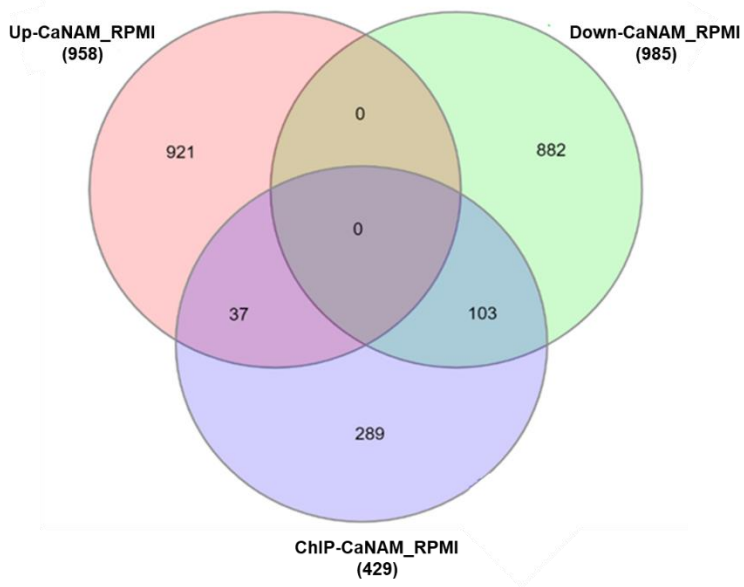

Fig. 46 - Venn diagram showing the overlapping genes between RNA-seq dysregulated transcripts and ChIP-seq regions enriched exclusively in CaNAM_RPMI.

Overall, these results reveal a complex mechanism behind the gene regulation mediated by H3K56 acetylation, underlining the importance of such histone mark in controlling a wide range of biological processes in *C. albicans*.

Chapter IX: Hst3 purification

9.1. Optimization of Hst3 protein expression in *Saccharomyces cerevisiae*

Antifungal resistance is a cause for great concern worldwide, given the difficulty in finding specific targets for the development of new antifungals due to the similarity between fungi and human cells. ChIP-seq and transcriptomic results, in addition to previous studies showing that Hst3 is essential for the fungus viability and virulence (109), make Hst3 an attractive and unique therapeutic target, (109). Moreover, a very important feature to keep in mind is that fungal Hst family members share sequence motifs that are absent in human sirtuins.

In order to obtain the recombinant protein rHst3 to be used for screening of new potential inhibitors, and considering that BLR(DE3) /pET28/*HST3* is not the optimal expression system since the recombinant protein remains unfolded and complexed to the bacterial chaperonine GroEL (data not shown), *HST3* was cloned in pYES/NT/A vector. The latter is optimized for the expression in *S. cerevisiae* INVSc1 competent cells, in which the recombinant protein (rHst3) is synthetized as a fusion protein with a N-terminal histidine tag. After selecting transformants from YNB/URA$^-$ plates, a time course was performed to optimize the expression conditions of the recombinant protein. A total amount of 0.4 OD from the overnight culture was used for the induction in SC Minimal Medium URA$^-$ containing 2% galactose at 30°C. Cells were collected at 0, 4, 6, 8, 24 h and analyzed by Western Blotting using an anti poly-Histidine. The optimal condition for the expression of the recombinant protein was 8 h of induction at 30°C (data not shown).

9.1.1. Recombinant protein purification

Once optimized the protein expression conditions, the total lysate from induced INVSc1/*HST3* cells was loaded on a His-Trap HP column for the His-tag affinity purification step. Flow-through and fractions samples were analyzed by Western Blotting, which indicates a higher accumulation of the recombinant protein in the flow-through compared to the fractions (Fig. 45) leading to the speculation that the protein structure might mask the recognition of the His-tag. However, His-tag affinity purification in denaturing conditions with 8 M Urea did not lead to any improvement. Since similar results were obtained using an ion exchange chromatography (Fig. 47), suggesting that the protein precipitates in any of the tested conditions, we decided to change expression system to improve the solubility and the purification yield.

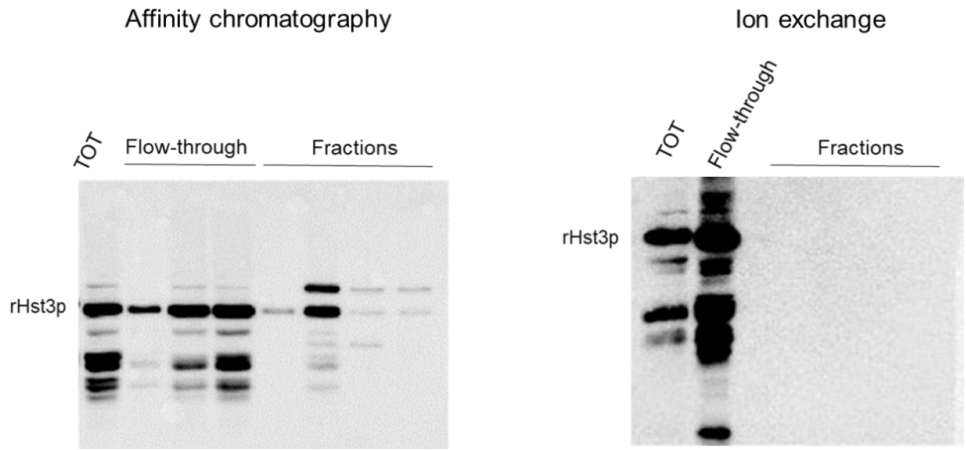

Fig. 47 - Western blot anti HisTag relative to rHst3 purification by affinity chromatography and ion exchange chromatography from *S. cerevisiae* expression host.

10.1. *HST3* cloning in pETM11-6xHis-SUMO3 vector and expression in *E. coli*

Given the technical issues in purifying the protein from INVSc1/*HST3* expression system, the sequence was cloned in pETM11-6xHis-SUMO3 vector and expressed in BL21-CodonPlus competent cells. SUMO fusion

technology has been shown to be superior to commonly used fusion tags in enhancing expression and solubility, and is largely used for difficult-to-express proteins (127; 128). To determine the optimum induction conditions, different temperatures, time of induction and IPTG concentrations were assayed. In particular, BL21/*HST3* cells were grown at 37°C up to OD_{600} of 0.8 before IPTG addition. The cultures were then incubated at 25° and 37°C with 1- or 2-mM IPTG up to 6 h. Every 2 h, 1.5 ml of each sample were taken, cells were lysed and analyzed by SDS-PAGE. Since the expression levels of the recombinant protein did not change significantly among all the condition assayed, of the induction condition 1 h with 1 mM IPTG at 37°C was chosen (data not shown). After the induction, cells were lysed and centrifuged to remove cellular debris. The supernatant was used for the purification using Ni-NTA agarose beads, whereas the pellet was resuspended in denaturing buffer to evaluate the insoluble fraction precipitated in the inclusion bodies. As shown in Fig. 48, the rHst3 protein was slightly soluble since it was more abundant in the inclusion bodies compared to the eluted fraction. Also, no significant enrichment in the eluted fraction compared to unbound was observed.

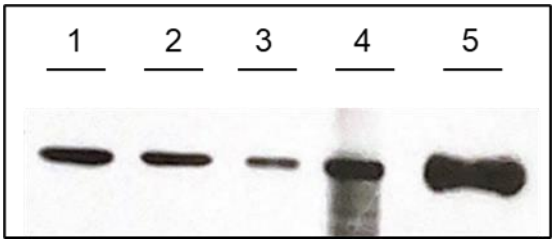

Fig. 48 - Western blot anti HisTag relative to rHst3 purification by affinity chromatography. 1) unbound; 2) washing 1; 3) washing 2; 4) eluted; 5) inclusion bodies.

DISCUSSION

The emergence of fungal strains resistant to the main antifungal drugs is an increasing concern due to the growing number of nosocomial infections caused by *Candida* spp. In particular, the opportunistic fungus *C. albicans* is the most prevalent species causing disease in both adult and pediatric populations, with a 30-day mortality rate approaching 40% in immunocompromised hosts (57). However, the identification and development of new potential drugs targeting the microbial cell without damaging the host is furtherly limited by the similarity between fungal and human cells (62).

In *C. albicans*, histone acetylation/deacetylation balance plays a crucial role in growth and virulence (107). In particular, H3K56 acetylation is the most abundant post-translational modification, regulated by the histone acetyltransferase Rtt109 and the histone deacetylase Hst3, which displays sequence motifs not shared with human sirtuins (109). Therefore, this histone deacetylase represents a promising therapeutic target for developing new antifungal agents. Several known deacetylase inhibitors have already been explored as new potential antifungal drugs, but the selectivity of such molecules remains the main problem (107). Belonging to the NAD+-dependent sirtuin family, Hst3 is inhibited by NAM. However, NAM is a non-specific and non-selective sirtuin inhibitor.

In the present work, three currently available sirtuin inhibitors (Inauhzin, Sirtinol, and SirReal2) were tested. Still, none of them showed activity on Hst3 since they did not induce either morphological alterations in *Candida* or a significant accumulation of H3K56ac, as demonstrated by Western blotting. Therefore, NAM was used as an Hst3 inhibitor to explore the effects of H3K56ac accumulation in *Candida albicans*. Consistent with previous studies, Hst3 inhibition resulted in abnormal phenotypes; specifically, when *Candida* is grown under hyphae-inducing conditions, there is a substantial filamentation

reduction. By contrast, as previously observed by Wurtele and colleagues (109), when Hst3 is inhibited under yeast-promoting conditions, *Candida* forms an abnormal phenotype, namely V-shaped hyphae.

Since the V-shaped hyphae is a peculiar morphology associated with increased levels of H3K56ac, those cells were used as a model to identify Hst3 targets. Preliminary transcriptomic studies showed a significant dysregulation following Hst3 inhibition with 1330 up-regulated and 1081 down-regulated transcripts in CaNAM_YPD compared to CTRL_YPD. Gene Ontology analysis confirmed that, among the up-regulated transcripts, there are mainly genes related to filamentation, cell wall organization, and adhesion giving rise to the possibility that H3K56, through its acetylation status, regulates these processes. Moreover, ChIP-seq analysis revealed a strong enrichment of H3K56ac across the TSS of genes.

Noteworthy, 447 regions were ChIP-enriched only upon NAM treatment, including HSGs, genes encoding for adhesin proteins, degradative enzymes, and white-opaque switching.

Interestingly, 87 genes showed a direct correlation between transcripts upregulation and H3K56 acetylation on their promoters. One of them is the zinc-finger transcription factor *OFI1*, whose over-expression promotes filamentous growth in several culture conditions (129). A second one is *WAL1*, required for the organization of the cortical actin cytoskeleton and the polarized hyphal growth (130). Notably, our ChIP-seq revealed the presence of H3K56ac in the promoter of *EFG1*, whose transcript abundance is lower in CaNAM_YPD compared to CTRL_YPD. This is consistent with previous studies showing that overexpression of *EFG1* facilitates hyphal initiation but, shortly after that, leads to Efg1-dependent transcript down-regulation (116; 117). Furthermore, *EFG1* is repressed both directly and indirectly by Wor1 (132), which is up-regulated upon NAM treatment. Efg1, acting via the cAMP-PKA pathway, regulates the expression of several genes involved in the

filamentation, such as *UME6*, a known hyphal extension regulator upregulated in the V-shaped conditions (131). These results might explain the abnormal phenotype, namely V-shaped hyphae, observed in *C. albicans* cells exposed to NAM in yeast-promoting conditions.

Another peculiar characteristic of this opportunistic fungus is the ability to escape the host immune response. Several mechanisms have been described by which *C. albicans* could evade the phagosome and/or mitigate the recognition by innate immune cells. However, a growing number of studies pointed out the role of *C. albicans* secretome in influencing host immune cells (91; 92; 93; 120). In this study, the secretomes recovered from *C. albicans* cultures treated (CaNAM-CM) or not (Ca-CM) with NAM were used to stimulate the murine macrophages J774A.1. Significant morphological changes were observed in the actin structure of cytoskeleton, with activated macrophages after only 4 h of exposure to CaNAM-CM. Interestingly, this effect was not observed in cells treated with Ca-CM, where the actin appears more localized around the nucleus and with abnormal membrane ruffle, suggesting that H3K56 acetylation levels influence the production of metabolites that compromise macrophages response by affecting the actin structure of the cytoskeleton.

Given the role of actin remodeling in phagocytosis, the effects of exposure to CaNAM-CM and Ca-CM on the phagocytic activity were investigated. Notably, the stimulation with CaNAM-CM resulted in an improved phagocytic activity compared to macrophages pre-exposed to CM, whose phagocytic activity was delayed. Finally, based on literature studies, some QSMs were quantified by MS analysis, to identify the molecules possibly responsible for the observed effects on the macrophages. Among them, we found farnesol significantly more abundant in CaNAM-CM than Ca-CM. This molecule has been shown to induce macrophage activation and migration through the infection site.

Since histone modifications are highly dynamic, transcriptomic and ChIP-seq studies were also performed in infection conditions. Surprisingly, in ChIP-CTRL_RPMI, a different genomic distribution of H3K56ac was observed. Indeed, even if most of the enriched regions mapped across the TSS of genes, a less localized distribution of the ChIP-enriched regions was also observed in intergenic regions. By contrast, the genomic distribution of the ChIP-enriched regions in ChIP-CaNAM_RPMI was more localized upstream of the TSS of the genes. In infection conditions, the regions ChIP-enriched only upon NAM treatment were 429, and GO analysis revealed a strong enrichment for GO terms relative to the transcription factors activity.

Moreover, a significant transcriptome dysregulation was observed in infection conditions as well, with 958 up-regulated and 985 down-regulated transcripts in CaNAM_RPMI *vs* CTRL_RPMI. Interestingly, an important dysregulation was observed in transcripts abundance of genes involved in PAMPs biosynthesis and exposure, pointing out a possible role of H3K56ac in interfering with the host-immune recognition and facilitating the host immune escaping.

Noteworthy, only 37 genes showed a direct correlation between promoter acetylation and transcript levels. Among them, *DPP1*, a pyrophosphatase with a possible role in farnesol biosynthesis, and *YWP1* encoding for the cell wall protein Ywp1, responsible for biofilm dispersion and in the β-glucan masking control. Intersecting both the RNA-seq experiments, 481 genes were up-regulated in both infection and yeast-promoting conditions. They were mainly transcripts of genes involved in the cell wall and β-glucan biosynthetic process. In addition, 294 down-regulated transcripts were common to both experiments, especially transcripts of genes involved in biosynthesis, processing, and transport of acetyl-CoA, suggesting that a balance mechanism would be activated in response to the hyperacetylation due to NAM treatment.

Overall, the present study represents the first genome-wide H3K56 acetylation analysis in *C. albicans* and provides the first map of H3K56ac distribution across the *C. albicans* genome in two different growth conditions, representing a rich resource for future studies. Nevertheless, the evidence that H3K56ac directly regulates the expression of several virulence-related genes, as well as genes involved in the regulation of host immune escaping, points out the relevance of such epigenetic modification in regulating *C. albicans* virulence, confirming that Hst3 is an appealing target for the development of new potential antifungal drugs.

BIBLIOGRAPHY

(1) Lopes JP, Lionakis MS. Pathogenesis and virulence of *Candida albicans*. Virulence. 2022 Dec;13(1):89-121

(2) Jaroš P, Vrublevskaya M, Lokočová K, Michailidu J, Kolouchová I, Demnerová K. *Boswellia* *serrata* Extract as an Antibiofilm Agent against *Candida* spp. Microorganisms. 2022 Jan 13;10(1).

(3) Legrand M, Jaitly P, Feri A, d'Enfert C, Sanyal K. *Candida albicans*: An Emerging Yeast Model to Study Eukaryotic Genome Plasticity. Trends Genet. 2019 Apr;35(4):292-307.

(4) Forche A, Alby K, Schaefer D, Johnson AD, Berman J, Bennett RJ. The parasexual cycle in *Candida albicans* provides an alternative pathway to meiosis for the formation of recombinant strains. PLoS Biol. 2008 May 6;6(5):e110.

(5) Bennett RJ, Johnson AD. Completion of a parasexual cycle in *Candida albicans* by induced chromosome loss in tetraploid strains. EMBO J. 2003 May 15;22(10):2505-15.

(6) Hickman MA, Paulson C, Dudley A, Berman J. Parasexual Ploidy Reduction Drives Population Heterogeneity Through Random and Transient Aneuploidy in *Candida albicans*. Genetics. 2015 Jul;200(3):781-94.

(7) Berman J. Ploidy plasticity: a rapid and reversible strategy for adaptation to stress. FEMS Yeast Res. 2016 May;16(3).

(8) Dunn MJ, Anderson MZ. To Repeat or Not to Repeat: Repetitive Sequences Regulate Genome Stability in *Candida albicans*. Genes (Basel). 2019 Oct 30;10(11).

(9) Todd RT, Wikoff TD, Forche A, Selmecki A. Genome plasticity in *Candida albicans* is driven by long repeat sequences. Elife. 2019 Jun 7;8.

(10) Moura GR, Lousado JP, Pinheiro M, Carreto L, Silva RM, Oliveira JL, Santos MA. Codon-triplet context unveils unique features of the *Candida albicans* protein coding genome. BMC Genomics. 2007 Nov 29;8:444.

(11) Garcia-Rubio R, de Oliveira HC, Rivera J, Trevijano-Contador N. The Fungal Cell Wall: *Candida*, *Cryptococcus*, and *Aspergillus* Species. Front Microbiol. 2019;10:2993.

(12) Childers DS, Avelar GM, Bain JM, Larcombe DE, Pradhan A, Budge S, Heaney H, Brown AJP. Impact of the Environment upon the *Candida albicans* Cell Wall and Resultant Effects upon Immune Surveillance. Curr Top Microbiol Immunol. 2020;425:297-330.

(13) Lenardon MD, Sood P, Dorfmueller HC, Brown AJP, Gow NAR. Scalar nanostructure of the *Candida albicans* cell wall; a molecular, cellular and ultrastructural analysis and interpretation. Cell Surf. 2020 Dec;6:100047. Ibe C, Munro CA. Fungal cell wall: An underexploited target for antifungal therapies. PLoS Pathog. 2021 Apr;17(4):e1009470.

(14) Basso V, d'Enfert C, Znaidi S, Bachellier-Bassi S. From Genes to Networks: The Regulatory Circuitry Controlling *Candida albican*s Morphogenesis. Curr Top Microbiol Immunol. 2019;422:61-99.

(15) Chen H, Zhou X, Ren B, Cheng L. The regulation of hyphae growth in *Candida albicans*. Virulence. 2020 Dec;11(1):337-348.

(16) Ciurea CN, Kosovski IB, Mare AD, Toma F, Pintea-Simon IA, Man A. *Candida* and Candidiasis-Opportunism Versus Pathogenicity: A Review of the Virulence Traits. Microorganisms. 2020 Jun 6;8(6).

(17) Noble SM, Gianetti BA, Witchley JN. *Candida albicans* cell-type switching and functional plasticity in the mammalian host. Nat Rev Microbiol. 2017 Feb;15(2):96-108

(18) Kadosh D. Regulatory mechanisms controlling morphology and pathogenesis in *Candida albicans*. Curr Opin Microbiol. 2019 Dec;52:27-34.

(19) Perry AM, Hernday AD, Nobile CJ. Unraveling How *Candida albicans* Forms Sexual Biofilms. J Fungi (Basel). 2020 Jan 15;6(1).

(20) Yue H, Hu J, Guan G, Tao L, Du H, Li H, Huang G. Discovery of the gray phenotype and white-gray-opaque tristable phenotypic transitions in *Candida dubliniensis*. Virulence. 2016 Apr 2;7(3):230-42.

(21) Nett JE. Special Issue: Candida and Candidiasis. J Fungi (Basel). 2018 Jun 21;4(3):74

(22) Zhang Y, Tang C, Zhang Z, Li S, Zhao Y, Weng L, Zhang H. Deletion of the ATP2 Gene in *Candida albicans* Blocks Its Escape From Macrophage Clearance. Front Cell Infect Microbiol. 2021 Apr 16;11:643121.

(23) Su C, Yu J, Lu Y. Hyphal development in *Candida albicans* from different cell states. Curr Genet. 2018 Dec;64(6):1239-1243.

(24) d'Enfert C, Kaune AK, Alaban LR, Chakraborty S, Cole N, Delavy M, Kosmala D, Marsaux B, Fróis-Martins R, Morelli M, Rosati D, Valentine M, Xie Z, Emritloll Y, Warn PA, Bequet F, Bougnoux ME, Bornes S, Gresnigt MS, Hube B, Jacobsen ID, Legrand M, Leibundgut-Landmann S, Manichanh C, Munro CA, Netea MG, Queiroz K, Roget K, Thomas V, Thoral C, Van den Abbeele P, Walker AW, Brown AJP. The impact of the Fungus-Host-Microbiota interplay upon *Candida albicans* infections: current knowledge and new perspectives. FEMS Microbiol Rev. 2021 May 5;45(3).

(25) Kornitzer D. Regulation of *Candida albicans* Hyphal Morphogenesis by Endogenous Signals. J Fungi (Basel). 2019 Feb 28;5(1).

(26) Mba IE, Nweze EI. Mechanism of *Candida* pathogenesis: revisiting the vital drivers. Eur J Clin Microbiol Infect Dis. 2020 Oct;39(10):1797-1819.

(27) Flanagan PR, Fletcher J, Boyle H, Sulea R, Moran GP, Sullivan DJ. Expansion of the TLO gene family enhances the virulence of *Candida* species. PLoS One. 2018;13(7):e0200852.

(28) Jenull S, Tscherner M, Gulati M, Nobile CJ, Chauhan N, Kuchler K. The *Candida albicans* HIR histone chaperone regulates the yeast-to-hyphae transition by controlling the sensitivity to morphogenesis signals. Sci Rep. 2017 Aug 16;7(1):8308.

(29) Veri AO, Miao Z, Shapiro RS, Tebbji F, O'Meara TR, Kim SH, Colazo J, Tan K, Vyas VK, Whiteway M, Robbins N, Wong KH, Cowen LE. Tuning Hsf1 levels drives distinct fungal morphogenetic programs with depletion impairing Hsp90 function and overexpression expanding the target space. PLoS Genet. 2018 Mar;14(3):e1007270.

(30) Shapiro RS, Uppuluri P, Zaas AK, Collins C, Senn H, Perfect JR, Heitman J, Cowen LE. Hsp90 orchestrates temperature-dependent *Candida albicans* morphogenesis via Ras1-PKA signaling. Curr Biol. 2009 Apr 28;19(8):621-9.

(31) Childers DS, Mundodi V, Banerjee M, Kadosh D. A 5' UTR-mediated translational efficiency mechanism inhibits the *Candida albicans* morphological transition. Mol Microbiol. 2014 May;92(3):570-85.

(32) Desai PR, Lengeler K, Kapitan M, Janßen SM, Alepuz P, Jacobsen ID, Ernst JF. The 5' Untranslated Region of the EFG1 Transcript Promotes Its Translation To Regulate Hyphal Morphogenesis in *Candida albicans*. mSphere. 2018 Jul 5;3(4).

(33) Padder SA, Ramzan A, Tahir I, Rehman RU, Shah AH. Metabolic flexibility and extensive adaptability governing multiple drug resistance and enhanced virulence in *Candida albicans*. Crit Rev Microbiol. 2022 Feb;48(1):1-20.

(34) Sellam A, Whiteway M. Recent advances on *Candida albicans* biology and virulence. F1000Res. 2016;5:2582.

(35) Qasim MN, Valle Arevalo A, Nobile CJ, Hernday AD. The Roles of Chromatin Accessibility in Regulating the *Candida albicans* White-Opaque Phenotypic Switch. J Fungi (Basel). 2021 Jan 9;7(1).

(36) Park YN, Pujol C, Wessels DJ, Soll DR. *Candida albican*s Double Mutants Lacking both EFG1 and WOR1 Can Still Switch to Opaque. mSphere. 2020 Sep 23;5(5).

(37) Nikou SA, Kichik N, Brown R, Ponde NO, Ho J, Naglik JR, Richardson JP. *Candida albicans* Interactions with Mucosal Surfaces during Health and Disease. Pathogens. 2019 Apr 22;8(2).

(38) Romo JA, Kumamoto CA. On Commensalism of Candida. J Fungi (Basel). 2020 Jan 17;6(1).

(39) Richardson JP, Ho J, Naglik JR. Candida-Epithelial Interactions. J Fungi (Basel). 2018 Feb 8;4(1).

(40) Wall G, Montelongo-Jauregui D, Vidal Bonifacio B, Lopez-Ribot JL, Uppuluri P. *Candida albicans* biofilm growth and dispersal: contributions to pathogenesis. Curr Opin Microbiol. 2019 Dec;52:1-6.

(41) Lohse MB, Gulati M, Johnson AD, Nobile CJ. Development and regulation of single- and multi-species *Candida albicans* biofilms. Nat Rev Microbiol. 2018 Jan;16(1):19-31.

(42) McCall AD, Pathirana RU, Prabhakar A, Cullen PJ, Edgerton M. *Candida albicans* biofilm development is governed by cooperative attachment and adhesion maintenance proteins. NPJ Biofilms Microbiomes. 2019;5(1):21.

(43) de Barros PP, Rossoni RD, de Souza CM, Scorzoni L, Fenley JC, Junqueira JC. *Candida* Biofilms: An Update on Developmental Mechanisms and Therapeutic Challenges. Mycopathologia. 2020 Jun;185(3):415-424.

(44) Pereira R, Dos Santos Fontenelle RO, de Brito EHS, de Morais SM. Biofilm of *Candida albicans*: formation, regulation and resistance. J Appl Microbiol. 2021 Jul;131(1):11-22.

(45) Mancera E, Nocedal I, Hammel S, Gulati M, Mitchell KF, Andes DR, Nobile CJ, Butler G, Johnson AD. Evolution of the complex transcription

network controlling biofilm formation in *Candida* species. Elife. 2021 Apr 7;10.

(46) Cauchie M, Desmet S, Lagrou K. *Candida* and its dual lifestyle as a commensal and a pathogen. Res Microbiol. 2017 Nov - Dec;168(9-10):802-810.

(47) Rapala-Kozik M, Bochenska O, Zajac D, Karkowska-Kuleta J, Gogol M, Zawrotniak M, Kozik A. Extracellular proteinases of *Candida* species pathogenic yeasts. Mol Oral Microbiol. 2018 Apr;33(2):113-124.

(48) Di Cosola M, Cazzolla AP, Charitos IA, Ballini A, Inchingolo F, Santacroce L. *Candida albicans* and Oral Carcinogenesis. A Brief Review. J Fungi (Basel). 2021 Jun 12;7(6).

(49) Schaller M, Borelli C, Korting HC, Hube B. Hydrolytic enzymes as virulence factors of *Candida albicans*. Mycoses. 2005 Nov;48(6):365-77.

(50) Aoki W, Kitahara N, Miura N, Morisaka H, Yamamoto Y, Kuroda K, Ueda M. Comprehensive characterization of secreted aspartic proteases encoded by a virulence gene family in *Candida albicans*. J Biochem. 2011 Oct;150(4):431-8.

(51) Harpf V, Rambach G, Würzner R, Lass-Flörl C, Speth C. *Candida* and Complement: New Aspects in an Old Battle. Front Immunol. 2020;11:1471.

(52) Moyes DL, Wilson D, Richardson JP, Mogavero S, Tang SX, Wernecke J, Höfs S, Gratacap RL, Robbins J, Runglall M, Murciano C, Blagojevic M, Thavaraj S, Förster TM, Hebecker B, Kasper L, Vizcay G, Iancu SI, Kichik N, Häder A, Kurzai O, Luo T, Krüger T, Kniemeyer O, Cota E, Bader O, Wheeler RT, Gutsmann T, Hube B, Naglik JR. Candidalysin is a fungal peptide toxin critical for mucosal infection. Nature. 2016 Apr 7;532(7597):64-8.

(53) Naglik JR, Gaffen SL, Hube B. Candidalysin: discovery and function in *Candida albicans* infections. Curr Opin Microbiol. 2019 Dec;52:100-109.

(54) Ho J, Yang X, Nikou SA, Kichik N, Donkin A, Ponde NO, Richardson JP, Gratacap RL, Archambault LS, Zwirner CP, Murciano C, Henley-Smith R, Thavaraj S, Tynan CJ, Gaffen SL, Hube B, Wheeler RT, Moyes DL, Naglik JR. Candidalysin activates innate epithelial immune responses via epidermal growth factor receptor. Nat Commun. 2019 May 24;10(1):2297.

(55) Lamoth F, Lockhart SR, Berkow EL, Calandra T. Changes in the epidemiological landscape of invasive candidiasis. J Antimicrob Chemother. 2018 Jan 1;73(suppl_1):i4-i13.

(56) Pappas PG, Lionakis MS, Arendrup MC, Ostrosky-Zeichner L, Kullberg BJ. Invasive candidiasis. Nat Rev Dis Primers. 2018 May 11;4:18026.

(57) Koehler P, Stecher M, Cornely OA, Koehler D, Vehreschild MJGT, Bohlius J, Wisplinghoff H, Vehreschild JJ. Morbidity and mortality of candidaemia in Europe: an epidemiologic meta-analysis. Clin Microbiol Infect. 2019 Oct;25(10):1200-1212.

(58) Mastrangelo A, Germinario BN, Ferrante M, Frangi C, Li Voti R, Muccini C, Ripa M; COVID-BioB Study Group. Candidemia in Coronavirus Disease 2019 (COVID-19) Patients: Incidence and Characteristics in a Prospective Cohort Compared With Historical Non-COVID-19 Controls. Clin Infect Dis. 2021 Nov 2;73(9):e2838-e2839.

(59) Nucci M, Barreiros G, Guimarães LF, Deriquehem VAS, Castiñeiras AC, Nouér SA. Increased incidence of candidemia in a tertiary care hospital with the COVID-19 pandemic. Mycoses. 2021 Feb;64(2):152-156.

(60) Kayaaslan B, Eser F, Kaya Kalem A, Bilgic Z, Asilturk D, Hasanoglu I, Ayhan M, Tezer Tekce Y, Erdem D, Turan S, Mumcuoglu I, Guner R. Characteristics of candidemia in COVID-19 patients; increased incidence, earlier occurrence and higher mortality rates compared to non-COVID-19 patients. Mycoses. 2021 Sep;64(9):1083-1091.

(61) R AN, Rafiq NB. Candidiasis. 2022 Feb 12. In: StatPearls [Internet]. Treasure Island (FL): StatPearls Publishing; 2022 Jan.

(62) Salazar SB, Simões RS, Pedro NA, Pinheiro MJ, Carvalho MFNN, Mira NP. An Overview on Conventional and Non-Conventional Therapeutic Approaches for the Treatment of Candidiasis and Underlying Resistance Mechanisms in Clinical Strains. J Fungi (Basel). 2020 Feb 10;6(1):23.

(63) Nami S, Aghebati-Maleki A, Morovati H, Aghebati-Maleki L. Current antifungal drugs and immunotherapeutic approaches as promising strategies to treatment of fungal diseases. Biomed Pharmacother. 2019 Feb;110:857-868.

(64) Mast N, Zheng W, Stout CD, Pikuleva IA. Antifungal Azoles: Structural Insights into Undesired Tight Binding to Cholesterol-Metabolizing CYP46A1. Mol Pharmacol. 2013 Jul;84(1):86-94.

(65) Szymański M, Chmielewska S, Czyżewska U, Malinowska M, Tylicki A. Echinocandins - structure, mechanism of action and use in antifungal therapy. J Enzyme Inhib Med Chem. 2022 Dec;37(1):876-894.

(66) Mroczyńska M, Brillowska-Dąbrowska A. Review on Current Status of Echinocandins Use. Antibiotics (Basel). 2020 May 2;9(5):227.

(67) Delma FZ, Al-Hatmi AMS, Brüggemann RJM, Melchers WJG, de Hoog S, Verweij PE, Buil JB. Molecular Mechanisms of 5-Fluorocytosine Resistance in Yeasts and Filamentous Fungi. J Fungi (Basel). 2021 Oct 27;7(11):909.

(68) Raj GM. Antifungal Drugs. 2021 March 14. In: Paul A, Anandabaskar N, Mathaiyan J, Raj GM. (eds) Introduction to Basics of Pharmacology and Toxicology. Springer, Singapore.

(69) Howard KC, Dennis EK , Watt DS , Garneau-Tsodikova S. A comprehensive overview of the medicinal chemistry of antifungal drugs: perspectives and promise. Chem Soc Rev. 2020 Apr 21;49(8):2426-2480.

(70) Costa-de-Oliveira S, Rodrigues AG. *Candida albicans* Antifungal Resistance and Tolerance in Bloodstream Infections: The Triad Yeast-Host-Antifungal. Microorganisms. 2020 Jan 22;8(2):154.

(71) Bhattacharya S, Sae-Tia S, Fries BC. Candidiasis and Mechanisms of Antifungal Resistance. Antibiotics (Basel). 2020 Jun 9;9(6):312.

(72) Nishimoto AT, Sharma C, Rogers PD. Molecular and genetic basis of azole antifungal resistance in the opportunistic pathogenic fungus *Candida albicans*. J Antimicrob Chemother. 2020 Feb 1;75(2):257-270.

(73) da Silva Dantas A, Lee KK, Raziunaite I, Schaefer K, Wagener J, Yadav B, Gow NA. Cell biology of *Candida albicans*-host interactions. Curr Opin Microbiol. 2016 Dec;34:111-118.

(74) Chen C, Huang X. *Candida albicans* Commensalism and Human Diseases. 2018 Jan 27 In: Sun J, Dudeja P. (eds) Mechanisms Underlying Host-Microbiome Interactions in Pathophysiology of Human Diseases. Physiology in Health and Disease. Springer, Boston, MA.

(75) Wang Y, Zhou J, Zou Y, Chen X, Liu L, Qi W, Huang X, Chen C, Liu NN. Fungal commensalism modulated by a dual-action phosphate transceptor. Cell Rep. 2022 Jan 25;38(4):110293.

(76) Bojang E, Ghuman H, Kumwenda P, Hall RA. Immune Sensing of *Candida albicans*. J Fungi (Basel). 2021 Feb 6;7(2):119.

(77) Cottier F, Hall RA. Face/Off: The Interchangeable Side of *Candida albicans*. Front Cell Infect Microbiol. 2020 Jan 28;9:471.

(78) Xu S, Shinohara ML. Tissue-Resident Macrophages in Fungal Infections. Front Immunol. 2017 Dec 12;8:1798.

(79) d'Enfert C, Kaune AK, Alaban LR, Chakraborty S, Cole N, Delavy M, Kosmala D, Marsaux B, Fróis-Martins R, Morelli M, Rosati D, Valentine M, Xie Z, Emritloll Y, Warn PA, Bequet F, Bougnoux ME, Bornes S, Gresnigt MS, Hube B, Jacobsen ID, Legrand M, Leibundgut-Landmann S, Manichanh C, Munro CA, Netea MG, Queiroz K, Roget K, Thomas V,

Thoral C, Van den Abbeele P, Walker AW, Brown AJP. The impact of the Fungus-Host-Microbiota interplay upon *Candida albicans* infections: current knowledge and new perspectives. FEMS Microbiol Rev. 2021 May 5;45(3):fuaa060.

(80) Valand N, Girija UV. *Candida* Pathogenicity and Interplay with the Immune System. Adv Exp Med Biol. 2021;1313:241-272.

(81) Loureiro A, Pais C, Sampaio P. Relevance of Macrophage Extracellular Traps in C. albicans Killing. Front Immunol. 2019 Dec 4;10:2767.

(82) Kumaresan PR, da Silva TA, Kontoyiannis DP. Methods of Controlling Invasive Fungal Infections Using CD8+ T Cells. Front Immunol. 2018 Jan 8;8:1939.

(83) Austermeier S, Kasper L, Westman J, Gresnigt MS. I want to break free - macrophage strategies to recognize and kill *Candida albicans*, and fungal counter-strategies to escape. Curr Opin Microbiol. 2020 Dec;58:15-23.

(84) Chen T, Wagner AS, Reynolds TB. When Is It Appropriate to Take Off the Mask? Signaling Pathways That Regulate ß(1,3)-Glucan Exposure in *Candida albicans*. Front in Fungal Biol. 2022 March 9; Vol 3.

(85) Pradhan A, Avelar GM, Bain JM, Childers D, Pelletier C, Larcombe DE, Shekhova E, Netea MG, Brown GD, Erwig L, Gow NAR, Brown AJP. Non-canonical signalling mediates changes in fungal cell wall PAMPs that drive immune evasion. Nat Commun. 2019 Nov 22;10(1):5315.

(86) Oliver JC, Ferreira CBRJ, Silva NC, Dias ALT. *Candida* spp. and phagocytosis: multiple evasion mechanisms. Antonie Van Leeuwenhoek. 2019 Oct;112(10):1409-1423.

(87) Luo S, Dasari P, Reiher N, Hartmann A, Jacksch S, Wende E, Barz D, Niemiec MJ, Jacobsen I, Beyersdorf N, Hünig T, Klos A, Skerka C, Zipfel PF. The secreted *Candida albicans* protein Pra1 disrupts host defense by broadly targeting and blocking complement C3 and C3 activation fragments. Mol Immunol. 2018 Jan;93:266-277.

(88) Hornby JM, Jensen EC, Lisec AD, Tasto JJ, Jahnke B, Shoemaker R, Dussault P, Nickerson KW. Quorum sensing in the dimorphic fungus *Candida albicans* is mediated by farnesol. Appl Environ Microbiol. 2001 Jul;67(7):2982-92.

(89) Pathak P, Sahu P. Perspective of Quorum Sensing Mechanism in *Candida albicans*. In: Pallaval Veera Bramhachari (eds) Implication of Quorum Sensing System in Biofilm Formation and Virulence. Springer, Singapore. 2019 Jan 29;

(90) Mehmood A, Liu G, Wang X, Meng G, Wang C, Liu Y. Fungal Quorum-Sensing Molecules and Inhibitors with Potential Antifungal Activity: A Review. Molecules. 2019 May 21;24(10):1950.

(91) Cottier F, Sherrington S, Cockerill S, Del Olmo Toledo V, Kissane S, Tournu H, Orsini L, Palmer GE, Pérez JC, Hall RA. Remasking of *Candida albicans* β-Glucan in Response to Environmental pH Is Regulated by Quorum Sensing. mBio. 2019 Oct 15;10(5):e02347-19.

(92) Leonhardt I, Spielberg S, Weber M, Albrecht-Eckardt D, Bläss M, Claus R, Barz D, Scherlach K, Hertweck C, Löffler J, Hünniger K, Kurzai O. The fungal quorum-sensing molecule farnesol activates innate immune cells but suppresses cellular adaptive immunity. mBio. 2015 Mar 17;6(2):e00143.

(93) Hargarten JC, Moore TC, Petro TM, Nickerson KW, Atkin AL. *Candida albicans* Quorum Sensing Molecules Stimulate Mouse Macrophage Migration. Infect Immun. 2015 Oct;83(10):3857-64.

(94) Zawrotniak M, Wojtalik K, Rapala-Kozik M. Farnesol, a Quorum-Sensing Molecule of *Candida albicans* Triggers the Release of Neutrophil Extracellular Traps. Cells. 2019 Dec 11;8(12):1611.

(95) Chen P, Li W, Li G. Structures and Functions of Chromatin Fibers. Annu Rev Biophys. 2021 May 6;50:95-116.

(96) Dai Z, Ramesh V, Locasale JW. The evolving metabolic landscape of chromatin biology and epigenetics. Nat Rev Genet. 2020 Dec;21(12):737-753.

(97) Klemm SL, Shipony Z, Greenleaf WJ. Chromatin accessibility and the regulatory epigenome. Nat Rev Genet. 2019 Apr;20(4):207-220.

(98) Barnes CE, English DM, Cowley SM. Acetylation & Co: an expanding repertoire of histone acylations regulates chromatin and transcription. Essays Biochem. 2019 Apr 23;63(1):97-107.

(99) Ramazi S, Allahverdi A, Zahiri J. Evaluation of post-translational modifications in histone proteins: A review on histone modification defects in developmental and neurological disorders. J Biosci. 2020;45:135.

(100) Millán-Zambrano G, Burton A, Bannister AJ, Schneider R. Histone post-translational modifications - cause and consequence of genome function. Nat Rev Genet. 2022 Mar 25.

(101) Zhang Y, Sun Z, Jia J, Du T, Zhang N, Tang Y, Fang Y, Fang D. Overview of Histone Modification. Adv Exp Med Biol. 2021;1283:1-16.

(102) Chen YC, Koutelou E, Dent SYR. Now open: Evolving insights to the roles of lysine acetylation in chromatin organization and function. Mol Cell. 2022 Feb 17;82(4):716-727.

(103) Shvedunova M, Akhtar A. Modulation of cellular processes by histone and non-histone protein acetylation. Nat Rev Mol Cell Biol. 2022 May;23(5):329-349.

(104) Park SY, Kim JS. A short guide to histone deacetylases including recent progress on class II enzymes. Exp Mol Med. 2020 Feb;52(2):204-212.

(105) Ho TCS, Chan AHY, Ganesan A. Thirty Years of HDAC Inhibitors: 2020 Insight and Hindsight. J Med Chem. 2020 Nov 12;63(21):12460-12484.

(106) Teixeira CSS, Cerqueira NMFSA, Gomes P, Sousa SF. A Molecular Perspective on Sirtuin Activity. Int J Mol Sci. 2020 Nov 15;21(22):8609.

(107) Su S, Li X, Yang X, Li Y, Chen X, Sun S, Jia S. Histone acetylation/deacetylation in *Candida albicans* and their potential as antifungal targets. Future Microbiol. 2020 Jul;15:1075-1090.

(108) Garnaud C, Champleboux M, Maubon D, Cornet M, Govin J. Histone Deacetylases and Their Inhibition in *Candida* Species. Front Microbiol. 2016 Aug 5;7:1238.

(109) Wurtele H, Tsao S, Lépine G, Mullick A, Tremblay J, Drogaris P, Lee EH, Thibault P, Verreault A, Raymond M. Modulation of histone H3 lysine 56 acetylation as an antifungal therapeutic strategy. Nat Med. 2010 Jul;16(7):774-80.

(110) Prigneau O, Porta A, Maresca B. *Candida albicans* CTN gene family is induced during macrophage infection: homology, disruption and phenotypic analysis of CTN3 gene. Fungal Genet Biol. 2004 Aug;41(8):783-93.

(111) Mawer JSP, Massen J, Reichert C, Grabenhorst N, Mylonas C, Tessarz P. Nhp2 is a reader of H2AQ105me and part of a network integrating metabolism with rRNA synthesis. EMBO Rep. 2021 Oct 5;22(10):e52435.

(112) Ford E, Nikopoulou C, Kokkalis A, Thanos D. A method for generating highly multiplexed ChIP-seq libraries. BMC Res Notes. 2014 May 22;7:312.

(113) Iqbal A, Duitama C, Metge F, Rosskopp D, Boucas J. Flaski. (2021).

(114) Enis Afgan, Dannon Baker, Bérénice Batut, Marius van den Beek, Dave Bouvier, Martin Čech, John Chilton, Dave Clements, Nate Coraor, Björn Grüning, Aysam Guerler, Jennifer Hillman-Jackson, Vahid Jalili, Helena Rasche, Nicola Soranzo, Jeremy Goecks, James Taylor, Anton Nekrutenko, and Daniel Blankenberg. The Galaxy platform for accessible, reproducible and collaborative biomedical analyses: 2018 update, Nucleic Acids Research, Volume 46, Issue W1, 2018 July 2, Pages W537–W544.

(115) Conte M, Eletto D, Pannetta M, Petrone AM, Monti MC, Cassiano C, Giurato G, Rizzo F, Tessarz P, Petrella A, Tosco A and Porta A. Effects of Hst3p inhibition in *Candida albicans*: a genome-wide H3K56 acetylation analysis. Front. Cell. Infect. Microbiol. 2022 Oct 27. 12:1031814.

(116) Tebarth B, Doedt T, Krishnamurthy S, Weide M, Monterola F, Dominguez A, Ernst JF. Adaptation of the Efg1p morphogenetic pathway in *Candida albicans* by negative autoregulation and PKA-dependent repression of the EFG1 gene. J Mol Biol. 2003 Jun 20;329(5):949-62.

(117) Lassak T, Schneider E, Bussmann M, Kurtz D, Manak JR, Srikantha T, Soll DR, Ernst JF. Target specificity of the *Candida albicans* Efg1 regulator. Mol Microbiol. 2011 Nov;82(3):602-18.

(118) Topal S, Vasseur P, Radman-Livaja M, Peterson CL. Distinct transcriptional roles for Histone H3-K56 acetylation during the cell cycle in Yeast. Nat Commun. 2019 Sep 26;10(1):4372.

(119) Tsarfaty I, Sandovsky-Losica H, Mittelman L, Berdicevsky I, Segal E. Cellular actin is affected by interaction with *Candida albicans*. FEMS Microbiol Lett. 2000 Aug 15;189(2):225-32.

(120) Schindler B, Segal E. *Candida albicans* metabolite affects the cytoskeleton and phagocytic activity of murine macrophages. Med Mycol. 2008 May;46(3):251-8.

(121) Kim J, Lee H, Yi SJ, Kim K. Gene regulation by histone-modifying enzymes under hypoxic conditions: a focus on histone methylation and acetylation. Exp Mol Med. 2022 Jul;54(7):878-889.

(122) Tams RN, Wagner AS, Jackson JW, Gann ER, Sparer TE, Reynolds TB. Pathways That Synthesize Phosphatidylethanolamine Impact *Candida albicans* Hyphal Length and Cell Wall Composition through Transcriptional and Posttranscriptional Mechanisms. Infect Immun. 2020;88(3):e00480-19. Published 2020 Feb 20.

(123) Strijbis K, van Roermund CW, van den Burg J, van den Berg M, Hardy GP, Wanders RJ, Distel B. Contributions of carnitine acetyltransferases to intracellular acetyl unit transport in *Candida albicans*. J Biol Chem. 2010 Aug 6;285(32):24335-46.

(124) Okazaki K, Tan H, Fukui S, Kubota I, Kamiryo T. Peroxisomal acyl-coenzyme A oxidase multigene family of the yeast *Candida tropicalis*; nucleotide sequence of a third gene and its protein product. Gene. 1987;58(1):37-44.

(125) Nickerson KW, Atkin AL. Deciphering fungal dimorphism: Farnesol's unanswered questions. Mol Microbiol. 2017 Feb;103(4):567-575.

(126) Granger BL. Accessibility and contribution to glucan masking of natural and genetically tagged versions of yeast wall protein 1 of *Candida albicans*. PLoS One. 2018 Jan 12;13(1):e0191194.

(127) Marblestone JG, Edavettal SC, Lim Y, Lim P, Zuo X, Butt TR. Comparison of SUMO fusion technology with traditional gene fusion systems: enhanced expression and solubility with SUMO. Protein Sci. 2006 Jan;15(1):182-9.

(128) Butt TR, Edavettal SC, Hall JP, Mattern MR. SUMO fusion technology for difficult-to-express proteins. Protein Expr Purif. 2005 Sep;43(1):1-9.

(129) Du H, Li X, Huang G, Kang Y, Zhu L. The zinc-finger transcription factor, Ofi1, regulates white-opaque switching and filamentation in the yeast *Candida albicans*. Acta Biochim Biophys Sin (Shanghai). 2015 May;47(5):335-41.

(130) Walther A, Wendland J. Polarized hyphal growth in *Candida albicans* requires the Wiskott-Aldrich Syndrome protein homolog Wal1p. Eukaryot Cell. 2004 Apr;3(2):471-82.

(131) Banerjee M, Thompson DS, Lazzell A, Carlisle PL, Pierce C, Monteagudo C, López-Ribot JL, Kadosh D. UME6, a novel filament-specific regulator

of *Candida albicans* hyphal extension and virulence. Mol Biol Cell. 2008 Apr;19(4):1354-65.

(132) Hernday AD, Lohse MB, Fordyce PM, Nobile CJ, DeRisi JL, Johnson AD. Structure of the transcriptional network controlling white-opaque switching in *Candida albicans*. Mol Microbiol. 2013 Oct;90(1):22-35.